Membranes made with zeolite and ZIF-8, and their applications to water separation from organic/water mixtures

ゼオライト膜及び ZIF-8 膜の合成と有機物水混合溶液分離への応用

北海道大学大学院　総合化学院

総合化学専攻　プロセス工学講座

Yaqi Zhang

Table of Contents

Chapter 1
Introduction

1.1. Development of porous materials and porous ma1terials based membranes

1.1.1. Development of porous materials

A porous material is a material containing pores. The atoms, ions and molecules which composed in the porous material distribute at the surface and throughout the bulk of the material. The types and performances of the porous materials are decided by their porosity, the size, volume and distribution of the porous space and atomic molecular structure.

Porous materials can be grouped into three classes based on their pore diameter (φ): microporous, φ<2.0 nm; Mesoporous, 2.0<φ<50 nm; and macroporous, φ> 50nm [1].

Porous materials attracted wide attention for application of adsorbents, catalysts, molecular sieves and ion exchangers due to their particular characteristic such as high surface area, homogeneous pore size. Among all of the porous materials, zeolite is most studied because of the uniform pore size and well-ordered structure. The uniform pore size of zeolite can efficiently separate molecules based on the size or shap differences, namely, selectively separate a small molecule from a bigger one. On the other hand, the hydrophobicity and hydrophility of the zeolite which decided by the atoms composed in zeolite is important [2]. The zeolite comprising pure silica can absorb organic molecules from water, whereas zeolite comprising aluminosilicate can absorb water from organic solvents.

The applications of zeolite with microporous were limited in the small size molecules adsorption and separation due to the basic unit of TO_4 (SiO_4 and AlO_4), which not suitable for the catalysis or adsorption of big organic and biological molecules [3, 4]. ExxonMobil discovered mesoporous zeolite called M41S in the early 1990s [5], opened new appraches to synthesize catalysts for reaction of relative large molecules. Mesoporous silicates such as MCM-41 and SBA-15, are porous silicates with huge surface areas (normally>1000 m^2/g), large pore sizes (2 nm < size < 20 nm)

and ordered arrays of cylindrical mesopores with very regular pore morphology.

Recently, a new family of microporous material named metal-organic frameworks (MOFs) has been developed rapidly [6, 7]. In MOFs, the metal ions are connected by the organic molecules and the frameworks are flexible. MOFs can be obtained by different synthesis methods, moreover, by adjusting the size and functional groups of the organic linkers, the surface area and the hydrophilicity or hydrophobility of MOF structures can be controlled. Hence many researchers invest their attention into MOFs development in the fields of adsorption, catalysis, storage, separation.

1.1.2. Development of porous materials based membrane

Membranes are widely divided into two parts: polymeric membranes and inorganic membranes. The polymeric membranes have been well developed because the simple synthesis method but limited in application since the vulnerability characters. Compared with the polymeric membranes, inorganic membranes have lots of merits: high pressure resistance; low activation energy; easy to cleaning.

Inorganic membranes generally include 2 primary categories according to the structure: pore and dense inorganic membrane. Applications of dense inorganic membranes are majorly used for low molecular weight gases separation. Porous inorganic membranes possess more merits than other kinds of membranes which playing a predominance role in commercial membrane market. Four types of inorganic materials attracted widest attentions: metallic membrane, ceramic membrane, carbon membranes and zeolitic membranes [8].

Dense inorganic membranes are usually used for hydrogen separation from gaseous mixtures. The main synthesis method of metallic membrane is by sintering of metal powders. The dominant material is palladium (Pd) and its alloys, which is highly soluble and permeable for hydrogen. But the surface of the metal membranes is easily be poisoned by a carbon-containing source which development is limited.

Ceramic membranes are synthesis by the combine of a metal with anion in the form of oxide, carbide or nitride. This kind of membrane is chemically stable in high temperature environment. Therefores, application is major in food, Pharmacy, bioindustry.

Carbon membranes can be used for gas separation according size sieving. Because of the uniform porous strcture in the carbon membrane, the membranes can separation the small size molecule with big size molecule with a high separation factor. Even differences bewteen two molecules is very small, the separation performance is very

good according to the strictly separation by the solid pores in carbon membranes.

Zeolites are composed by Si-Al-O units and possess the micro-size uniform pores in the crystalline frameworks. The applications of zeolite membranes are mainly in separation and act as supplymentary to distillation tower or reaction actor. But there are still some problems when using zeolite membrane to separate small size molecule, expecially gas mixture separation. During the zeolite membrane preparation, the non-zeolite pores or defect points are unavoidable among the zeolite crystals. Therefore, gas fluxes through zeolite membrane are low compared to other inorganic membranes. Moreover, the zeolite membranes are usually prepared by using template or surfactant to help zeolite crystal formation. After the synthesis procedure, the membranes need to calcinate in a high temperature to remove the template. In the high temperature, zeolite crystal will shink, but the support which made by different materials go on to expansion, which made membrane broken.

Recently, a new class of materials, MOFs structure are studied and developed. MOFs structures contain single metal atoms connected with elongated organic molecules as ligand. MOFs can be made with millions of different combinations of metal atoms, molecules and structure. Zeolite imidazolate frameworks (ZIFs) are a subclass of MOFs. The membranes prepared by using ZIFs materials are interesting for gas storage and molecular separation [9-10].

Metallic membrane, ceramic membrane, carbon membranes and zeolitic membranes possess the same metrits such as metallic membrane, ceramic membrane, carbon membranes and zeolitic membranes. However in the past, the application of inorganic membranes is mainly focus on porous ceramic membranes [11]. Nowadays all kinds of application have been found and examples of important applications are [12]:

- Separation of H_2 from coal-derived gas.
- Separation of CO_2 from natural gas and coal plant flue gas.
- Separation of O_2 from air for use in efficient combustion, and (petro-) chemical applications.

The applications of membrane are classified according to their connected pore size. Dense and micro-porous membranes are applied for gas and liquids separation but can be permeable for single molecules. Zeolite MFI membrane could use for p/o-xylene separation [13] and Zeolite A membranes have been commercialized for the removal of water from organic solution [14] selective transport in dense and micro-porous materials occurs by a diffusion mechanism.

Meso-porous membrane can be used for selective permeate of ions and small molecules in liquids by nano-filtration [15]. Supported meso-porous r-alumina

membranes have been used for ^{235}U isotope enrichment. Gas phase transport in meso-porous membrane occurs by a Knudsen mechanism but liquids transport is generally by viscous flow.

Macro-porous membranes are commercially available for water filtration applications. These structures are sometimes used as support for gas separation membranes. Both gas and liquid phase transport in macro-porous membrane occurs by viscous flow.

1.2. Zeolite molecular sieve

Zeolites are derived from natural volcanic minerals with unique performances, especially when the volcanic ash diffused in ancient alkaline water areas, the salts media altered and rebuilt the ash into different zeolite materials [16].

Zeolites are 3D microporous crystals which contain Al, Si and O in the regular frameworks [17]. The corresponding crystallographic structure is formed by tetrahedras of (AlO_4) and (SiO_4). Figure 1.1 shows the typical tetrahedral structures. They are the basic building blocks of zeolites. Since the network of SiO_4 tetrahedral is neutral and AlO_4 tetrahedron in the framework takes a negative charge, zeolite frameworks need to combine with charge compensating cations (Na^+, K^+ or NH^{4+}) to maintain electrical neutrality.

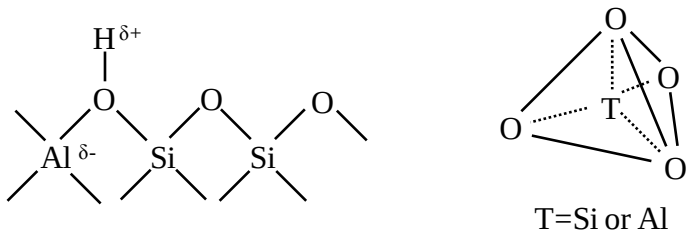

Figure 1.1 Tetrahedron-Basic building units of zeolites

The zeolite framework includes channels, channel intersections and cages, which are agree with the dimensions range of most molecules. According to pore size, most zeolites can be divided into three species (Fig. 1.2): small pore zeolites of 8 membrane ring apertures, e.g. zeolite A; medium pore zeolites with 10 membrane ring apertures, e.g. zeolite ZSM-5 and large pore zeolites with 12 membrane ring apertures, 6.0-8.0 Å e.g. zeolite MOR.

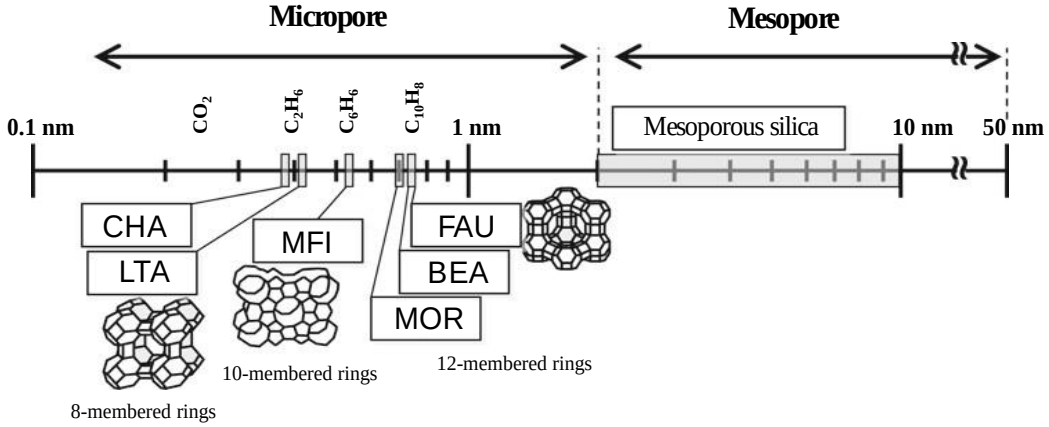

Figure 1.2 the comparation of zeolitic pore size and the hydrocarbon

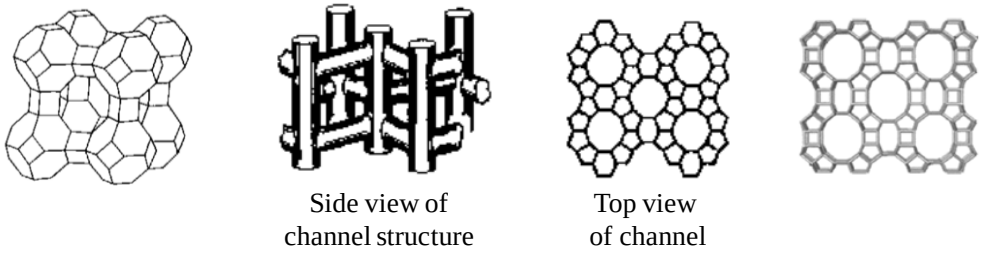

(a) A zeolite (b) ZSM-5 zeolite (c) MOR

Figure 1.3 zeolite molecular sieve structure (a) A type zeolite, (b) ZSM-5 zeolite, (c) MOR

1.2.1. Representative structures of zeolites [18]

- Zeolite A (LTA)

Zeolite A has 3D pore structure and the pores arranged perpendicular to each other in x, y, z axis (Fig. 1.3 (a)). The pore size is fixed by eight oxygen ring and the pore size is about 4.2 Å. the large cavity is about 11.4 Å and it is surrounded by eight sodalite cages (truncated octahedral) connected by their square faces of cubic structure. The inner cavity of zeolite A is large enough for the reaction of structure changing occurred, however this kind small pore can only allow specific shape like olefins and n-paraffins. For example, the pore of zeolite A is selective to paraffins and the cracking reaction will

occur on the sites within the cage to form smaller alkane chain. Every year huge amount of this kind zeolite are produced [19] for many application such as water softening detergents, addition of polyvinyl chloride (PVC) thermoplastics, gas drying and hydrocarbons separation.

- Zeolite ZSM-5 (MFI)

The zeolite ZSM-5 is consisted of five rings which are arrayed as columns and connected with each other as showed the figure 1.3b. There are two obvious ten-ring channels of nominally 5.6 Å apertures. A straight channel run along the [0 1 0] direction and sinusoidal channel runs along the [100] direction. Zeolite ZSM-5 are most potential and versatile catalysts because we can prepare ZSM-5 with Si/Al ratios from 8 to infinity. Moreover, it can be prepared zeolites into MFI framework with Ga, B, Co, Ti, and Fe. This flexibility provides the chance of industrial or chemical engineer to desire the optimum for catalytic application [20].

- Mordenite (MOR)

Mordenite zeolite has 12-ring pores of about 6.5 ×7.0 Å running along the [001] direction. There are connected by smaller eight-ring pores along [010] direction (Fig. 1.3 (C)). Mordenites offer some interesting performances which are valuble at electrochemical interface, such as size, shape and charge selectivity, chemical stability, capacity of ion exchange in micro-environment and ionic conductivity [21]

1.2.2. The application of the zeolite

- Catalyst

Zeolite could be used in many areas but mostly is applied for catalyst [22-23], for example use of various small pore zeolites for converting methanol to olefins (MTO), the C_2-C_4 olefin concentration is about 60% at 100% conversion. Zeolites promote a diverse catalytic reaction array of acid or metal include reactions. The reactions can occur in zeolite channel, only small size and certain shape moleclues can enter and leave from the channel of zeolite. It makes zeolite become a shape selective catalyst.

- Gas separation

The characteristics of zeolite such as uniform multiapertures can be used to sieve molecules, make it widely used for gas separation [24-25]. This property can be optimum by balancing the structure by adjusting the shape and number of cations nearby the pertures. The polymerization of semiconductors and conducting polymers can occur within the aperture of the zeolites.

- Ion exchange

Zeolite acted as ion exchange, is maimly applicated in toothpaste, water softening, soaps and detergents fields because of the hydrated cations within the zeolite pores can exchange with other cations when in water solutions.

1.3. Zeolite membrane

1.3.1. Membrane and Membrane process

Membrane can be used for two phase`s separation; selective separation is the main function of a membrane and membrane process. Membranes can be classified into two parts: biofilm and prepared membranes. The biofilm like liposomes and vesicles are now applied in pharmaceutical industry. Prepared membranes can be subdivided into organic and inorganic membranes. In accordance with specific condition, the membrane can be prepared differently in morphology, thickness, homogeneous and heterogeneous. By changing the opration condition such as pressure, concentration or a temperature, the membrane prosess can be transformed from active to passive..

The properties and characterization of the membrane decide membranes` application. The structural of membrane materials, the pore size of the membrane materials and even the distribution of the pore in the membrane affect the membrane characterization and the application of the membranes

Membrane separation means using permeable membrane to transport of substances between two fractions. Because the operation which carried in the membrane separation process without heating, therefore the separation using membrane is less energy than conventional thermal separation process.

According to the separation system, the membrane separation process can be divided into three types: microfiltration separation, ultrafiltration and reverse osmosis separation [26].

When the diameter of particles is smaller than 100 nm and it is act as permeate component, the high flux could be obtained only with low hydrodynamic resistance and small driving forces. This kind of membrane process is called micro size particle filtration.

Ultrafiltration can be used to separate the macro size molecules. Compared with the microfiltration, the increased in permeate resisitance of bigger size particles need larger driving force to meet the separation requirement.

When the separation system is the small molecular weight and the molecule size of the two components is nearly the same, the high dense membrane is needed and during

the separation process, a high hydrodynamic resistance will exist and this process can be defined as reverse osmosis.

Membrane separation is mainly depends on the size and shape of the pores existed in the membrane. The geometries, size and the structure of the pores are difference. There are lots of pore structures in membranes. Figure 1.4 gives a part of examples of pores which consist in either organic membrane or inorganic membranes [26].

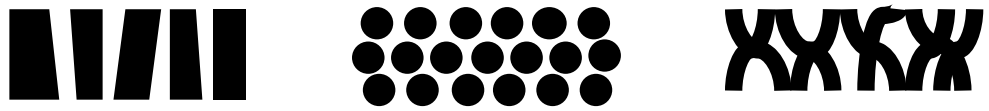

Figure 1.4 Some characteristic pore geometries found in porous membranes.

As shown in Figure 1.4 (a), some of the pores go through the membrane with the cylindrical shape to the surface of membrane. When the pores were considered as the same diameter, the volume flux through the pores can be calculated by the Hagen-Poiseuille equations [26]:

$$J = \frac{\varepsilon r^2}{8\eta\tau}\frac{\Delta P}{\Delta x} \quad (1)$$

ΔP stands for pressure difference; Δx is the thickness of the membrane; η is inversely proportional to the viscosity.The quantity ε is the surface porosity, which is the fractional pore area, while τ is the pore tortuosity. It is found that the flux through the membrane is proportional to the pressure difference (ΔP) and surface porosity (ε), but inverse proportional to the thickness of the membrane (Δx).

When the membrane is composed by amont of the round crystals as shown in figure 1.4 (b), the solution flux through the membrane can be described as follow [26].

$$J = \frac{\varepsilon^3}{K\eta S^2(1-\varepsilon)^2}\frac{\Delta p}{\Delta x} \quad (2)$$

Here, ε is the volume fraction of the pores, S the internal surface area, and K is constant which affected by the pore morphology and the tortuosity.

The membrane showed in figure 1.4 (c) maily exists in organic membrane. The membrane show the structure like a sponge, which materials connect with each other. The volume through this kind of membrane can not be calculated directly but estimate by using the model describe above ((1)-(2)).

1.3.2. Zeolite membrane

Zeolites are crystalline microporous aluminasilicates which built up by a three dimensional network of SiO_4 and AlO_4 retrathedra [27]. Zeolites have been used for as toothpaste, adsorbent and catalysts. However, the most fundamental application by zeolite is molecular sieving. The zeolite membrane separation mainly based on the molecule size and shape selective separation. The molecule with a kinetic diameter too large to pass through the zeolite internal adsorption surface will be effectively sieved. Table 1.1 shows some properties of zeolites [28, 29]. Zeolite LTA is a very hydrophilic zeolite because of a high amount of aluminium contains. The pore size is dependent on the type of the cation and Ca^{2+}, Na^{+} and K^{+} gives 5A, 4A and 3A, respectively. On the other hand silicalite-1 is a very hydrophobic zeolite since without aluminium contain. Specific separation can be operated when use the zeolite as a material for membrane synthesis [30-35].

1.3.3. Zeolite Membrane synthesis

Typically, a zeolite membrane is prepared by hydrothermal synthesis under a high temperature or pressure in a traditional autoclave. For membrane synthesis, the silica source and aluminum source are mixed together and add in to water alkaline solution. Some time the surfactants or templates such as structure directing agents are also used to help crystal formation, and after the membrane synthesis, the template can be deleted by calcination methods. The pH of the mother liquids, the ratio of silica by alumina and the ratio of metal ion and silica are the important factors affect membrane preparation.

There are all kinds of zeolite membrane synthesis methods and they were been conclude as follow:

- In situ hydrothermal synthesis methods

"In situ hydrothermal synthesis" means synthesize a membrane only in one step. During the hydrothermal synthesis, the alumina filter which acting as membrane support is immersed in the mother solution, the nucleation on the surface of alumina filter is requied. The crystal nucleus can grow into the zeolite crystals at a high temperature and high pressure condition [36, 37].

- Ex situ hydrothermal synthesis or second growth methods

The method which using the seed to synthesis membrane was first appear in 1993 [38], and follow the patent was submitted in 1994 [39]. This method includes two synthesis steps. The first step is formation of the first layer of the membrane on the

surface of the membrane support by adsorbing the same zeolite as seed crystals. These first layer seed crystals will further growth under hydrothermal synthesis condition in the second stage. Since it is easy for the neclei get growth than the neclei formation, therefore, the crystal growth take place from the existed seed and the nucleation from the mother liquid decreased. There are some merits of the method about ex situ hydrothermal synthesis methods likes: firstly, the purity of crystallization is increased and in some extent to prevent the formation of the zeolite crystal into the support pores [40]. Secondly, the second growth method can keep the nuclei at the same growth rate as well as the crystal growth directions. In generally, the membrane prepared by second growth method usually showed the c-orientation [41, 42]. However the b-orientation membrane was also successfully prepared by Lai et al. [43], and the membranes they prepared shown high separation performance [44, 45].

- Other synthesis methods

Microwave-assisted crystallization provides an efficient method for preparing the zeolite membrane in short times [46]. The zeolite crystallization process was carried out by using microwaves for heating the autoclaves. There were all kinds of zeolite have been successfully synthesis by using this method [47-50].

1.3.4. Zeolite membrane characterization

Some of the methods can be used to analysis the zeolite characterization such as: scanning electron microscopy (SEM), X-ray diffraction (XRD), X-ray Fluorescence Analysis (XRF), energy dispersive X-ray spectroscopy (EDS).

SEM can be used to observe membrane morphology and the thickness of the membrane. The membrane quality and layer uniformity can also be checked by observing the crystal size, shape and the connection between the crystals.

XRD can measure the zeolite crystallinity. During the membrane preparation process, some zeolite powder also formed in the mother liquid and become deposit. Since these crystals show similar to the membranes, they can used to make XRD analysis to determine the membrane`s crystallinity purity.

EDS is used to check zeolite composition and usually with help of XRF. In zeolite membrane, the alumina contains ratio in the membrane is important factor affect membrane performance, and this alumina ratio can be detect using EDS analysis. Some reasearchers also use EDS to check the mix area of the membrane and membrane support [51, 52].

The property of the membrane is usually checked by the separation experiments.

For usually, membrane separation is used for gas mixtures or liquid mixtures separation. Gas separation mainly depends on the size sieving. For an ideal membrane, small size molecule can go through the pore of the membrane, but big size molecule is left on the feed side. The pressure acts as driving force for gas separation. But some materials` frameworks are flexible which can be permeated by bigger molecules.

Compared with sigle gas permeation, some mixtures permeate are different. The reason include two aspects: the partial pressure is different and there is competitive adsorption among the gas mixtures in feed side. N-C_4H_{10}/i-C_4H_{10} could be separated by using 10-membrane ring (MR) zeolite membrane [53]. Small pore, such as 8 MR zeolite membranes can be characterized by separation of light gas, like H_2/CH_4 [54], CO_2/CH_4 [55] or H_2/N_2 [56].

Separation by pervaporation usually refers to liquid mixture separation. Different with gas separation, liquid separation is not only depends on molecule size sieving but also hydrophilic and hydrophobic ability of molecules. During the pervaporation, small size molecules which possess high polarity will adsorb on the surface of the membrane and go through the membrane, at last get vaporization at permeate side. The driving force for liquid mixture separation is partical concentration which refered by using vacuum or carried gas at permeate side. The section 1.4 will give further discussion.

1.3.5. The application of zeolite membranes for separation [57]

- Gas separation

The gas separation is mainly conducted by polymeric membranes. However, in the separation process of refining, petrochemical, and nature gas industries, zeolite membranes still have large opportunities since they are more robust to support high partial pressure.

Zeolite membranes for gas separations are mainly carried out on the laboratory scale. MFI zeolite membranes were widely studies because of their pores sizes (0.55 nm) are suitable for gas separation of many industrial mixtures.

Table 1.2 summarizes some results concerning gas separation.

- Alcohol dehydration

A mixture of two or more liquids whose proportions cannot be altered by simple distillation is an azeotrope. Azeotropic separation usually refers to the specific techniques and pervaporation by using zeolite membranes is one of the choices.

Table 1.2 Gas separation results with zeolite membranes

Zeolitic Structure	Support	Thickness (μm)	Permeance 10^7 [mol/(m^2 s pa)]	Mixture Separation	Maximum Separation Factor (-)	Ref.
SAPO-34	α-Al_2O_3	25	1.6 [CO_2 at 298 k]	CO_2/CH_4	67	[58]
FAU	α-Al_2O_3	3	10 [CO_2 at 308 k]	CO_2/N_2	149	[59]
MFI	α-Al_2O_3	1	3 [p-Xylene at 298 k]	p/o-xylene	500	[60]
MFI	α-Al_2O_3	3	0.08 [n-C_4 at 300 k]	H_2/n-butane	520	[61]
MFI	α-Al_2O_3	10	1.2x10^{-7} [H_2 at 773 K]	H_2/H_2O	180	[62]
LTA	α-Al_2O_3	5	5.7 [H_2 at 298 k]	H_2O/CH_4	11.4	[63]

A-type zeolite membrane is most commonly employed for separation water from organic mixtures, because they are highly alumina contents and has a small pore, which is little larger than water molecular but smaller than most of organic moleculars. Many researchers have attempted to synthesize the A-type membrane and using them for organic dehydration by pervaporation method. Table 1.3 shows the result of the experiments. Usually the water flux through the membrane is affected by the concentration of water in the feed side and pervaporation temperature. because water flux through the membrane depends on the driving force which separation system refer. However, the temperature has little effect on the separation factor of the membranes.

The Si/Al ratio in A type zeolite is low. Therefore, A type zeolite displays high hydrophilicity which can be used for dehydration of alcohols. But the generally the fluxes and separation factor is lower than A-type zeolite because their Si/Al ratio is lower showed lower hydrophilicity.

Table 1.3 Pervaporation performance of zeolite NaA in alcohol dehydration

Temperature (K)	Water in feed (wt. %)	Water flux (kg/h m^2)	Separation Factor	Ref.
298	10	4.0	3000	[64]
323	10.09	0.772	46000	[65]
348	10.09	2.08	42000	[65]
393	10.09	8.37	47000	[65]
323	5.02	0.396	4800	[65]
348	5.02	1.10	5900	[65]
393	5.02	4.30	5600	[65]

Except A-type zeolite, zeolite X, Y, ZSM-5, MOR and T also been used in the dehydration of alcohols. But the generally the fluxes and separation factor is lower than A-type zeolite because their Si/Al ratio is lower showed lower hydrophilicity.

- Acid solution dehydration

The separation water from the esterification reaction for equilibrium, and the acid solution dehydration required an acid resistant hydrophilic membrane. However, hydrophilic zeolite is not stable in acid solution, since the alumina-oxygen bond is broken easily in acid solution. The zeolite T, MOR, and ZSM-5 were invested for water/acid mixture separation, MOR and zolite T show the high water permeability. Both of MOR and T zeolite possess 12 membrane ring which providing alternate pathways for H_2O but organic molecular could not permeate.

High slica contents membrane silicalite-1 membrane can also used for water/acetic acid mixtures separation. The membranes need some post treatment before using for separation. Our laboratory has been focus on this study for a long time. It is founded that the (-OH) group which on the surface of the zeolite membrane help for zeolite membrane separation and not destroyed by acid solution. The channel for water separation is not only include zeolite pore in the zeolite frameworks, but also the zeolitic-pores among the zeolite crystals.

- Organic separation

Separation of organic molecules from water required using hydrophpbic membranes. Among those membranes, silicalite-1, ZSM-5, and β type zeolite were mostly studied. Compare with the hydrophilic zeolite membrane, hydrophobic membranes possess low permeability and separation ability. This is because organic molecular is larger than water molecular and easily diffuse through the membrane. Separation is only depend on the hydrophobility zeolite preferentially adsorb organic molecular. Non-zeolitic pores and structure defects decrease the membrane separation ability.

Bowen` group [66] studied the separation ability of Ge-ZSM-5 membrane by separation organic compounds from organic/water mixtures. The result shows that the separation ability and flux are proportion to the organic component` fugacity in the mixture.

- Organic/Organic separation

Methy-tert-butyl ether (MTBE) can be used as an additive in gasoline, however as a potential human carcinogen, the separation MTBE from the mixture and safely discharge attracted much interest in the industries. The separation of MEOH from MTBE can be conducted by using zeolite silicalite-1 [67] and X, Y type zeolite

membranes. Zeolite Y and X showed good results in the separation process. NaY zeolite membranes were prepared by a research group and are used to separation the methanol/MTBE solution, it was found that different with other kinds of membrane, the separation factor decreased when increase the permeate molecule concentration (methanol molecule).

1.4. Pervaporation

In chemical industry and chemical processes, a separation is one of most important unit operation, which is mainly carried out by distillation. In high purity separation by distillation, the number of trays as well as the reflux ratio increase. Moreover, the azeotropic distillation such as water/ethanol, 3rd component of benzene need to be added in the distillation system, which is complex process with large energy consumption. It is important to build a new separation process composed of a distillation tower and other separation method. After separation by a distillation at a certain level, further purification is carried out by the new separation method, by which enable us to reduce energy consumption and to design a simple separation process. One method is prevaporation.

1.4.1. Pervaporation process

Pervaporation is a process method for separation of mixture of liquids by selective sorption and diffusion of a component through the membrane. Different from other separation process, there is a phase change during the pervaporation process.

Binning et al. [69] described the pervaporation process by the solution-diffusion mechanism. The pervaporation process can be divided into three steps according to the model, adsorption, diffusion and evaporation. In the mixture solution, the membrane adsorbs the components and the adsorbed components diffuse across the membrane under a chemical potential gradient and get evaporation at the downside of the membrane.

The adsorption is affected by the organic molecule polarities of the solution and the size, shape and molecular weight of the solute. The thermodynamic properties are the driving force during the whole process.

There is not selection during the desorption process. Therefore, the organic molecules diffuse in the final step of transport and get evaporation from the downside of the membrane with only small transport thermodynamics activities to be separated.

1.4.2. Pervaporation mechanism in zeolite membrane

In ideal situation, zeolite membranes possess only zeolite pores, as shown in Fig. 1.5 (a), the water molecules could be selectively permeated the zeolite pores of the hydrophilic membrane. However, zeolite membranes are composed by zeolite crystals. There are spaces among zeolite crystals which named non-zeolitic pores in zeolite membranes. The non-zeolitic pores can be affected by the preparation method, zeolite structure, and the post treatment of the membrane. The contributions of non-zeolitic pore to the whole flux of the membrane have been estimated by some researchers [70-73].

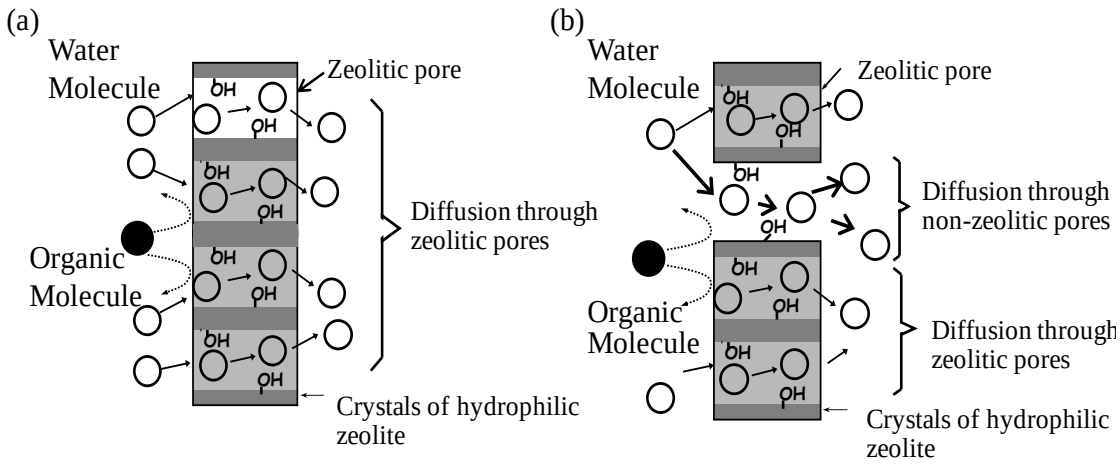

Figure 1.5 Representation of transport of an organic/water mixture through: (a) a hydrophilic zeolite membrane with only zeolitic pores; (b) a hydrophilic zeolite membrane containing hydrophilic non-zeolitic pores.

In addition, since the surface of the zeolite crystal is covered by (-OH) groups, just as shown in Fig. 1.5 (b), hydrophilic molecules become easily to adsorb on to the zeolite membrane surface or even the spaces among the zeolie crystals (non-zeolitic pore), therefore, increasing the hydrophilic molecules permeability of the membrane. Some research groups have reported that non-zeolitic pores can be used for separation for some mixtures and by controlling the non-zeolitic pore size, non-zeolitic pores can positively affected pervaporation [74, 75].

During membrane separation process, molecules in the solution selectively adsorbed into the membrane, permeate through it, and are removed as vapor from permeate side. The flux of molecules through the zeolite membrane from feed side to permeate side strongly affects the performance of the membrane, and the flux of

molecules through the membrane can be expressed as follow when adsorption of molecules do follows Langmuir isotherm and effect of counter diffusion could be ignored [76].

$$J_i = \frac{\rho_s \varepsilon D^s_{i,v}(0)}{\delta}(q_{i,f} - q_{i,p}) \quad (1)$$

here, ρ_s, ε, $D^s_{i,v}(0)$, δ, $q_{i,f}$, and $q_{i,p}$ are the zeolite membrane density, porosity, the intracrystalline surface diffusivity, thickness of membrane, quantities of component *i* on the feed side and the permeate side, respectively.

1.4.2.1. Adsorption

Adsorption is usually a heat release process. In zeolite membrane, the affinity of organic molecules and water molecules are decided by the hydrophilic and hydrophobic ability of the zeolite. Usually, the Si/Al ratio affects the hydrophilicity and hydrophobicity characters of zeolite, and the Si/Al ratio of the zeolite structure could be change in a wide range.

For example, Silicalite-1 is the most hydrophobic zeolite since the Si/Al ratio in silicalite-1 structure equal to infinity, and silicalite-1 could be used to separate the organic molecules from water. Howerer, zeolite A can be used for organic solution dehydration because of the hydrophilicity of zeolite A (Si/Al=1).

The hydrophilicity and hydrophobicity of the materials is difficult to description. A hydrophobicity index (HI) is defined as follow [77], which helping to make measurement. ($q_{organic}$: organic amount adsorbed by a solid; q_{water}: water amount adsorbed by a solid)

$$HI = \frac{q_{organic}}{q_{water}} \quad (2)$$

1.4.2.2. Diffusion

The molecules which adsorbed on the surface of membrane can diffuse along the zeolite pore or non-zeolitic pore, and reach to the downside of the zeolite membrane. During the diffusion process, the concentration gradient of adsorbed molecules is considered to be the driving force. The molecule diffusion in zeolite membrane is in the range of solution-diffusion, molecular sieving, surface diffusion, Knudsen diffusion.

When the diameter of permeate molecule is bigger than the diameter of the zeolite pore, usually, the diffusivity follows an Arrhenius-type equation [78]:

$$D = D_0 \exp(-\frac{E_d}{RT}) \quad (3)$$

1.4.3. The advantage and application of pervaporation

By combination with distillation and other rectification processes, pervaporation has many potential applications and the separation process become simplicity, efficiency and favorable economics. The advantages of pervaporation can be concluded as follows:
a. The new separation process which combining the distillation and pervaporation is less cost and low energy demand.
b. The pervaporation can be used in the azeotropes separation.
c. Pervaporation is a green separation technology which freedom from environmental pollution.
d. Pervaporation can be applied in a wide range according to the membrane properties.

Pervaporation technology has a wide application such as dehydration of the organic solution, separation of organic from water and organic separations. The examples described below show the application of the new separation process which combining the distillation and pevaporation.

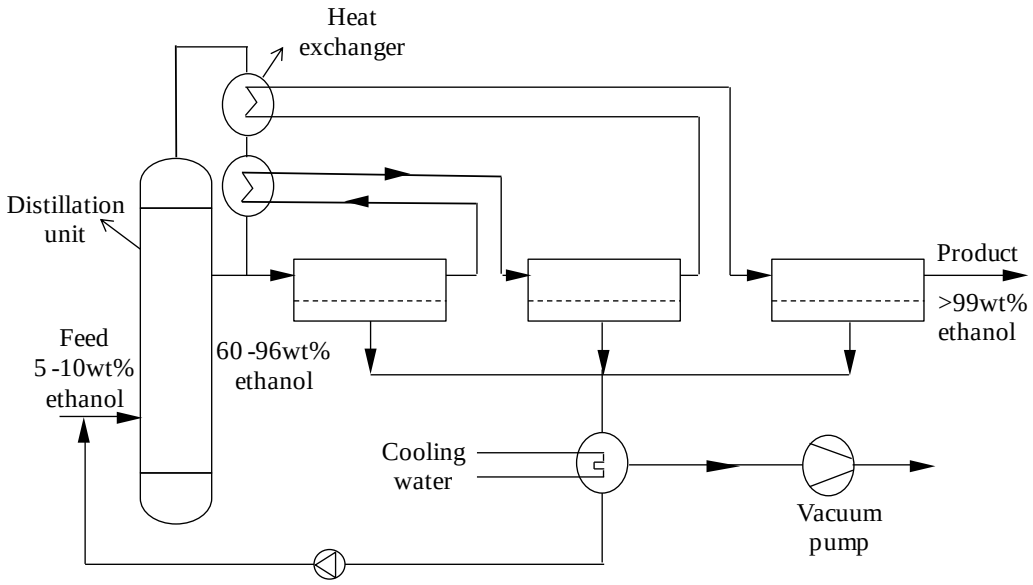

Figure 1.6 Flow diagram of a hybrid process for pure alcohol production,

Pervaporation technologies are usually used for dehydration of ethanol and iso-propanol. As show in Figure 1.6, the pervaporation technology and ditllation process are combined together to separate water from water/ethanol mixtures. The distillation process can remove bulk of the water and followed by the pervaporation process to reach 99.8wt% ethanol. By combining the distillation and pervaporation the hybrid system is less energy consumption. There is only phase change during the pervaporation need energy consumption. And the retentate steam from the distillation uint can be reused to offer the energy. In order to enhance the efficiency, the membrane separator can be divided in small section and connected in series [79].

Lurgi Company compared the pervaporation method with the azeotropic distillation from the ethanol dehydration (enrichment of ethanol from 94wt% to 99.85%). Table 1.4 show the cost in every operation section and according to the data run for one year operation, the cost of pervaporation technology could save 60% compared with azeotropic distillation.

Table 1.4 Operation cost compared the azeotropic distillation with pervaporation by dehydration ethanol from 94wt% to 99.85wt% /Mark・t^{-1}

Program	Azeotropic distillation (Cyclohexane as entrainer)	pervaporation
Low-pressure steam	50~75	6.25
Cooling water	7.5	2
Electricity cost	2.25	5.7
Entrainer	2.4 ~ 4.5	—
Membrane	—	8 ~ 16
Total	62 ~ 89	22 ~ 30

1.5. Zeolitic imidazolate frameworks (ZIFs)

Metal organic frameworks (MOFs) are a new kind of materials made by inorganic and organic unit combinations [80]. They are also known as “hybrid organic inorganic frameworks” or “coordination polymers”. In some cases, the structures are stable in certain pressure and could be used for the storage of gases such as H_2 and CO_2. Other possible applications of MOFs are in gas purification, in gas separation, in catalysis and as sensors [81].

MOFs are made by two parts: inorganic part – a metal ion and organic unit (a linker) [81]. The combination of inorganic part and organic unit dictates the structure and hence properties of the MOF. For example, the metal's coordination preference influences the morphorlogy of the apertures by determinating the ligand number by connection with the metals and the connection angle. In MOFs, the framework is template by the secondary building unit (SBU) and the organic ligands. Figure 1.7 shows some of MOFs materials structures which synthesis by the SBU ($Zn_4O(CO_2)_6$, $Cu_2(CO_2)_4$, $Zn_2O_2(CO_2)_2$) [82].

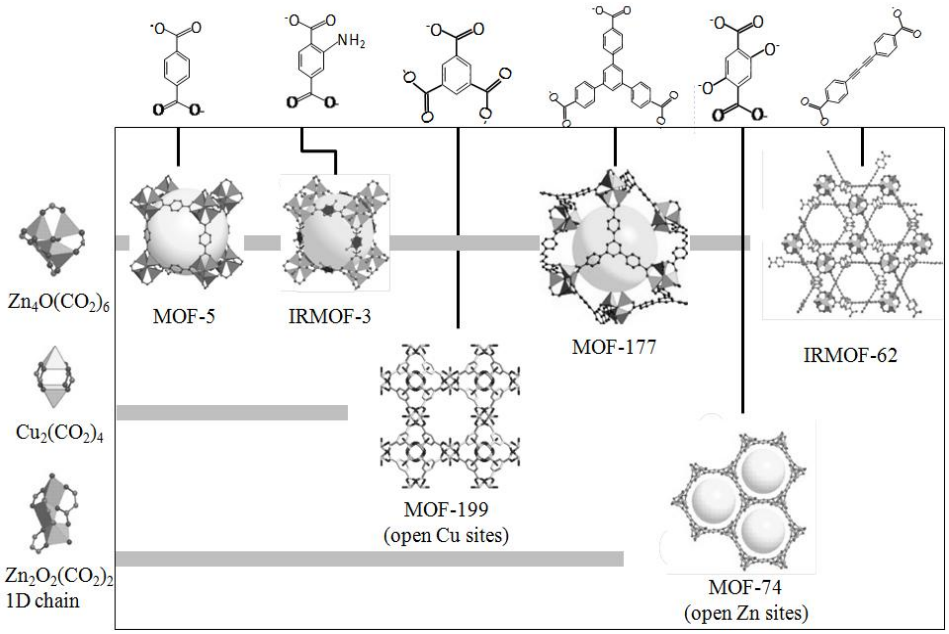

Fig. 1.7 The single-crystal x-ray structures of the benchmark MOFs: the $Zn_4O(CO_2)_6$ cluster linked by terephthalate (MOF-5), 2-aminoterephthalate (IRMOF-3), benzene-1,3,5-tris(4-benzoate) (MOF-177), and diacetylene-1,4-bis(4-benzoic acid) (IRMOF-62); the $Cu_2(CO_2)_4$ cluster linked by trimesate (MOF-199); and 1D $Zn_2O_2(CO_2)_2$ chains linked by 2,5-dihydroxyterephthalate (MOF-74).

Zeolitic imidazolate frameworks (ZIFs) are a subclass of MOFs which composed by the metal ions like Ferrum, Cobalt, Copper, or Zinc by organic imidazole linkers form the one, two or three dimensional structural with uniform porous. Since the metal-imidazole-metal angle is similar to the 145° Si-O-Si angle in zeolites, ZIFs possess the similar topology structure with zeolite. Moreover, ZIFs have the advantages

of both zeolites and MOFs, such as large surface areas, high crystallinities and exceptional thermal and chemical stabilities. ZIFs hold great promise in many application areas including catalysis, separation and sensing [83-85].

1.5.1. Synthesis of ZIF crystals

ZIFs have been rapidly developed and lots of new type ZIFs were synthesis and named in the past 5 years, traditional method such as hydrothermal synthesis in water or organic solvents, respectively. The synthesis temperatures range from room temperature up to 200 °C and reaction time from hours to days. So far, there are two methods have been developed to synthesis of the ZIF crystals, which ZIFs synthesis with solvent and ZIFs synthesis without solvent.

1.5.1.1. ZIFs synthesis with solvent

- Solvothermal synthesis.

ZIFs, which are synthesis with the organic solvents called solvothermal synthesis. ZIF-1 to ZIF-12, the twelve kinds of ZIF crystals were firstly prepared by using organic solvent systems such as N, N-dimethylformamide (DMF), N, N-diethylformamide (DEF) and N-methylpyrrolidine (NMP) [86]. Other kind of ZIF materials like ZIF-60 to ZIF-77 [87], ZIF-78 to ZIF-82 [88], ZIF-90 [89] and ZIF-100 [90] were successfully prepared by using DMF/DEF/NMP as reaction medium solvents. Recently, some deprotonating agents were added to facilitate the ZIF materials formation, including some organic amines such as pyridine and triethylamine (TEA). ZIF-78 crystals were prepared with assistance of TEA [91], while ZIF-90 was prepared with adding of pyridine to DMF at room temperature [92].

Methanol also can be used as the reaction medium to form ZIFs materials [93]. ZIF-8 crystals can be obtained by using methanol as the reaction medium [94, 95], moreover, the crystal size and morphology can be controlled by some methods. The nanosized and hexagonally shaped ZIF-8 crystals can be obtained when using poly (diallyldimethylammonium chloride) as a stabilizer in methanol [96]. The micron-sized crystals can be obtained by using modulating ligands such as sodium formate/1-methylimidazole and *n*-butylamine in methanol solution [97]. Other alcohols such as ethanol [98] and isopropyl alcohol [99] were also successfully used as organic solvents in ZIFs synthesis.

- Hydrothermal synthesis

The organic solvents are expensive, flammable and not environmentally, recently, water was used for ZIFs formation [100]. However, the stoichiometric molar ratio of zinc ions and MIm is high and the large amount usage of MIm was wasted. By adding the deprotonation agents, the purity ZIFs could be prepared in a low ration of zinc ions and MIm. Gross et al. [101] prepared ZIF-8 and ZIF-67 in an aqueous system with addition of TEA at room temperature and the molar ratio of Zn^{2+}: MIm = 1: 4.

Some surfactants were used to control the ZIFs crystal size and morphology, such as polyvinylpyrrolidone (PVP). The micron sized ZIF-90 crystals could be obtained in a water solution by using PVP as surfactant and it was considered that PVP can prevent the aggregation of crystal seeds to control the morphology and size of the crystals [102]. Moreover, ammonium hydroxide can be used for ZIF-8 formation, the particle sizes and the structures of ZIF-8 crystals could be easily controlled by change the ammonia concentration in the synthesis solution [103].

1.5.1.2. ZIFs synthesis without solvent

There are still some problems in the ZIFs formation such as the excessively use of imidazole sources and the collection of products ZIF-8 needed massive solvent washing. For this reason, ZIFs formation without usage of solvent has been developed. Shi et al. [104] obtained ZIF-8 and ZIF-67 by a steam-assisted conversion method. During the formation process, the solid phase containing metal salts and excess ligands were placed in a small Teflon cup where surrounded by water vapor at 120 °C for 24h. Moreover, Zhang et al. [105] have successfully prepared ZIF-8 from the solvent-free reaction by simply mixing of ZnO and MIm with a molar ratio of 1 : 2, the mixture was heated at 180 °C for 12 h. Beobibe et al. [106] have also prepared ZIFs by a solvent-free method, in which ZIFs were formed by the acid-base reaction between ZnO/CoO/$Co(OH)_2$ and imidazolic ligands at a temperature from 100 °C to 160 °C in a closed vessel and the high yield of product about 97% were obtained by adding small amount of structure directing agents.

1.5.2. Application of ZIF materials

ZIFs possess the high porosity, controllable structures and high stable ability even at a high temperature environment. The application of ZIF materials looks to be promising. Both ZIF crystals and ZIF membranes have been developed as adsorbents and catalysts. And even contribute to the fields of sensing and drug delivery.

1.5.2.1. Separation

Because of the uniform mutiaperture and superficial area, ZIF materials hold great potential in gas separation. Both ZIF crystals and ZIF membranes have been widely focused on the application of the gas separations, just as shown in Table 1.5. Generally, the separation performance of ZIF membranes can be affected by many factors such as the separated system condition, phase system, operating environment and the type of ZIFs materials. In the case of ZIF-7, the pore limiting diameter is 0.24nm and the largest cavity diameter is about 0.56 nm. The separation factor is between 6.5 ~ 9.6, when using ZIF-7 membrane to separate the mixed gases of H_2 and CO_2. The results indicate the pore size of the ZIFs materals is the key point to decide the separation. As shown in the Table 1.5, ZIF-8 is also used for mixed gas separation. The pore limiting diameter of ZIF-8 is 0.34nm and the lagest cavity diameter is 1.14nm. The ZIF-8 membrane showed a high separation factor of 11.2 when separate gas mixtures of H_2/CH_4. Moreover, ZIF-8 membrane can be used for separation the C2 and C3 hydrocarbon mixtures and showed the high separation factor of 167 for separation the gases mixture of ethylene-propane. The detail of ZIF membranes for separation application will discuss in next section.

Table 1.5 Gas separation performances of ZIF membranes

ZIF membrane	Gases	Separation performance	Reference
ZIF-7	H_2/CO_2	Ideal selectivity 6.7; separation factor 6.5	[107]
ZIF-7	H_2/CO_2	Separation factor 9.6	[108]
ZIF-8	H_2/CO_2	Ideal selectivity 11.0; separation factor 9.5	[109]
ZIF-8	H_2/N_2; H_2/CH_4	Ideal selectivity 11.6; 13	[110]
ZIF-8	H_2/CO_2; H_2/Ar; H_2/O_2; H_2/N_2;	Ideal separation factor 4.9; 7.0; 13.6; 15.1 and 9.8	[111]
ZIF-8	C_2H_6/C_3H_8; C_2H_4/C_3H_6;	Separation factors 80; 10 and 167	[112]
ZIF-8	H_2/C_3H_8; C_3H_6/C_3H_8	The ideal separation factors 2000 and 59 (298 K)	[113]
ZIF-69	CO_2/CO	Permselectivity 3.5	[114]
ZIF-69	CO_2/N_2; CO_2/CO; CO_2/CH_4	Separation factor 6.3; 5.0; 4.6	[115]

1.5.2.2. Catalyst

ZIFs are kind of porous materials which been considered as one of the most active catalysts. A number of reactions including the Knoevenagel reaction [116, 117], the Friedel-Crafts acylation [118], the esterification [119], transesterification [120],

oxidation [121] alcoholysis [122], and the hydrogen production [123, 124], can be actively catalyzed by ZIFs.

ZIF-8 can effectively catalyze for the Friedel-Crafts acylation reaction, the anisole and benzoyl chloride proceeded well by using ZIF-8 and the high product yield was obtained [118]. Furthermore, ZIF-8 can be used for monoglycerides by esterification of oleic acid with glycerol. Compared with the reaction without using calalyst (the conversion is about 10%), the oleic acid conversion is above 50% by using ZIF-8 as a catalyst. Moreover, ZIF-8 crystals can be easily recovered by filtration methods and can be reused without losing lots of the activities [119]. Oxidation can also been catalyzed by ZIFs, for examples, ZIF-9 exhibited catalytic activity for the oxidation of tetralin [121] and small aromatic molecules such as vanilly alcohol, syringol, and cinnamyl alcohol [122]. ZIF-9 can also catalyze for the hydrogen production in $NaBH_4$ hydrolysis reaction. ZIF-9 showed high catalytic activity and thermal stability, the porous structure of ZIF-9 offer a good support point for Co element. The ZIF-10 and ZIF-8 also act as a expective materials for calalyze reactions [123].

Moreover, due to the similar characteristic with zeolite materials such as large surface area and multipoles, some of ZIFs can be used as supports for the incorporation of various metals to form catalysts [125, 126].

1.5.2.3. Sensing and drug delivery

The high thermal and chemical stabilities of ZIF marterials enable ZIFs to be used as sensors and even drug deliveries.

ZIFs as the matrix for constructing integrated dehydrogenase electrochemical biosensors for in vivo measurement of neurochemicals are prepared successfully [127]. In that study, ZIFs act as a matrix for coimmobilizing electrocatalysts and dehydrogenases onto the electrode surface. Different ZIFs materials were choiced for the experiment, including ZIF-7, ZIF-8, ZIF-70 which a series of goup marterials with different pore sizes, channels and functional groups [127]. Based on the luminescence intensity, ZIF-8 nano-size crystals can be used as a sensing platform for fluorescence-enhanced detection of nucleic acids [128]. Moreover, caffeine can be inserted into the ZIF-8 cages [129]. ZIF-8 materials keep stable even in high temperature, therefore, by combining the caffeine molecules into ZIF-8 cages, the ZIF-8 can control the release of caffeine and provide thermal protection during the high temperature process.

1.6. Preparation methods of ZIF based membranes

ZIF materials possess promising future and can be applied in many areas. ZIF based membranes using for separation is one of the most attractive applications. So far, various synthesis methods for ZIF membranes have been studied. Generally, the synthesis method can be classified into: in situ preparation, secondary growth preparation and the counter-diffusion preparation.

1.6.1. In situ preparation method

ZIF membrane can be synthesis through one-step solvothermal or hydrothermal synthesis on the disks or some porous structural support. This kind of method also acted as a traditional method for zeolite membrane preparation.

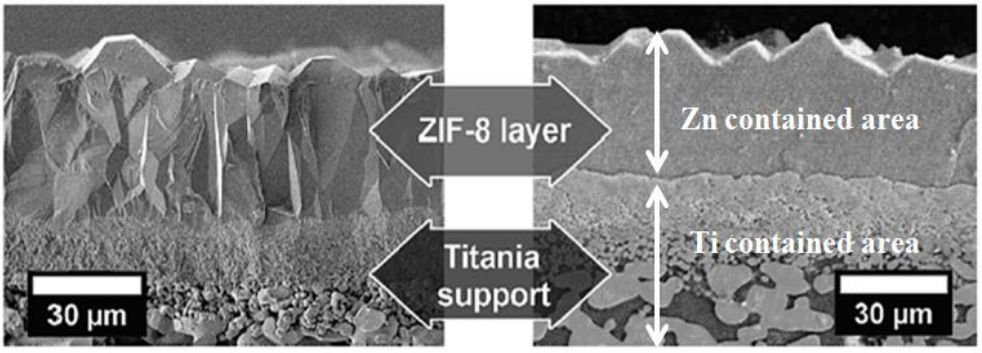

Figure 1.8 Left: SEM image of the cross section of a simply broken ZIF-8 membrane. Right: EDXS mapping of the sawn and polished ZIF-8 membrane.

Bux's group [130] prepared the ZIF-8 membrane (as shown in Fig. 1.8) using a microwave assisted, in situ preparation method, which the solution with a porous titania support was put into an autoclave and heated in a microwave oven. The permeability of ZIF-8 membrane is no as high as zeolite membrane when keep the same selectivity according to hydrogen permeance experiment. The modified in situ preparation method for ZIF membrane preparation was developed by using a kind of covalent linker to promote the heterogeneous nucleation such as 3-aminopropyltriethoxysilane (APTES). ZIF membrane with a compact layer can be formed on the APTES-modified support by

solvothermal synthesis method such as ZIF-22, ZIF-95 [131-134]. This method makes a big improvement of membrane quality.

1.6.2. Second growth preparation method

The membrane prepared by second growth method usually realized through two parts: (1) depositing the crystal seeds by thermal seeding, dip-coating or rubbing; (2) put the support with the crystal seed layer into the autoclave to go on solvothermal synthesis or hydrothermal synthesis for the second ZIF membrane layer. The membrane prepared by this method has the same crystal orientation and the membrane thickness and grain boundary structure could be controlled by this method.

ZIF-8 membrane was successfully prepared by a second growth method in Carreon research group [135]. The alumina support was at first seeded with ZIF-8 crystals by rubbing, then the support with the first layer of the ZIF-8 seed crystals was go on to hydrothermal synthesis for the second layer formation. In secondary growth methods, seeding step is very important which decided the membrane quality. The technology to increase the connection between ZIF crystals and the support is important. Therefore, many seeding approaches such as reactive seeding [136, 137], pre-coating [138, 139], and microwave-assisted seeding [140] have been explored.

1.6.3. Counter diffusion preparation method

ZIF membranes can be prepared by a counter diffusion method [141]. In this method, a support was used to separate the metal ions from the organic linker molecules. This method enables to synthesis membrane inside of the support which made the poorly intergrown membranes to be healed and in some avoided the obscission of the membrane. Yamaguchi's group [141] used a counter diffusion method to obtain an 80 micron meter thick ZIF-8 layer on the outer section of a porous alumina capillary substrate. The Figure 1.9 shows the procedure for the membrane preparation. The membranes prepared possess high permeances of hydrogen and propylene molecules. The ideal separation factors of H_2/C_3H_8 and C_3H_6/C_3H_8 at 25^{o}C were found to be 2000 and 59, respectively [141].

In conclusion, there are many of synthesis methods can be used for the ZIF membrane. The remaining challenge is to produce ZIFs on a large scale to meet the potential commercial application and the methods for ZIF membrane which with high reproducibility, low cost and large-scale preparation in the future.

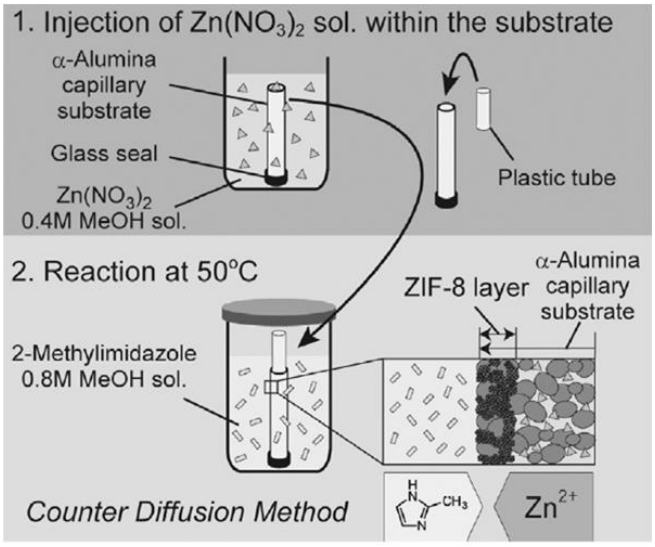

Figure 1.9 Schematic illustration of the counter diffusion method

1.7. Research objective

A new separation process has been proposed which instead of the traditional separation by distillation which can consume less amount of energy but achieve a high purity separation. A pervaporation by using membrane is a promising technique to achieve this goal. The membrane process can separate certain molecular mixtures effectively and economically without any toxic or by-production. The materials used for membrane preparation are not limited but cover in a wide range. The structures and properties of the materials decided the membrane performance and the field of membrane applications. The objective of this study is selective separation of water from water/organic mixtures by pervaporation using membrane technology. We studied the method of membrane preparation including the zeolite membrane (modenite type and MTW type membrane), ZIF materials based membrane (ZIF-8 membrane). We optimized the synthesis method for increasing the performance of the membrane and the membranes were used in the different separation system for application. The whole work is constituted by 6 sections from chapter 1 to chapter 6.

In chapter 1, the industrial separation process using distillation columns is

intriduced, and its problems are extracted. Furehtmore, the nature of zeolites is overviewed, and the expection of zeolite membranes is described for a new separation process.

In chapter 2 and 3, the methods of preparation, optimization of the Mordenite membranes and application were discussed, respectively. In chapter 2, Mordenite nanocrystal-layered membranes consisting of a mordenite nanocrystal layer and protection layer were successfully prepared. The effect of nanocrystal layer thickness was discussed to determine the appropriate condition for membrane preparation. The basic conditions were detected in order to use the membrane for pervaporation. The membrane acid stability was examined by separation of water from acetic acid/water solution. In chapter 3, four types of water/organic solvent solutions were prepared for pervaporation experiments using the mordenite nanocrystal-layered membranes to detect the effect of the polarity of the organic solvent in the feed solution on the permeance of water through the mordenite nanocrystal-layered membrane. The mechanism of the mordenite type zeolite membrane was studied and using for directing the membrane preparation. In order to prepare the membrane with high separation ability and permeability, the effects of synthesis conditions on the membranes performance, such as hydrothermal temperature, pre-aging time for the mother liquid which using for hydrothermal synthesis and heating rate during the hydrothermal synthesis were discussed. Moreover, the obtained mordenite membranes were applied to the separation of water from water/organic solutions (organic solvents: ethanol, acetone, 2-propanol, or acetic acid) using a pervaporation method.

In chapter 4 and chapter 5, a new type high-silica material with a unidimensional 12-membered ring channel were used to prepare the membrane. At first, the MTW nanocrystals synthesis with different Si/Al ratios and different kinds of the organic structure directing agent (OSDA) were discussed to dicide the seed crystals for membrane preparation. A MTW-type zeolite nanocrystal-layered membrane composed of nanocrystal and protection layers were successfully prepared by a secondary growth method under hydrothermal conditions. The acidic proof ability of MTW membrane was detected by separation of water from acetic acid/water solution. Since the MTW can be synthesized in a wide range of Si/Al and the crystals morphology can be controlled by using different kind of the OSDA molecules, in chapter 5, the effects of crystal morphology, Si/Al ratio and thickness of MTW zeolite membrane on water/2-propanol separation by pervaporation were discussed, respectively. In order to get better understanding of the membrane preparation and separation, the mechanisms of the MTW type zeolite membrane were discussed in the chapter. The function of the

protection layer and the nanocrystal layer in the membrane separation is studied, respectively.

In capter 6, zeolitic imidazolate frameworks (ZIFs) as metal-organic frameworks (MOF) were focused. ZIFs possess the advantages of both zeolites and MOFs, namely molecular sieving effect, hydrophilic and hydrophobic properties. Therefores, the nanocrystals and the membranes of ZIF-8 as a model ZIFs were prepared. In order to understand the properties of ZIF-8 materials, the gas adsorption isotherms of ZIF-8 crystals were measured in advance. The permeance performance of single component (water, ethanol, butanol, benzene, hexane) through ZIF-8 membrane was found to follow the adsorption properties obtained through the gas adsorption experiment using ZIF-8 crystals.

Reference

[1] K.S.W. Sing, D.H. Everett, W.R.A. Haul, L. Moscou, J. Pierotti, J. Ruquerol, T. Siemieniewska, *pure appl. Chem.* 57 (1985) 603
[2] M.E. Davis, *Nature* 417(2002)813
[3] C.T. Kresge, M.E. Leonowicz, W.J. Roth, J.C. Vartuli, J. S. Beck, *Nature* 359 (1992) 710
[4] F. Schuth, W. Schmidt, *Adv. Mater,* 14 (2002) 629
[5] C.T. Kresge, M.E. Leonowicz, W.J. Roth, J.C. Vartuli, *J.S. Nature* 359 (1992) 710
[6] R. Matsuda, R. Kitaura, S. Kitagawa, Y. Kubota, R. V. Belosludov, T. C. Kobayashi, H. Sakamoto, T. Chiba, M. Takata, Y. Kawazoe, Y. Mita, *Nature* 436 (2005) 238
[7] J. S. Seo, D. Whang, H. Lee, S. I. Jun, J. Oh, Y. Jin, K. Kim, *Nature* 404 (2000) 982
[8] Introduction to membrane
http://www.separationprocesses.com/Membrane/MT_Chp07a.htm
[9] R. Banerjee, A. Phan, B. Wang, C. Knobler, H. Furukawa, M O'Keeffe, O.M. Yaghi, *Science* 319 (2008) 939
[10] X.L. Dong, K. Huang, S.N. Liu, R.F. Ren, W.Q. Jin, Y.S. LIN, *J. Mater, Chem.* 22 (2012) 19222
[11] P. HsiehH, Inorganic membranes. *AIChE Sym. Ser., New York* 84 (1988) 1
[12] H. Verweij, Inorganic membranes, *Chem. Eng.* 1(2012)156
[13] T. Gallego-Lizon, E. Edwards, G. Lobiundo, L.F. dos Santos, *J. Membr. Sci.* 197 (2002) 309

[14] Y.S. Lin, I. Kumakiri, B.N. Nair, H. Alsyouri, *Sep. Purify. Methods* 31(2002) 229
[15] L. Cot, A. Ayral, J. Durand, C. Guizard, N. Hovnanian, A. Julbe, A. Larbot, *Solid State Sci.* 2 (2000) 313
[16] V. Faraon, R.M. Ion, *Mater. Mech.* 5 (8) 2010
[17] J.A. Schwarz, C.I. Contescu, K. Putyera, *Dekker Encyclopedia of Nanoscience and Nanotechnology* 2(2004)1157
[18] Website: http://www.personal.utulsa.edu/~geoffrey-price/zeolite/index.html
[19] T. Maesen, B. Marcus, *Studies in surface science and catalysis* 137(2001)1
[20] K. Tanabe, WF Holderich. *Appl Catal A Gen* 181 (1999) 399
[21] M. Arvand, S. Sohrabnezhad, M.F. Mousavi, M. Shamsipur, M.A. Zanjanchi, *Analytica Chimica Acta* 491(2, 8) (2003)193
[22] W. Wang, Y. Jiang, M. Hunger, *Catal. Today* 113 (2006) 102
[23] J. Kim, M. Choi, R. Ryoo, *J. Catal.* 269 (2010) 219
[24] K. Kusakabe, T. Kuroda, A. Murata, S. Morooka, *Ind. & Eng. Chem. Res.* 36 (1997) 649
[25] T. Tomita, K. Nakayama, H. Sakai, *Micropor. Mesopor. Mater.* 68 (2004) 71
[26] M. Marcel, Basic principles of membrane technology, 1997, p224
[27] D.W. Breck, Zeolite Molecular Sieves: Structure, Chemistry and use, John Wiley & Sons, 1974
[28] W.M. Meier, D.H. Olson, Atlas of zeolite structure types, 3rd edition, Butterworth Heineman 1992
[29] D.M. Ruthven, *Chem. Eng. Progr.* 84 (1988) 42
[30] M. Matsukata, E. Kikuchi, *Chem. Soc. Jp.* 70 (10) (1997) 2341
[31] J. Coronas, J. Santamaría, *Sep Purif method* 28 (1999) 127
[32] J. Caro, M. Noack, P. Kölsch, R. Schäfer, *Micropor. Mesopor. Mater.* 38 (2000) 3
[33] S. Nair, M. Tsapatsis, Synthesis and properties of zeolitic membranes. In: S. M. Auerbach, K.A. Carrado, P.K. Dutta (Eds.) Handbook of Zeolite Science and Technology. New York: Marcel Dekker, 2003; 867-919
[34] J. Coronas, J. Santamaría, *Topics Catal.* 29(1-2) (2004) 29
[35] J. Coronas, J. Santamaría, *Chem. Eng. Sci.* 59 (2004) 4879
[36] J.D.F. Ramsay, S. Kallus, in: N.K. Kanellopoulos (ED.), membrane science and technology series, *Amsterdam* 6 (2000) 373
[37] S. Komarneni, H. Katsuki, S. Furuta, Novel honeycomb structure: a microporous ZSM-5 and macroporous mullite composite, *J. Mater. Chem.* 8 (1998) 2327
[38] K. Horii, K. Tanaky, K. Kita, K. Okamoto, in: proc. 26th Autumn Meeting of Soc. Chem. Eng., Japan, 1994, P.99

[39] W.F. Lai, H.W. Deckman, J.A. mcHenry, J.P. Verdujin, US patent 5.871.650, filed on July 8, 1994
[40] J. Hedlund, J. Sterte, M. Anthonis, A.J. Bons, B. Carstensen, N. Corcoran, D. Cox, H. Deckman, W.D. Gijinst, P.P de Moor, F. Lai, J. McHenry, W. Mortier, J. Reinoso, J. Peters, *Micropor. Mesopor. Mater.* 52 (2002) 179
[41] M.C. Lovallo, M. Tsapatsis, *AIChE J* 42 (11) (1996) 3020
[42] G. Xomeritakis, S. Nair, M. Tsapatsis, transport properties of alumina-supported MFI membranes made by secondary (seeded) growth. *Micropor. Mesopor. Mater.* 38 (2000) 61
[43] Z.P. Lai, G. Bonilla, I. Díaz, J.G. Nery , K. Sujaoti, M.A. Amat, E. KOkkoli, O. Terassaki, R.W. Thompson, M. Tsapatsis, D.G. Vlachos, *Science* 300 (2003) 456
[44] J.S. Lee, K. Ha, Y.J. LEE, K.B. Yoon, *Adv. Mater.* 17 (2005) 837
[45] K. Ha, Y.J. Lee, K.B. Yoon, *Adv. Mater.* 12 (2000) 1114
[46] C.S. Cundy, Collect. Czech. *Chem. Commun.* 63 (1998) 1699
[47] P. Chu, F.G. Dwyer, V.J. Clarke, *EP* 358 (1990) 827
[48] A. Arafat, J.C. Jansen, A.R. Ebaid. H. van Bekkum, *Zeolites* 13 (1993) 162
[49] I. Girnus, K. Hoffmann, F. Marlow, J. Caro, G. Döring, *Micropor. Mater.* 2 (1994) 537
[50] I. Girnus, M.M. Pohl, J. Richter-Mendau, J. Caro, *Zeolite* 15 (1995) 33
[51] J.C. Poshusta, V.A. Tuan, E.A. Page, R.D. Noble, J.L. Falconer, *AIChE J.* 46 (2000) 779
[52] J. Coronas, J.L. Falconer, R.D. Noble, *AIChE J.* 43 (1997) 1797
[53] W.J.W. Bakker, F. Kapteijn, J. Poppe, J.A. Moulijn, *J. Membr. Sci.* 117 (*1996*) 57
[54] J.C. Poshusta, R.D. Noble, J.L. Falconer, *J. Membr. Sci.* 186 (2001) 25
[55] K. Aoki, K. Kusakabe, S. Morooka, *J. Membr. Sci.* 141 (1998) 197
[56] S.G. Li, J.L. Falconer, R.D. Noble, *J. Membr. Sci.* 241(2004)121
[57] A.K. Pabby, S.S.H. Rizvi, A.M. Sastre, Handbook of Membrane Separations, 2009
[58] S.G. Li, J.L. Falconer, R.D. Noble, *J. Membr. Sci.* 241 (2004) 121
[59] Y. Hasegawa, K. Watanabe, K. Kusakabe, S. Morooka, *J. Membr. Sci.* 208(1-2) (2002) 415
[60] Z.P. Lai, G. Bonilla, I. Díaz, J.G. Nery, K. Sujaoti, M.A. Amat, E. Kokkoli, O. Terasaki, R.W. Thompson, M.Tsapatsis, D.G. Vlachos, *Sci.* 300(2003)456
[61] J.H. Dong, Y.S. Lin, M.Z.C. Hu, R.A. Peascoe, E.A. Payzant, *Micropor. Mesopor. Mater.* 34 (3) (2000) 241
[62] H.B. Wang, X.L. Dong, Y.S. Lin, *J. Membr. Sci.* 450(2014)425
[63] S. Shirazian, S.N. Ashrafizadeh, *J. Indus. Eng. Chem.*, Accepted at 2014

[64] S. Basak, D. Kundu, M.K. Naskar, *Cera. Inter.* 40 (8B) (2014) 12923
[65] M. Kondo, M. Komori, H. Kita, K. Okamoto, *J. Membr. Sci.* 133 (1997) 133
[66] T.C. Bowen, S. Li, R.D. Noble, J.L. Falconer, *J. Membr. Sci.* 225 (2005) 165
[67] T. Sano, M. Hasegawa, Y. Kawakami, H. Yanagishita, *J. Membr. Sci.* 107 (1995) 193
[68] H. Kita, K, Fuchida, T. Horita, H. Asamura, K. Okamoto, *Sep. Purif. Technol.* 25 (2001) 261
[69] D.W. Breck, Zeolite Molecular Sieves : Structure, Chemistry and use, John Wiley & Sons, 1974
[70] T. Tsuru, Y. Takata, H. Kondo, F. Hirano, T. Yoshioka, M. Asaeda, *Sep. Purif. Tech.* 32 (2003) 23
[71] J.M. van de Graaf, F. Kapteijn, J.A. Moulijn, *Chem. Eng. Sci.* 54 (1999) 1081
[72] T.E. Clark, H.W. Deckman, D.M. Cox, R.R. Chance, *J. Membr. Sci.* 230 (2004) 91
[73] F. Jareman, J. Hedlund, D. Creaser, J. Sterte, *J. Membr. Sci.* 236 (2004) 81
[74] K. Okamoto, H. Kita, K. Horii, K. Tanaka, M. Kondo, *Ind. Eng. Chem. Res.* 40 (2001) 163
[75] M. Nomura, T. Yamaguchi, S. Nakao, *J. Membr. Sci.* 187 (2001) 203
[76] D. Shah, K. Kissick, A. Ghorpade, R. Hannah, D. Bhattacharyya, *J. Membr. Sci.*179 (2000) 185
[77] A.A. Giaya, R.W. Thompson, R. Denkewicz, *Micropor, Mesopor. Mater.* 40 (2000) 205
[78] T.C. Bowen, R.D. Noble, J.L. Falconer, *J. Membr. Sci.* 245 (2004) 1
[79] M. Mulder, Basic Principles of Membrane Technology, 2003
[80] P.K. Pahwa, G.K. Pahwa, Hydrogen economy, P164
[81] Website: http://en.wikipedia.org/wiki/Metal-organic_framework
[82] D. Britt, H. Furukawa, B. Wang, T.G. Glover, D.M. Yaghi, *PNAS* 106 (2009) 20637
[83] S.A. Moggach, T.D. Bennett, A.K. Cheetham, *Angew. Chem.* 121 (2009) 7221
[84] D. Fairen-Jimenez, S. A. Moggach, M.T. Wharmby, P.A. Wright, S. Parsons, T. Düren, *J. Am. Chem. Soc.* 133(2011) 8900
[85] F. Wang, Y.X. Tan, H. Yang, H.X. Zhang, Y. Kang, J. Zhang, *Chem. Commun.* 47 (2011) 5828
[86] K.S. Park, Z. Ni, A.P. Côté, J.Y. Choi, R. Huang, F.J. Uribe-Romo, H.K. Chae, M. O'Keeffe, O.M. Yaghi, Proc. Natl. *Acad. Sci. U. S. A.*103 (2006) 10186
[87] R. Banerjee, A. Phan, B. Wang, C. Knobler, H. Furukawa, M. O'Keeffe, O. M. Yaghi, *Science* 319 (2008) 939
[88] R. Banerjee, H. Furukawa, D. Britt, C. Knobler, M. O'Keeffe, O. M. Yaghi, *J. Am.*

Chem. Soc. 131 (2009) 3875
[89] W. Morris, C. J. Doonan, H. Furukawa, R. Banerjee, O. M. Yaghi, *J. Am. Chem. Soc.* 130 (2008) 12626
[90] H. Hayashi, A. P. Cote, H. Furukawa, M. O'Keeffe, O. M. Yaghi, *Nat. Mater.* 6 (2007) 501
[91] Y. Ban, Y. Li, X. Liu, Y. Peng, W. Yang, *Micropor. Mesopor. Mater.* 173(2013) 29
[92] T. Yang, T.S. Chung, *J. Mater. Chem.* A 1 (2013) 6081
[93] X.C. Huang, Y.Y. Lin, J.P. Zhang, X.M. *Chen, Angew. Chem., Int. Ed.* 45 (2006) 1557
[94] J.P. Zhang, A.X. Zhu, R.B. Lin, X.L. Qi, X.M. Chen, *Adv. Mater.* 23 (2011) 1268
[95] A.X. Zhu, R.B. Lin, X.L. Qi, Y. Liu, Y.Y. Lin, J.P. Zhang, X.M. Chen, *Micropor.Mesopor. Mater.* 157 (2012) 42
[96] S.K. Nune, P.K. Thallapally, A. Dohnalkova, C. Wang, J. Liu, G. J. Exarhos, *Chem. Commun.*46 (2010) 4878
[97] J. Cravillon, R. Nayuk, S. Springer, A. Feldhoff, K. Huber, M. Wiebcke, *Chem. Mater.* 23 (2011) 2130
[98] M. He, J.F. Yao, L.X. Li, K. Wang, F.Y. Chen, H.T. Wang, *Chem Plus Chem* 78 (2013) 1222
[99] T.D. Bennett, P.J. Saines, D.A. Keen, J.C. Tan, A.K. Cheetham, *Chem. Eur. J.*19 (2013) 7049
[100] Y. Pan, Y. Liu, G. Zeng, L. Zhao, Z. Lai, *Chem. Commun.* 47 (2011) 2071
[101] A.F. Gross, E. Sherman, J.J. Vajo, *Dalton Trans.* 41 (2012) 5458
[102] F.K. Shieh, S.C. Wang, S.Y. Leo, K.C.W. Wu, *Chem. Eur. J.* 19 (2013) 11139
[103] M. He, J. Yao, Q. Liu, K. Wang, F. Chen, H. Wang, *Micropor. Mesopor. Mater.* 184 (2014) 55
[104] Q. Shi, Z. Chen, Z. Song, J. Li, J. Dong, *Angew. Chem. Int. Ed.* 50 (2011) 672
[105] J.B. Lin, R.B. Lin, X.N. Cheng, J.P. Zhang, X.M. Chen, *Chem. Commun.* 47 (2011) 9185
[106] M. Lanchas, D. Vallejo-Sanchez, G. Beobide, O. Castillo, A.T. Aguayo, A. Luque, P. Roman, *Chem. Commun.* 48(2012) 9930
[107] Y.S. Li, F.Y. Liang, H. Bux, A. Feldhoff, W.S. Yang, J. Caro, *Angew. Chem., Int. Ed.* 49 (2010) 548
[108] V.M. Aceituno Melgar, H.T. Kwon, J. Kim, *J. Membr. Sci.* 459 (2014) 190
[109] X. Dong, K. Huang, S. Liu, R. Ren, W. Jin, Y. S. Lin, *J. Mater. Chem.* 22 (2012) 19222
[110] M.C. McCarthy, V. Varela-Guerrero, G.V. Barnett, H.K. Jeong, *Langmuir* 26

(2010) 14636
[111] L. Ge, A. Du, M. Hou, V. Rudolph, Z. Zhu, *RSC Adv.* 2 (2012) 11793
[112] Y. Pan, Z. Lai, *Chem. Commun.* 47 (2011) 10275
[113] N. Hara, M. Yoshimune, H. Negishi, K. Haraya, S. Hara, T. Yamaguchi, *J. Membr. Sci.*450 (2014) 215
[114] Y. Liu, E. Hu, E. A. Khan, Z. Lai, *J. Membr. Sci.* 353 (2010) 36
[115] Y. Liu, G. Zeng, Y. Pan, Z. Lai, *J. Membr. Sci.* 379 (2011) 46
[116] U.P.N. Tran, K.K.A. Le, N. T. S. Phan, *ACS Catal.* 1 (2011) 120
[117] L.T L. Nguyen, K.K.A. Le, H.X. Truong, N.T.S. Phan, *Catal. Sci. Technol.* 2 (2012) 521
[118] L.T.L. Nguyen, K.K.A. Le, N.T.S. Phan, Chin. *J. Catal.* 33 (2012) 688
[119] L.H. Wee, S.R. Bajpe, N. Janssens, I. Hermans, *Chem. Commun.* 46 (2010) 8186
[120] M. Savonnet, S.Aguado, U. Ravon, D.B. Bachi, V. Lecocq, N. Bats, C. Pinel, D. Farrusseng, *Green Chem.* 11 (2009) 1729
[121] F.X. Llabrés i Xamena, O. Casanova, R. Galiasso Tailleur, H. Garcia, A. Corma, *J. Catal.* 255 (2008) 220
[122] L.H. Wee, C. Wiktor, S. Turner, W. Vanderlinden, N. Janssens, S.R. Bajpe, J. Am. Chem. Soc. 134 (2012) 10911
[123] S.B. Kalidindi, D. Esken, R.A. Fischer, *Chem. Eur. J.* 17 (2011) 6594
[124] Q. Li, H. Kim, *Fuel Process. Technol.* 100 (2012) 43
[125] H.L. Jiang, B. Liu, T. Akita, M. Haruta, H. Sakurai, Q. Xu, *J. Am. Chem. Soc.* 131 (2009) 11302
[126] P. Wang, J. Zhao, X. Li, Y. Yang, Q. Yang, C. Li, *Chem. Commun.* 49 (2013) 3330
[127] W. Ma, Q. Jiang, P. Yu, L. Yang, L. Mao, *Anal. Chem.* 85 (2013) 7550
[128] S. Liu, L. Wang, J. Tian, Y. Luo, G. Chang, A.M. Asiri, A.O. Al-Youbi, X. Sun, *ChemPlusChem* 77 (2012) 23
[129] N. Liédana, A. Galve, C. Rubio, C. Téllez, J. Coronas, *ACS Appl. Mater. Interfaces* 4 (2012) 5016
[130] H. Bux, F. Liang, Y. Li, J. Cravillon, M. Wiebcke, J.R. Caro, *J. Am. Chem. Soc.* 131 (2009) 16000
[131] A. Huang, H. Bux, F. Steinbach, J. Caro, Angew. *Chem., Int. Ed.* 49 (2010) 4958
[132] A. Huang, W. Dou, J. Caro, *J. Am. Chem. Soc.* 132 (2010) 15562
[133] A. Huang, J. Caro, Angew. *Chem., Int. Ed.* 50 (2011) 4979
[134] A. Huang, Y. Chen, N. Wang, Z. Hu, J. Jiang, J. Caro, *Chem. Commun.* 48 (2012) 10981
[135] S.R. Venna, M.A. Carreon, *J. Am. Chem. Soc.* 132 (2009) 76

[136] X. Dong, Y.S. Lin, *Chem. Commun.* 49 (2013) 1196
[137] X. Dong, K. Huang, S. Liu, R. Ren, W. Jin, Y.S. Lin, *J. Mater. Chem.* 22 (2012) 19222
[138] Y.S. Li, F.Y. Liang, H. Bux, A. Feldhoff, W.S. Yang, J. Caro, *Angew. Chem., Int. Ed.* 49 (2010) 548
[139] Y. Li, F. Liang, H. Bux, W. Yang, J. Caro, *J. Membr. Sci.* 354 (2010) 48
[140] H. T. Kwon, H.-K. Jeong, *Chem. Commun.* 49 (2013) 3854
[141] N. Hara, M. Yoshimune, H. Negishi, K. Haraya, S. Hara, T. Yamaguchi, *J. Membr. Sci.*450 (2014) 215

Chapter 2
Mordenite nanocrystal-layered membrane preparation

2.1. Introduction

In chemical processes, liquid mixtures are usually separated by distillation, which utilizes the vapor-liquid equilibrium difference. Purification of chemicals derived from biomass, such as ethanol, acetic acid, and acetone [1], requires a distillation column with a large number of plates and a high reflux ratio, plus a complex process for purification of azeotropes, which consumes a large amount of energy. Thus, a new high-purity, low-energy consumption separation process is needed. A pervaporation technique is a promising technique to achieve this goal.

Pervaporation using zeolite membranes has been studied because of the greater chemical and hydrothermal stability of the zeolite membranes compared to polymer membranes [2, 3]. Permeability of water through several types of zeolite membranes, *e.g.*, zeolite A [4-6], ZSM-5 [7-11], mordenite [12-14], and others [15-17], from a water/organic solution has been investigated. Water molecules in the solution adsorb into the membrane, permeate through it, and are removed as vapor. Therefore, the hydrophilic properties of the membrane, *e.g.*, Si/Al ratio of zeolites, are important because water separation depends on selective adsorption to the hydrophilic sites of the membrane [18]. However, for zeolites containing Al_2O_3, dealumination proceeds in acidic solutions, decreasing the separation factor due to generation of defects with long-term use.

In these zeolite membranes, because mordenite possesses resistance to acidic solutions [19], a mordenite membrane is a promising candidate as the separation membrane for acidic solutions [12, 13]. The high concentration of Al within the framework of the mordenite structure allows the mordenite membrane to separate water from water-acetic acid mixtures due to its high hydrophilicity.

The main objective of the present study was to prepare a mordenite membrane and investigation of its ability to separate water from water/organic solutions by pervaporation. We have previously reported the preparation of a silicalite-1 membrane composed of silicalite-1 protection layer, silicalite-1 nanocrystal layer and porous alumina filter [20, 21], in which the application of nano-sized silicalite-1 crystal as a

seed crystal was effective in improving the membrane performance. Compared with the dense membrane prepared by in situ hydrothermal synthesis methods, the water flux of the layer membrane prepared using the nanocrystals with a diameter of 60 nm was approximately 100 times high. In the present study, nano-sized mordenite crystals [22] were used as the seeds.

2.2. Experimental

2.2.1. Nanometer size Mordenite crystals synthesis

Mordenite nanocrystals (Si/Al=12.5) approximately 120 nm in size were prepared *via* hydrothermal synthesis in a water-surfactant-oil solution. An aqueous solution containing Si and Al was prepared by hydrolysis of tetraethylorthosilicate (Si source, Wako Chemicals) and aluminum isopropoxide (Al source, Wako Chemicals) with a dilute aq. tetraethyl-ammonium-hydroxide (TEA-OH) solution (Wako Chemicals) at room temperature. Polyoxyethylene-(15)-oleyl ether (O-15, Nikko Chemicals) and cyclohexane were employed as a surfactant and organic solvent, respectively.

2.2.2. Preparation of mordenite nanocrystal-layered membranes

A cylindrical alumina ceramic filter (NGK insulators, LTD.) was used as a membrane support. The inner and outer diameters and the length of the filter were 6 mm, 11 mm, and 50 mm, respectively. This filter was constructed in two porous regions; the pore diameter of the inner region was about 2-3 μm (rough region), and the outer region was dense and its pore diameter was 0.1μm. The filter was immersed in a 0.1 N hydrochloride solution for 6 h, and washed in distilled water. The mordenite nanocrystals were dispersed ultrasonically in an alkaline (approximately pH 12) aqueous solution at a concentration between 0.58 and 14.5 $g \cdot m^{-3}$. The dispersed nanocrystals were layered on the outer surface of cylindrical alumina ceramic filters using a filtration method under low-pressure vacuum on the permeate side. The thickness of the nanocrystal layer is from 0.8 to 20 μm. To protect the nanocrystal layer against mechanical shock, a protection layer with micrometer-sized mordenite was formed hydrothermally (secondary growth) on the nanocrystal layer without organic structure directing agents (OSDA). Aqueous solutions (mother liquid) containing Si and Al sources prepared by of tetraethylorthosilicate and aluminum isopropoxide were used to form the protection layer and the molar composition were:

SiO_2:Na_2O:Al_2O_3:H_2O=1:0.32:0.04:111. Then the alumina filter with a mordenite nanocrystal layer was immersed in the precursor solution and heated to 180 °C and kept at the hydrothermal temperature for 12 h to form the protection layer on the nanocrystal layer.

2.2.3. Analysis methods

The powders obtained in the solution during hydrothermal synthesis for the protection layer of mordenite membrane were characterized by X-ray diffraction (XRD, JEOL JDX-8030) and X-ray Fluorescence Analysis (XRF, Rigaku Supermini) for the detection of the Si/Al ratio in the mordenite crystals. The membrane morphology was characterized by scanning electron microscopy (SEM, JEOL JSM-6500F).

2.2.4. Pervaporation trials

Pervaporation experiments were conducted using a conventional method at temperatures ranging from 60 to 100 °C using the stainless-steel autoclave vessel shown in Fig. 2.1. Water/organic solutions (organic solvent: ethanol, iso-propanol or acetic acid) were used as feed solutions for the pervaporation experiment.

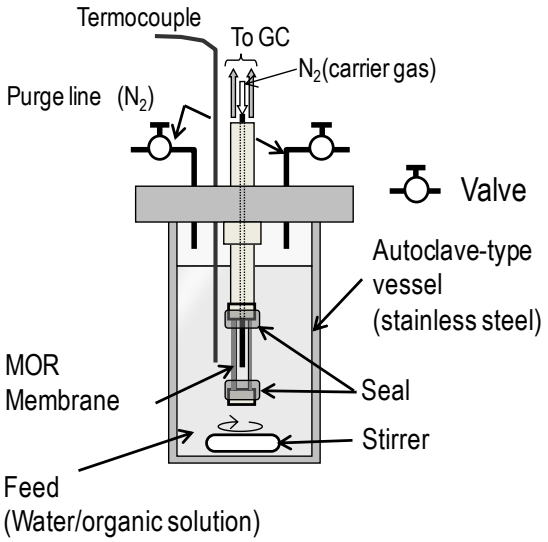

Figure 2.1 Schematic of the stainless steel autoclave vessel used for pervaporation experiments

The new water/organic solutions were used at each pervaporation temperature. The acid-stability of the membranes was checked by pervaporation experiments using water/acetic acid mixture (acetic acid concentration is 90 wt %) as a feed solution. The water/acetic acid solution was renewed at every 6 h and the whole pervaporation experiments were continuous to carry out for 32.6 h. After the membrane was immersed in the feed solution, nitrogen was fed into the gas phase of the vessel at room temperature to replace the air. The vessel was then heated to pervaporation temperatures. Molecules that permeated through the membrane were swept out with the nitrogen. The composition of the exit gas obtained from the permeate side of the membrane was analyzed using an on-line gas chromatograph equipped with a Porapak-Q column and TCD and FID detectors. The procedure has been described in detail previously [20, 21] The separation factor, α, is defined as:

$$\alpha = \frac{F_w / F_o}{C_w / C_o} \qquad \text{(Eq. 2.1)}$$

where F_w and F_o are the molar flux of water and organic solvent on the permeate side, respectively, and C_w and C_o are the molar concentrations of water and organic solvent, respectively, on the feed side. The total amount of water and organic solvent permeating through the membrane during each experiment was less than 3%. Accordingly, the initial concentrations of C_w and C_o were used to calculate the separation factor.

The permeance, P_i, is defined as:

$$P_i = \frac{F_i}{C_i} \qquad \text{(Eq. 2.2)}$$

F_i is the molar flux of water or organic molecules that permeate through the mordenite nanocrystal-layer membrane and C_i stands for the molar concentration of water or organic solvent in the feed side solution. The permeance indicated the permeability of the component (water or organic molecules) in the organic solution through the mordenite nanocrystal-layer membrane.

2.3. Results and Discussion

2.3.1 Mordenite nanocrystal-layered membrane preparation

Fig. 2.2 shows FE-SEM photographs of a surface area (A) and a cross-sectional area (B) of mordenite nanocrystal-layered membrane in which the protection layer was formed at a hydrothermal temperature of 180 °C and hydrothermal period of 12 h. A

protection layer with micrometer-sized crystals was formed on the nanocrystal layer with a thickness of about 5μm. The crystal size in the protection layer was much larger than that in the nanocrystal layer, indicating that secondary growth of mordenite nanocrystals occurred during formation of the protection layer.

The Fig. 2.2 (c) shows the magnified areas between the nanocrystal layer and the protection layer of the membrane. From the photograph, the crystals consisted in the protection layer of the membrane were grew from the nanocrystal consisted in the first layer and the place between the nanocrystal layer and the protection layer of the membrane is the most compact area.

In order to prepare the membrane with separation ability, the membrane preparation conditions such as the thickness of the membranes, the hydrothermal synthesis time were discussed, respectively.

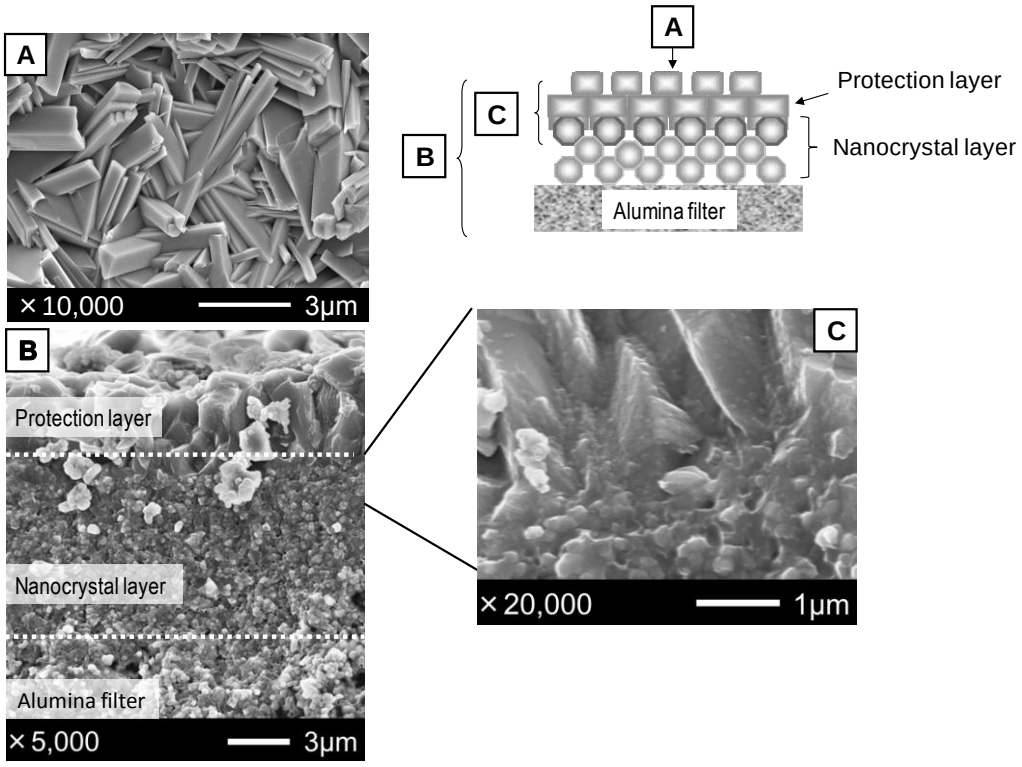

Figure 2.2 FE-SEM photographs of mordenite nanocrystal-layered membranes (A) top view, (B) cross-sectional area, and (C) magnified view of the indicated area.

2.3.2. Performance of mordenite nanocrystal-layered membranes in the pervaporation experiment

In order to check the pervaporation performances of the membrane prepared in last section, the membrane was used for separation the ethanol/water solutions (the weight percentage of ethanol: 90 wt %) and the feed temperature was 80 °C. Fig. 2.3 shows the permeance of the water and organics through the membrane and the separation factor during pervaporation experiment according to the pervaporation time.

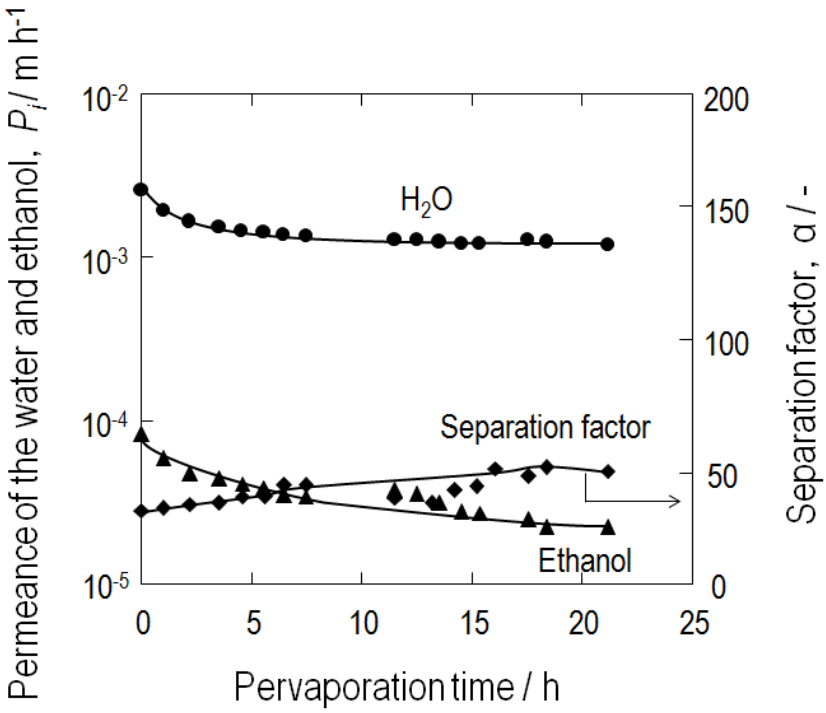

Figure 2.3 Permeance of the water and ethanol through the membrane and the changes of separation factors according to the pervaporation time.

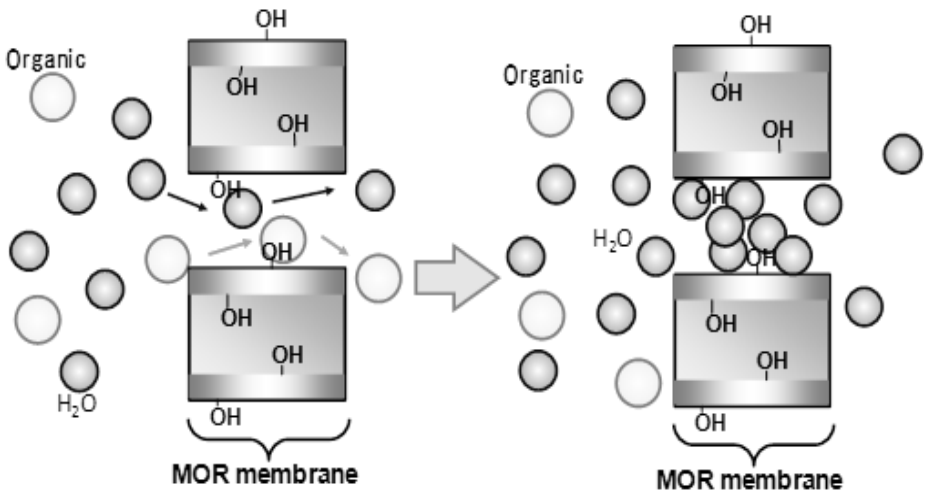

Figure 2.4 Formation of the water-acid site network.

From Fig. 2.3, it can be concluded that the membrane possesses the water separation ability and as times go on, the separation factor was increasing and keep stable after the 15 h. As shown in Fig. 2.4, it was considered that the water molecules permeate through the mordenite nanocrystal-layered via membrane water-acid site networks because water molecules have high polarity and selectively adsorb on the acid site of mordenite. The separation factors of the membrane keep stable indicates the finishing of the formation of the water-acid site networks after 15 h of pervaporation experiment. Therefore, the pervaporation data obtained in the follow sections were detected in the stable condition.

2.3.3 Effect of nanocrystal layer thickness on membrane preparation

Nanocrystal layer makes the connection between the alumina filter and the protection layer, and it is an important part which decides the membrane qualities. In order to check the optimization membrane preparation condition, membranes with nanocrystal layer thicknesses of (a) 0.8, (b) 4, (c) 8 and (d) 20 μm were prepared, respectively. The layer thickness was controlled by varying the concentration of nanocrystals in the water solution while loading the alumina filter. Fig. 2.5 presents cross-sectional FE-SEM images of the resulting membranes and Fig. 2.6 shows the effect of nanocrystal layer thickness in MOR membranes on water flux and separation ability from water/iso-propanol solutions at the feed temperature of 80 °C. From Fig. 2.5, an MOR protection layer was evidently formed over the nanocrystal layer which with decided thickness of each membrane. According to Fig. 2.6, the separation factors increased as the thickness of the nanocrystal layer increased and keep stable until the thickness more than 4μm. In contrast, the water flux decreasing with increasing thickness and plateaued at thicknesses above 4 μm. This result indicated that both the flux and separation ability were keep stable when the thickness of the nanocrystal layer equal to 4 μm or 8 μm.

On the other hand, the membrane formed was found easily falling off when the thickness of the nanocrystal layer equal to 20 μm. From the results above, MOR membranes approximately between 4 μm to 8 μm thick appear to possess adequate separation ability when applied to the pervaporation of water/iso-propanol mixtures. In order to make unification for comparison, the membranes discussed below were prepared with the nanocrystal thickness of 8 μm.

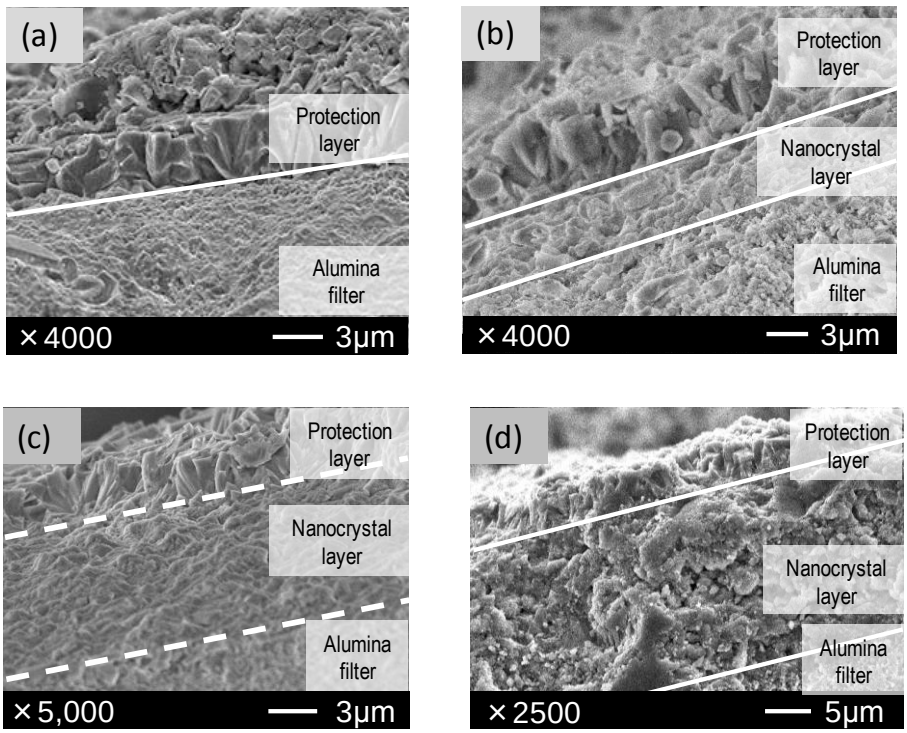

Figure 2.5 FE-SEM images of nanocrystal- layered MOR membranes prepared with different thickness of (a) 0.8μm, (b) 4μm, (c) 8μm, and (d) 20μm.

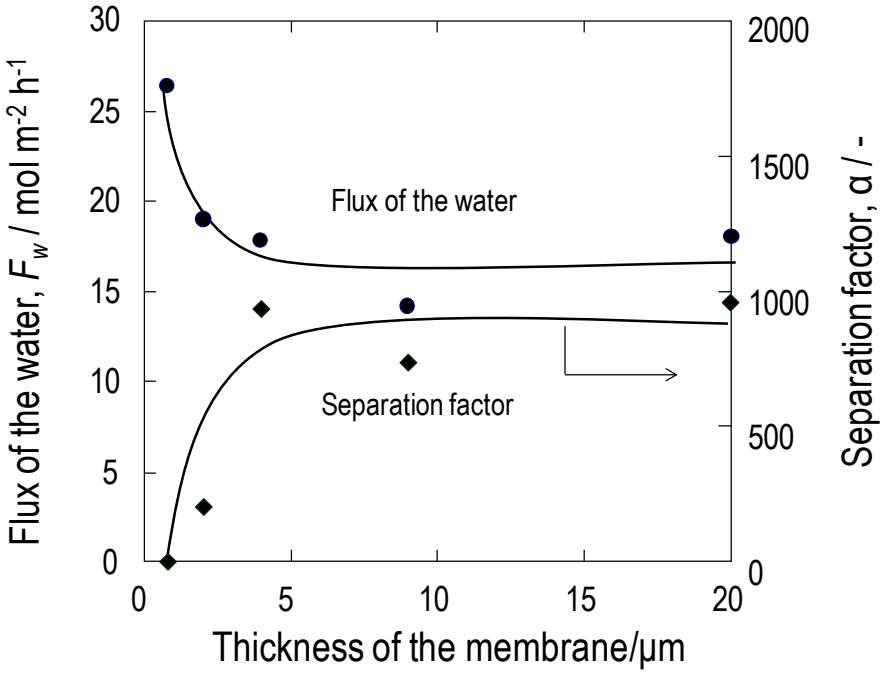

Figure 2.6 Effect of nanocrystal layer thickness in MOR membranes on water flux and separation ability from water / 2-propanol solutions.

2.3.4. The acid-stability of the mordenite membrane

As mention above, the mordenite possesses resistance to the acidic solution. The membrane acid stability was examined by separation of water from acetic acid/water solution (acetic acid concentration is 90 wt %) by pervaporation. The membrane was prepared at the hydrothermal temperature of 180 °C. Table 3 shows the water flux and separation factor of the membrane during the pervaporation experiment at 100 °C. As shown in the table, the membrane maintained the separation performance for 32.6 h even at the high acetic acid concentration. Li et al. [13] did the same pervaporation experiment to test the acid stability of the mordenite membranes. A separation factor of 50 was obtained when the membrane used for separating water from water/acetic acid mixtures (acetic acid concentration is 90 wt %). Compared with the A-type zeolite membranes, although lower in the water fluxes and separation factors, the acid stability makes mordenite membranes good candidates for the separation of acid mixtures and wide usage in organic dehydration.

Table 2.1 Pervaporation experiments for separation water from acetic acid/water mixtures.

Pervaporation time period (h)	5.8	12.3	25.8	32.6
Water flux through the membrane (kg $m^{-2}h^{-1}$)	0.179	0.195	0.159	0.133
Separation factor (-)	83	90	138	158

* Feed: acetic acid/water solution (90 wt %), pervaporation temperature: 100 ˚C.

3.4. Conclusions

Mordenite nanocrystal-layered membranes were successfully prepared using the secondary growth method. Mordenite nanocrystals were laminated onto an alumina filter and a mordenite protection layer was clearly formed on the nanocrystal layer. The effect of nanocrystal layer thickness was discussed to determine the appropriate condition for membrane preparation. The membrane acid stability was examined by separation of water from acetic acid/water solution (acetic acid concentration is 90

wt %) by pervaporation.

References

[1] S. Funai, T. Tago, T. Masuda, *Catal. Today* 164 (2011) 443
[2] R.W. Baker, Membrane Technology and Applications, Chapter 9 Pervaporation, McGraw-Hill, 2000
[3] F. Mizukami, *Study in Surface Science and Catalysis* 125 (1999) 1
[4] H. Kita, K. Horii, Y. Ohtoshi, K. Tanaka, K. Okamoto, *J. Mater. Sci. Lett.* 14 (1995) 206
[5] M. Kondo, M. Komori, H. Kita, K. Okamoto, *J. Membr. Sci.* 133 (1997) 133
[6] K. Okamoto, H. Kita, K. Horii, K. Tanaka, M. Kondo, *Ind. & Eng. Chem. Res.* 40 (2001) 163
[7] T. Sano, M. Hasegawa, Y. Kawakami, H. Yanagishita, *J. Membr. Sci.* 107 (1995) 193
[8] G. Li, E. Kikuchi, M. Matsukata, *Micropor. Mesopor. Mater.* 62 (2003) 211
[9] M. Noack, P. Kolsch, J. Caro, M. Schneider, P. Toussaint, I. Sieber, *Micropor. Mesopor. Mater.* 35 (2000) 253
[10] T. Sano, H. Yanagishita, Y. Kiyozumi, F. Mizukami, K. Haraya, *J. Membr. Sci.* 95 (1994) 221
[11] T. Masuda, S. Otani, T. Tsuji, M. Kitamura, S.R. Mukai, *Sep. Purif. Technol.* 32 (2003) 181
[12] X. Lin, E. Kikuchi, M. Matsukata, *Chem. Comm.* 11 (2000) 957
[13] G. Li, E. Kikuchi, M. Matsukata, *Sep. Purif. Technol.* 32 (2003) 199
[14] A. Navajas, R. Mallada, C. Téllez, J. Coronas, M. Menéndez, J. Santamaría, *J. Membr. Sci.*270 (2006) 32
[15] Y. Cui, H. Kita, K. Okamoto, *J. Membr. Sci.* 236 (2004) 17
[16] T. Nagase, Y. Kiyozumi, Y. Hasegawa, T. Inoue, T. Ikeda, F. Mizukami, *Chem. Lett.* 36 (2007) 594
[17] Y. Kiyozumi, Y. Nemoto, T. Nishide, T. Nagase, Y. Hasegawa, F. Mizukami, *Micropor. Mesopor. Mater.* 116 (2008) 485
[18] J. Čejka, J. van Bekkum, A. Corma, F. Schuth, Characterization and Application, Elsevier, 2007
[19] K. Sato, K. Sugimoto, T. Kyotani, N. Shimotsuma, T. Kurata, *J. Membr. Sci.* 385 (2011) 20
[20] T. Tago, Y. Nakasaka, A. Kayoda, T. Masuda, *Sep. Purif. Technol.* 58 (2007) 7

[21] T. Tago, Y. Nakasaka, A. Kayoda, T. Masuda, *Micropor. Mesopor. Mater.* 115 (2008) 176
[22] T. Tago, D. Aoki, K. Iwakai, T. Masuda, *Topics in Catal.* 52 (2009) 865

Chapter 3
Optimization of Mordenite Nanocrystal-layered Membrane for Dehydration by Pervaporation

3.1. Introduction

Compared with polymer membrane, there are lots of merits of zeolite membrane such as the stability in the high temperature and acid solution.

There are various methods to improve the performance of zeolite membranes such as use the new method for membrane preparation, the use of the new supports [1], improving the synthesis condition for membrane formation [2], decrease the thickness of the membrane [3], the control of the size or orientation of the crystals of the membranes.

A pre-aging treatment, which is defined as the mixing of reagents before onset of heating to crystallization temperature, can control the morphology and size of the zeolite crystals [4]. Chen et al. [5] reported morphology control of the zeolite crystal by a pre-aging treatment during preparation of a silicalite membrane.

The Mordenite nanocrystal-layered membranes consisting of a mordenite nanocrystal layer and protection layer were successfully prepared in last section. The main objective of the present study was to discuss the separation mechanism of the zeolite membrane and improve the performance of the zeolite membrane such as membrane permeability and separation ability. It is considered the pre-aging temperature of the mother liquid and the heating rate for formation of the protection layer affected the secondary growth process that formed the protection layer, leading to different morphologies and sizes of the crystals in the protection layer. Water flux increased with decreasing crystal size in the protection layer because the number of non-zeolitic pores among the mordenite crystal increased as the crystal size decreased.

3.2. Experimental

3.2.1. Preparation of mordenite nanocrystal-layered membranes

Mordenite nanocrystals (Si/Al=12.5) approximately 120 nm in size were prepared by the same method refer in chapter 2 (2.2.1. Nanometer size Mordenite crystal synthesis).

A cylindrical alumina ceramic filter (NGK insulators, LTD.) was used as a membrane support. The inner and outer diameters and the length of the filter were 6 mm, 11 mm, and 50 mm, respectively. This filter was constructed in two porous regions; the pore diameter of the inner region was about 2-3 μm (rough region), and the outer region was dense and its pore diameter was 0.1μm. The filter was immersed in a 0.1 N hydrochloride solution for 6 h, and washed in distilled water. The mordenite nanocrystals were dispersed ultrasonically in an alkaline (approximately pH 12) aqueous solution at a concentration of 5.8 $g \cdot m^{-3}$. The dispersed nanocrystals were layered on the outer surface of cylindrical alumina ceramic filters using a filtration method under low-pressure vacuum on the permeate side. The thickness of the nanocrystal layer is about 8μm. To protect the nanocrystal layer against mechanical shock, a protection layer with micrometer-sized mordenite was formed hydrothermally (secondary growth) on the nanocrystal layer without organic structure directing agents (OSDA). An aqueous solution (mother liquid) containing Si and Al sources prepared by of tetraethylorthosilicate and aluminum isopropoxide was used to form the protection layer and the molar composition was: SiO_2:Na_2O:Al_2O_3:H_2O=1:0.32:0.04:111. The aqueous solution was stirred at room temperature, 60 °C and 80 °C for 24 h, as pre-aging treatment. Then the alumina filter with a mordenite nanocrystal layer was immersed in the precursor solution and heated to 150-200 °C with heating rate of 4.2-8.3 °C/h and kept at the hydrothermal temperature for 0-12 h to form the protection layer on the nanocrystal layer.

3.2.2. Analysis methods

The powders obtained in the solution during hydrothermal synthesis for the protection layer of mordenite membrane were characterized by X-ray diffraction (XRD, JEOL JDX-8030) and X-ray Fluorescence Analysis (XRF, Rigaku Supermini) for the detection of the Si/Al ratio in the mordenite crystals. The membrane morphology and composition (Si/Al ratio) were characterized by scanning electron microscopy (SEM, JEOL JSM-6500F) and energy dispersive X-ray spectroscopy (EDS, JEOL JSM-6510LA), respectively.

3.2.3. Pervaporation trials

Pervaporation experiments were conducted using a conventional method at temperatures ranging from 60 to 100 °C using the stainless-steel autoclave vessel shown in Fig. 1. Water/organic solutions (organic solvent: ethanol, iso-propanol, acetone, or acetic acid) were used as feed solutions for the pervaporation experiment. Concentrations of the water/organic solutions and dielectric constants of organic solvents used are listed in Table 1. The new water/organic solutions were used at each pervaporation temperature. After the membrane was immersed in the feed solution, nitrogen was fed into the gas phase of the vessel at room temperature to replace the air. The vessel was then heated to pervaporation temperatures. Molecules that permeated through the membrane were swept out with the nitrogen. The composition of the exit gas obtained from the permeate side of the membrane was analyzed using an on-line gas chromatograph equipped with a Porapak-Q column and TCD and FID detectors. The procedure has been described in detail previously [9, 10].

Table 3.1 Apparent activation energy of the water flux through a mordenite nanocrystal-layered membrane from a water/organic solvent solution and the dielectric constant of the organic solvents.

Organic solvent	Organic concentration in solution (wt%)	Dielectric constant (-)**	Apparent activation energy ($kJ \cdot mol^{-1}$)
ethanol	90	25.02 [6]	38
acetone	90	19.56 [7]	30
iso-propanol	88	18.62 [7]	32
acetic acid	90	6.15 [6]	41
water*	—	80.1 [8]	38

*Apparent activation energies of water flux through the membranes from water (without organic solvent)

** The dielectric constant at 20 ºC

The separation factor, α, is defined as:

$$\alpha = \frac{F_w / F_o}{C_w / C_o} \quad (1)$$

where F_w and F_o are the molar flux of water and organic solvent on the permeate side, respectively, and C_w and C_o are the molar concentrations of water and organic solvent, respectively, on the feed side. The total amount of water and organic solvent permeating through the membrane during each experiment was less than 3%. Accordingly, the initial concentrations of C_w and C_o were used to calculate the separation factor.

The permeance, P_i, is defined as:

$$P_i = \frac{F_i}{C_i} \qquad (2)$$

F_i is the molar flux of water or organic molecules that permeate through the mordenite nanocrystal-layer membrane and C_i stands for the molar concentration of water or organic solvent in the feed side solution. The permeance indicated the permeability of the component (water or organic molecules) in the organic solution through the mordenite nanocrystal-layer membrane.

3.3. Results and Discussion

3.3.1. Effect of hydrothermal temperature on membrane preparation

The effect of the hydrothermal temperature on mordenite protection layer formation and its separation properties was examined to determine the appropriate hydrothermal temperature. Hydrothermal temperatures of 150, 180, and 200 °C were used for the formation of the protection layer. Fig. 3.1 shows the XRD patterns of the powder samples obtained during protection layer formation and commercial mordenite. Powder samples synthesized at 150 °C and 180 °C showed the same pattern as the commercial mordenite. On the other hand, the powder sample synthesized at 200 °C possessed low crystalline mordenite containing an impurity phase which was ascribed to moganite type crystal, indicating that there was a possibility to form other crystal types in the protection layer during the synthesis. In some cases, the structure of the powder is not exactly the same as the crystals constituting the membrane layer [11]. Accordingly, all of these membranes were used for separation of water from a water/2-propanol solution by pervaporation at 80°C and water fluxes and separation factors are listed in Table 3.2. From the table, all of the membranes possess the water separation ability and the separation factor are more than 500 in each membrane, and the membrane synthesized at 180 °C exhibited better separation properties and permeability compared with the membrane obtained at 150 °C and 200°C. Therefore, all of the membranes discussed below were prepared at the hydrothermal temperature of 180 °C

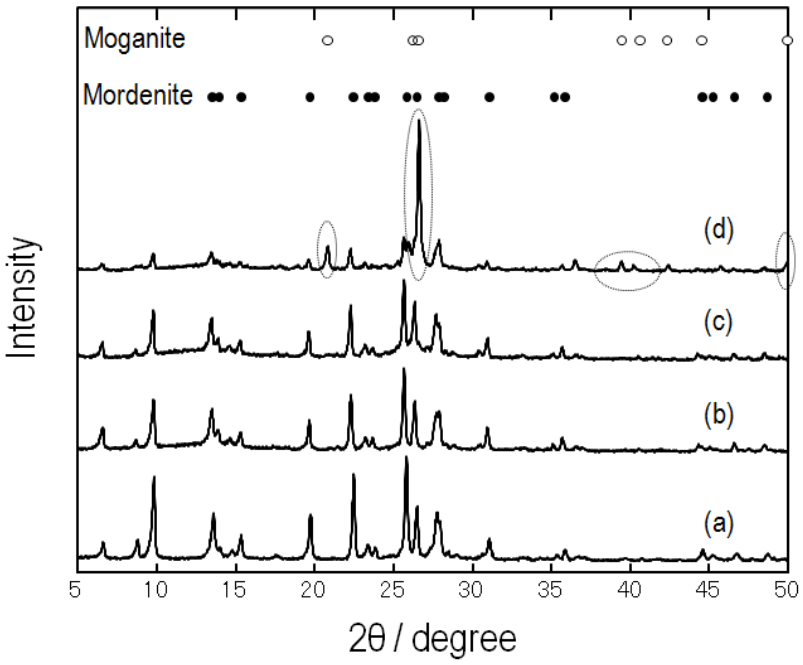

Figure 3.1 XRD patterns of (a) commercial mordenite, and powders obtained in solution after protection layer formation at (b) 150˚C (c) 180˚C and (d) 200˚C.

Table 3.2 Effect of hydrothermal temperature on membrane separation property from water/2-propanol solution.

Pre-aging		Hydrothermal synthesis conditions				Water flux through the membrane (kg $m^{-2}h^{-1}$)	Separation factor (-)
Temperature (^oC)	Period (h)	Heating Rate (^oC/h)	Heating Period (h)	Hydrothermal Temperature (^oC)	Hydrothermal Period (h)		
R.T.	24	5.0	24	150	12	0.199	648
R.T.	24	6.3	24	180	12	0.254	734
R.T.	24	7.1	24	200	12	0.186	538

* Feed: iso-propanol/water solution (88 wt %), pervaporation temperature:80 ˚C

3.3.2. Effect of organic polarity in feed on water and organic solvent permeation

Water molecules permeate through the mordenite nanocrystal-layered via membrane water-acid site networks because water molecules have high polarity and selectively adsorb on the acid site of mordenite. Meanwhile, polar organic molecules, which have high affinity with acidic sites, affect the permeance of organic solvents and the separation factor. To investigate the effect of organic solvent polarity on the permeance of water and organics through the membrane, dielectric constants were used to evaluate the polarity of the organic solvents. Dielectric constants of each organic solvent are listed in Table 3.1. A greater dielectric constant value indicates greater polarity.

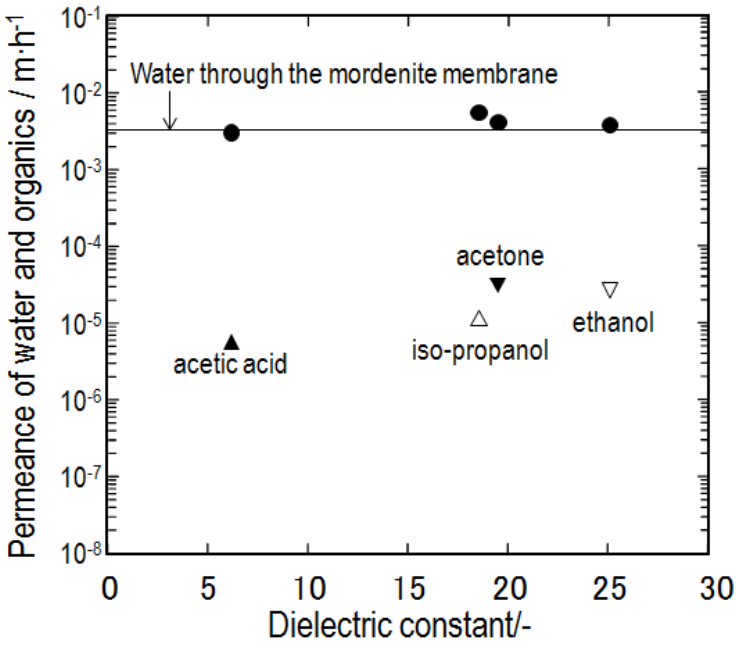

Figure 3.2 Permeance of water (circles) and organic molecules (triangles) through a mordenite nanocrystal-layered membrane. The solid line is water permeance from water (without organics) through the mordenite nanocrystal-layered membrane.

Figure 3.2 shows the relationship between the permeance of each component through the mordenite nanocrystal-layered membrane and the dielectric constant of the organic solvent. The greater water permeance of nearly 10^3 times than organic molecules in all of the water/organic systems proved that the mordenite

nanocrystal-layered membrane possess high water separation ability from the mixtures. Since the high Al element existed in mordenite zeolite structure generated high hydrophilicity, water molecules have higher affinity to the mordenite surface compared with organic molecules. Moreover, water permeance from a water/organic solution through a membrane was identical regardless of the organic solvent in the feed, and exhibited nearly the same value as the permeance of water through a membrane from a pure water solution (*i.e.*, without organic solvent), indicating that the dominant mechanism of the permeation of water is the same regardless of coexisting organic molecules.

Table 3.1 shows the apparent activation energies of water flux through the membranes from the water/organic solutions. The apparent activation energies of water flux through the membranes from pure water (without an organic solvent) are also showed for comparison. The apparent activation energies of water flux through the mordenite nanocrystal-layered membrane were similar regardless of the organic solvent in the feed and were close to the apparent activation energy of water flux through the membrane from a pure water feed. The apparent activation energy of water flux through the hydrophilic silicalite-1 nanocrystal-layered membrane from water/acetone solution (acetone concentration is 90 wt %) [9, 10] was 35 kJ/mol and the value was similar to that of the mordenite nanocrystal-layered membrane. In the hydrophilic silicalite-1 nanocrystal-layered membrane, water-silanol networks that formed on non-zeolitic pore spaces among the crystals acted as the main channel for water permeation, and the interface between the nanocrystal layer and protection layer was important for the separation because this area became the densest area in the membrane [10]. Since the mordenite membrane was prepared by the same procedure as the silicalite-1 membrane [10], it was considered that there were some non-zeolitic pores among the crystals. During the pervaporation to separate water from water/organic mixtures, water molecules were adsorbed on the surfaces of zeolitic and non-zeolitic pores. As compared with silanol groups on the surface of silicalite-1 crystal, the affinity of water molecules to the surface of mordenite crystal was much higher due to the strong ionic sites. However, since the mordenite membrane showed almost the same activation energy as the slilicalite-1 membrane, the non-zeolitic pores among the crystals, on which the water adsorption layer was formed, were the important channel for water permeation. The water molecules can diffuse through the non-zeolitic pore surrounded by the water adsorption layer, and consequently the size of non-zeolitic pores mainly affects the separation properties.

3.3.3 Effects of pre-aging and heating rate for synthesis of the protection layer on performance of mordenite nanocrystal-layered membranes

Ideally, the zeolite membranes must be continuous with good cross-linking between crystals and free of pinholes and cracks to get high selectivities. However, most of the synthesis procedures render membranes with some intercrystalline gaps and defects [12, 13]. The amount of these crystals and their sizes play an important role in the overall quality of the membranes [14]. It is suggested that the non-zeolitic pores have size distributions and the pores smaller than the zeolite pores may also affect flux and selectivity [15]. Moreover, some studies showed that the non-zeolitic pores are selective for some mixtures and pervaporation separations even positively affected by non-zeolitic pores [16].

In order to investigate the effect of the non-zeolitic pores on membranes quality, mordenite nanocrystal-layered membranes at conditions of hydrothermal period of 0, 12 and 24 h were prepared. Table 3.3 shows the results of membrane performance of water flux and separation factor as a function of hydrothermal period. In the case of M1, though prepared without hydrothermal period, the membrane exhibited the separation ability. Moreover, the separation factor of membranes (M1, M2, and M3) increased with increasing the hydrothermal period, implying that non-zeolitic pores were exist among the crystals and that the size of the non-zeolitic pore decreased to the appropriate size for water separation. On the other hand, the long hydrothermal period led to the excessive secondary growth of zeolite, thereby resulting in the decrease in water flux. Such an appropriate pore space was expected to be formed around the interface between the nanocrystal and protection layers [10].

The morphology and crystal size around the interface formed by hydrothermal synthesis are the important factors affecting the membrane permeability and separation ability. There are two parameters by which to modify the crystal growth during the secondary growth; the pre-aging treatment of the mother liquid and the heating rate to the hydrothermal temperature. To achieve high flux of water and high separation ability, the effects of pre-aging temperature and the heating rate on the crystal morphology and membrane performance were examined. The pre-aging temperatures of room temperature, 60 °C, and 80 °C with a pre-aging time of 24 h were tested for protection layer formation. After the autoclave temperature reached 180 °C, hydrothermal treatment to form the protection layer (secondary growth) was stopped. Table 3.3 shows the experimental conditions used for protection layer formation and the separation properties of the membranes using a water/iso-propanol solution. Compared with

pre-aging at room temperature (M1), the mordenite membrane prepared using a higher pre-aging temperature had a greater separation factor. On the other hand, compared with 24 h hydrothermal period (M3), the mordenite membrane (M5) showed higher water fluxes meanwhile nearly the same separation factor above 1000.

Table 3.3 Experimental conditions for formation of the protection layer and separation properties of the membranes prepared.

Sample	Pre-aging		Hydrothermal synthesis conditions			Pervaporation temperature					
						60 °C		80 °C		100 °C	
	Temperature (°C)	Period (h)	Heating rate (°C/h)	Heating Period (h)	Hydrothermal Period (h)	F_w [a]	a [b]	F_w [a]	a [b]	F_w [a]	a [b]
M1	R.T.	24	6.3	24	0	0.147	420	0.383	400	0.459	130
M2	R.T.	24	6.3	24	12	0.137	1200	0.254	730	0.454	470
M3	R.T.	24	6.3	24	24	0.126	1800	0.237	1200	0.423	1000
M4	60	24	5.0	24	0	0.293	570	0.482	330	0.664	170
M5	80	24	4.2	24	0	0.322	1420	0.455	1370	0.597	1170
M6	80	24	6.3	16	0	0.435	1920	0.806	2020	1.013	2600
M7	80	24	8.3	12	0	> 1	—	> 1	—	> 1	—

* Feed: iso-propanol/water solution (88 wt %)

a: water flux through the membrane (kg $m^{-2}h^{-1}$).

b: separation factor (-).

Figure 3.3 shows FE-SEM photographs of mordenite nanocrystal-layered membranes in which the protection layer was hydrothermally synthesized after pre-aging of the mother liquid. The crystal size of the mordenite in the protection layer became slightly smaller by increasing the pre-aging temperature from room temperature (M1) to 80 °C (M5). As pre-aging temperature increased, the concentration of the mordenite precursor increased, leading to a small crystal size of mordenite in protection layer. Moreover, increasing the mordenite precursor may improve the crystallinity of mordenite in the protection layer as well as the separation ability of the membrane.

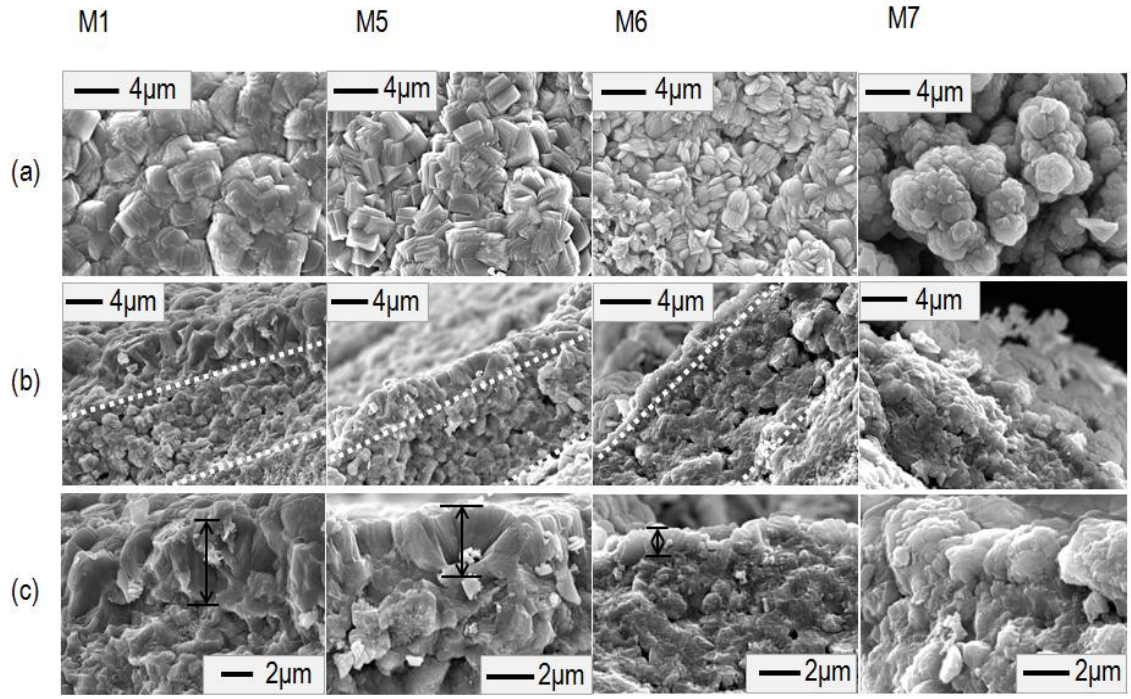

Figure 3.3 FE-SEM photographs of mordenite nanocrystal-layered membranes, containing a protection layer synthesized after pre-aging of the mother liquid: (a) top view, (b) cross-sectional area, and (c) interface area by large magnification.

In the next step, the effect of the heating rate from pre-aging temperature to 180°C during hydrothermal synthesis for protection layer formation was examined. Water flux as well as separation factor increased with heating rate from 4.2°C/h (M5) to 6.3°C/h (M6) and M6 showed a separation factor greater than 1900 at each pervaporation temperature. The Si/Al ratios in the protection layer of the membranes (M1, M5 and M6) are listed in Table 3.4. In all membranes, the Si/Al ratios of the protection layer are smaller than the Si/Al ratios of the obtained powder after hydrothermal synthesis. This is probably because the seed mordenite crystal preferentially enhanced the crystal growth with higher Al concentration in the frameworks [17]. On the other hand, the Si/Al ratios of the protection layer among these membranes showed almost the same values (Si/Al=5.6~6.5). So these membranes possess almost the same hydrophilicity. By increasing the heating rate to 8.3°C/h (M7), the obtained membrane showed no separation ability. As shown in Fig. 5, micrometer-size mordenite crystals were clearly

formed on the nanocrystal layer in membranes M5 and M6. In contrast, the protection layer was not successfully formed in the case of M7 because large pore spaces were observed from the top view of the membrane, leading to no separation ability. It is considered that the hydrothermal synthesis time was too short to form a protection layer dense enough for pervaporation due to insufficient crystal growth. From the top view of the membranes M5 and M6, crystal size in protection layer was decreased by increasing heating rate. By decreasing crystal size in the protection layer, the number of non-zeolitic pores among the mordenite crystals increased, leading to an increase in water flux. In addition, it is considered that the pore space of the interface between nanocrystal layer and protection layer, which is an important area for separation, became small enough to selectively separate water from a water/iso-propanol solution (iso-propanol concentration is 88 wt%). Furthermore, FE-SEM cross-sectional photographs showed that the thickness of the protection layer also decreased with increasing heating rate, which enhanced water flux due to the shorter diffusion length from the feed solution to the interface between the nanocrystal layer and protection layer. Compared with those of other reports [18-20], the mordenite nanocrystal-layered membranes prepared in this study exhibits almost the same as or higher in both of the water flux and separation factor. By pre-aging the mother liquid in the high temperature and increasing the heating rate for the protection layer formation, a high performance mordenite membrane with thin layer (protection layer about 1μm) could be successfully synthesized.

Table 3.4 Si/Al ratio of protection layer in mordenite membrane

Samples	Si/Al ratio of powder obtained in the solution during hydrothermal synthesis (mol%) *	Si/Al ratio of as-synthesized mordenite membrane (mol%) **
M1	10.3	6.48
M5	9.75	5.63
M6	8.87	5.87

* Analyzed by XRF

** Analyzed by EDS

3.4. Conclusions

Mordenite nanocrystal-layered membranes were successfully prepared using the secondary growth method. Mordenite nanocrystals were laminated onto an alumina filter and a mordenite protection layer was clearly formed on the nanocrystal layer. Four types of water/organic solvent solutions were prepared for pervaporation experiments using the mordenite nanocrystal-layered membranes. Permeance of water through the mordenite nanocrystal-layered membrane was similar regardless of the polarity of the organic solvent in the feed solutions however the permeances of the organic molecules depended on their polarities. The mechanisms of water permeation through the mordenite nanocrystal-layered membranes can be considered as the adsorbed water layer formed on both of the zeolitic pores and non-zeolitic pores among crystals for water permeation. The appropriate pore space was formed around the interface between the nanocrystal and protection layer which was expected to be the main separation area of the membranes. Formation of small size mordenite crystals in the protection layer enhanced the separation ability as well as permeability of the mordenite nanocrystal-layered membranes.

References

[1] J.J. Jafar, P.M. Budd, *Micropor. Mesopor. Mater.* 12 (1997) 305
[2] S. Li, V.A. Tuan, J.L. Falconer, R.D. Noble, *Micropor. Mesopor. Mater.* 53 (2002) 59
[3] Z.P. Lai, G. Bonilla, I. Diaz, J.G. Nery, K. Sujaoti, M.A. Amat, E. Kokkoli, O. Terasaki, R.W. Thompson, M.Tsapatsis, D.G. Vlachos, *Science* 300 (2002) 456

[4]Q. Li, B. Mihailova, D. Creaser, J. Sterte, *Micropor. Mesopor, Mater.* 43 (2001) 51
[5] H. Chen, C. Song, W, Yang, *Micropor. Mesopor, Mater.* 102 (2007) 250
[6] M.M. Nia, H. Amiri, J. Chem. Thermodynamics 57 (2013) 68
[7] G. Åkerlöf, *J. Amer. Chem. Soc.* 54 (11) (1932) 4125
[8] C.G. Malmberg, A.A. Maryott, Journal of Research of the National Bureau of Standards 56 (1) (1956) 2641
[9] T. Tago, Y. Nakasaka, A. Kayoda, T. Masuda, *Sep. Purif. Technol.* 58 (2007) 7
[10] T. Tago, Y. Nakasaka, A. Kayoda, T. Masuda, *Micropor. Mesopor, Mater.* 115 (2008) 176
[11] X. Li, H. Kita, H. Zhu, Z. Zhang, K. Tanaka, *J. Membr. Sci.* 339 (2009) 224
[12] A.K. Pabby, S.S.H. Rizvi, A.M. Sastre, Handbook of Membrane Separations, 2008, P289
[13] M. Nomura, T. Yamaguchi, S. Nakao, *J. Membr. Sci.* 187 (2001) 203
[14] T.C. Bowen, R.D. Noble, J.L. Falconer, *J. Membr. Sci.* 245 (2004) 15
[15] T.C. Bowen, H. Kalipcilar, J.L. Falconer, R.D. Noble, *J. Membr. Sci.*215 (2003) 235
[16] K. Okamoto, H. Kita, K. Horii, K. Tanaka, M. Konodo, *Ind. Eng.Chem.Res.* 40 (2001) 163
[17] M. Noack, P. Kölsch, V. Seefeld, P. Toussaint, G. Georgi, J. Caro, *Miropor. Mesopor. Mater.* 79 (2005) 329
[18] Y.F. Zhang, Z.Q. Xu, Q.L. Chen, *J.Membr. Sci.* 210 (2002) 361
[19] G. Li, E. Kikuchi, M. Matsukata, *Micropor. Mesopor. Mater.* 62 (2003) 211
[20] X. Lin, E. Kikuchi, M. Matsukata, *Chem. Comm.*11 (2000) 957

Chapter 4
MTW nanocrystal-layered membrane preparation

4.1. Introduction

Zeolites are among the most important porous materials used in industrial operations and have been widely applied as catalysts and adsorbents [1-5]. The use of zeolite membranes for separations has attracted considerable attention due to the inherent high thermal and chemical stability of these substances compared with polymeric materials. To date, membranes made using zeolites with the framework codes LTA [6, 7], FAU [8, 9], MOR [10, 11], BEA [12,13] and MFI [14, 15] have been studied and based on the different characteristics such as pore size and hydrophilic/hydrophobic ability, these different type membranes can be widely used for gas or liquid separation and zeolite-membrane reactors [16, 17]. In addition, the Mitsui Engineering and Shipbuilding Co. has demonstrated the separation of aqueous solutions by pervaporation using zeolite membranes [18].

MTW-type zeolite is a high-silica material with a unidimensional 12-membered ring channel system [19], in which the Si/Al ratio can be controlled over a wide range of values. This zeolite has been successfully prepared using conventional hydrothermal synthesis [20-22], and it has been shown that the crystal size obtained can be varied by using different organic structure directing agents (OSDAs) due to the resulting differences in the nucleation and crystallization rates [23, 24]. Applications of MTW zeolite to structure-sensitive catalytic reactions have been developed recently [25, 26], but there have been only a few reports concerning the use of MTW zeolite in separation membranes.

The main objective of the present work was to prepare an MTW nanocrystal layered membrane and apply it to the selective separation of water from a water/2-propanol solution by pervaporation. Previously, we succeeded in preparing hydrophilic MFI and MOR zeolite nanocrystal layered membranes consisting of a zeolite nanocrystal layer and a protection layer for the removal of water from water/organic solutions [27-29]. The application of nano-sized MTW crystal as a seed crystal was effective in improving the membrane performance. The water flux of the layer membrane prepared using the nanocrystals was approximately 100 times high compared with the dense membrane

prepared by in situ hydrothermal synthesis methods [30]. The protection layer is growth from the seed layer (nanocrystal layer) during the hydrothermal synthesis. It was found that the interface between the nanocrystal and protection layer is the densest area in the membrane which was considered to be the main separation region of the membrane [27-29]. The zeolite nanocrystal in this study, the same preparation method reported previously was applied to make the MTW zeolite membrane.

4.2. Experimental

4.2.1. Preparation of MTW zeolite powders

MTW nanocrystals approximately 50 nm in size were obtained *via* hydrothermal synthesis with tetraethylammonium bromide (TEABr, Wako Chemicals) as the OSDA. An aqueous solution containing sodium aluminate (Wako Chemicals), TEABr and sodium hydroxide (Wako Chemicals) was prepared and stirred at room temperature for 3 h. Subsequently, LUDOX HS-40 colloidal silica (Si source, Aldrich Chemicals) was added followed by further stirring at room temperature for 3 h to ensure a homogeneous mixture. The composition ratio of the resulting mixture was $20Na_2O$:120TEABr:$200SiO_2$:xAl_2O_3:$11110H_2O$, where x = 1 to 2. The mixture was transferred to a Teflon-sealed stainless steel bottle and this container was heated to 150 °C and held at this temperature for 6 days with stirring. The product was washed thoroughly three times each with deionized water and 2-propanol and then dried overnight at 110 °C. The OSDA was removed by calcination in air at 550 °C for 12 h. The morphology, composition (Si/Al ratio) and crystallinity of the resulting zeolite were assessed by field emission scanning electron microscopy (FE-SEM; JEOL JSM-6500F), energy dispersive X-ray spectroscopy (EDS, JEOL JSM-6510LA) and X-ray diffraction (XRD; JEOL JDX-8020), respectively. The porous and Brunauer-Emmett-Teller (BET) surface areas of the zeolite were determined from N_2 adsorption isotherms (BELSORP-mini).

4.2.2. Preparation of MTW nanocrystal-layered membranes

The MTW nanocrystals were subsequently ultrasonically dispersed in a sodium hydroxide aqueous solution (approximately pH 12) at concentrations of 3.5 to 6.5 $g \cdot m^{-3}$. The dispersed nanocrystals were layered on the outer surfaces of cylindrical alumina ceramic filters (NGK insulators) *via* a filtration method driven by the application of a

vacuum to the permeate side. The inner and outer diameters and the length of the filters were 6, 11 and 50 mm, respectively. Each filter consisted of two porous regions; an inner region with a pore diameter of approximately 2-3 μm (the rough region) and a dense outer region with a pore diameter of 0.1 μm. Each filter was immersed in 0.1 M HCl for 6 h and then washed in distilled water prior to preparation of the membranes. The thickness of the MTW nanocrystal layer on the ceramic filter could be controlled by changing the concentration of nanocrystals in the sodium hydroxide aqueous solution. Finally, to protect the nanocrystal layer against mechanical shock, a protection layer was hydrothermally formed on the nanocrystal layer using either TEABr or methyltriethylammonium chloride (MTEACl, Tokyo Chemical Industry) as the OSDA. The composition of the synthesis mixture when using TEABr as the OSDA was $20Na_2O$:100TEABr:$500SiO_2$:xAl_2O_3:$11110H_2O$, where x = 1.25 to 5, while the composition with MTEACl was $20Na_2O$:60TEABr:$300SiO_2$:$5Al_2O_3$:$11110H_2O$. The aqueous solution containing the MTW nanocrystal-layered membrane was heated to 150 °C for 6 days to form a protection layer on the nanocrystal layer. The zeolite membrane thus prepared was washed with distilled water and then dried in air.

4.2.3. Pervaporation trials

Pervaporation trials were carried out using a conventional method at temperatures ranging from 60 to 100 °C in a stainless steel autoclave shown in Fig. 4.1, with water/2-propanol (2-propanol concentration is 88 wt %) as the feed solution. The acid-stability of the membranes was checked by pervaporation experiments using water/acetic acid mixture (acetic acid concentration is 90 wt %) as a feed solution. The water/acetic acid solution was renewed at every 6 h and the whole pervaporation experiments were continuous to carry out for 18 h. After the membrane was immersed in this solution, the air in the autoclave was replaced with room temperature nitrogen and the vessel was heated to the desired pervaporation temperature. Molecules permeating through the membrane were swept out with a flow of nitrogen that was continuously fed to the permeate side of the membrane. The composition of the exit gas from the permeate side was analyzed using an on-line gas chromatograph equipped with a molecular sieve 5Å column and TCD and FID detectors.

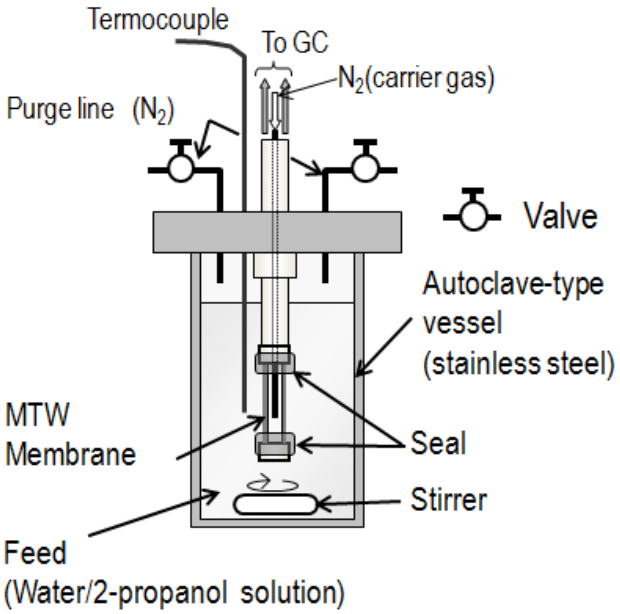

Figure 4.1 Schematic of the stainless steel autoclave vessel used for pervaporation experiments

The separation factor, α, was defined as

$$\alpha = \frac{F_w / F_i}{C_w / C_i}$$

where F_w and F_i are the molar flux of water and 2-propanol on the permeate side, respectively, and C_w and C_i are the molar concentrations of water and 2-propanol on the feed side, respectively.

The membrane separation ability and water flux are tested to become stable after the pervaporation test carried out for 5 h in the same temperature. Therefore, all of the pervaporation data were detected in the membrane stable condition (after 5 h pervaporation experiment in the same temperature). The duration of the every test was 8 h and after each pervaporation test, the membranes were at first washed with water and then dry in air for 12 h. The total amount of water and organic solvent permeating through the membrane during each experiment was less than 3 wt%. Accordingly, the initial concentrations were used to calculate the separation factor.

4.3. Result and discussion

4.3.1. MTW nanocrystals synthesis with different Si/Al ratios

MTW zeolite nanocrystals with Si/Al ratios of 50, 100 and 200 in the mother liquid were hydrothermally synthesized using TEABr as the OSDA, and were found to have Si/Al ratios of 34.5, 77.7 and 191.8, respectively, by EDS analysis. Figs. 4.2 and 4.3 show XRD patterns and FE-SEM images for the obtained MTW zeolites, respectively. The XRD patterns exhibit peaks corresponding to an MTW-type zeolite. As can be seen in Fig. 4.3, small, rounded crystals approximately 50 nm in size were obtained and the crystal size and morphology were unchanged as the Si/Al ratio was varied.

Nitrogen adsorption isotherms for the obtained MTW zeolite nanocrystals were acquired at 77 K (Fig. 4.4). The isotherms exhibited Type-I behavior according to the Langmuir isotherm model, indicating the presence of micropores. The amount of adsorbed nitrogen was relatively consistent regardless of the Si/Al ratio. The BET surface areas obtained from the isotherms were approximately 350 m^2/g, a value that is in good agreement with previously reported data [22]. These MTW zeolite nanocrystals were used to prepare the MTW zeolite nanocrystal-layered membranes.

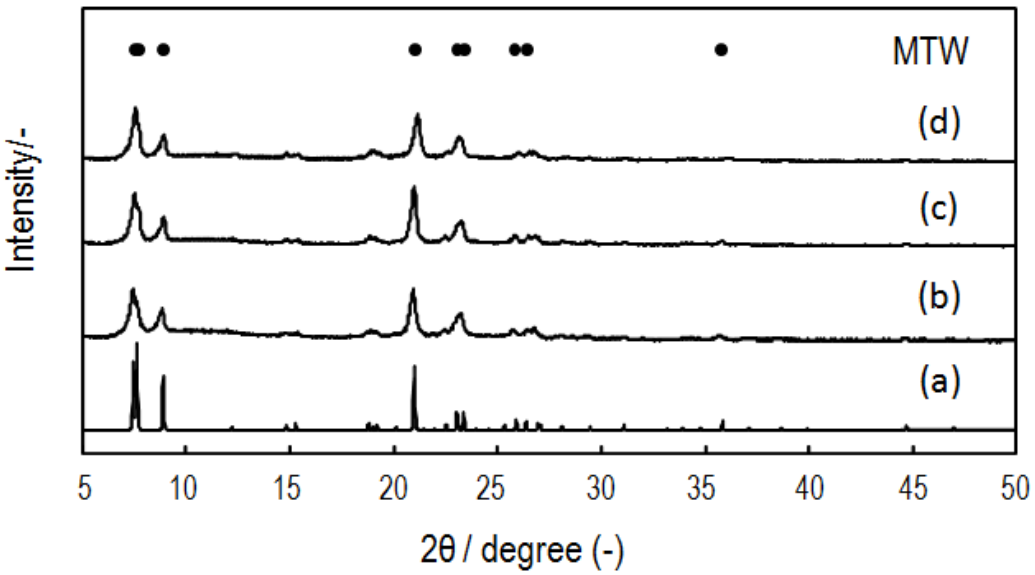

Figure 4.2 XRD patterns for (a) MTW zeolite [30] and MTW specimens prepared using Si/Al ratios in the crystal formation solution of (b) 50, (c) 100 and (d) 200.

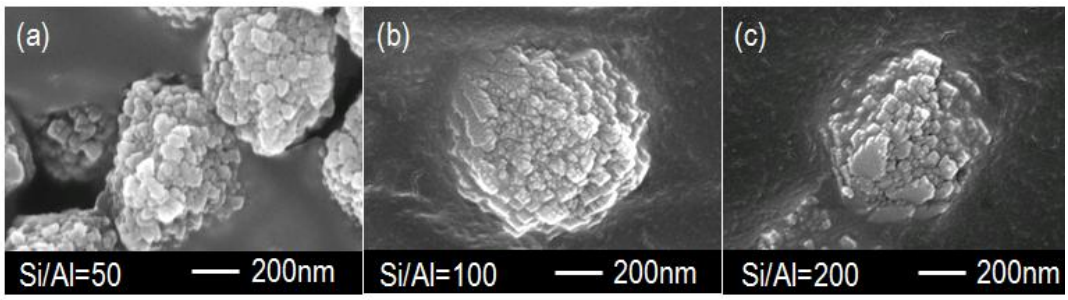

Figure 4.3 FE-SEM images of nanometer-sized MTW crystals synthesized with different Si/Al ratios.

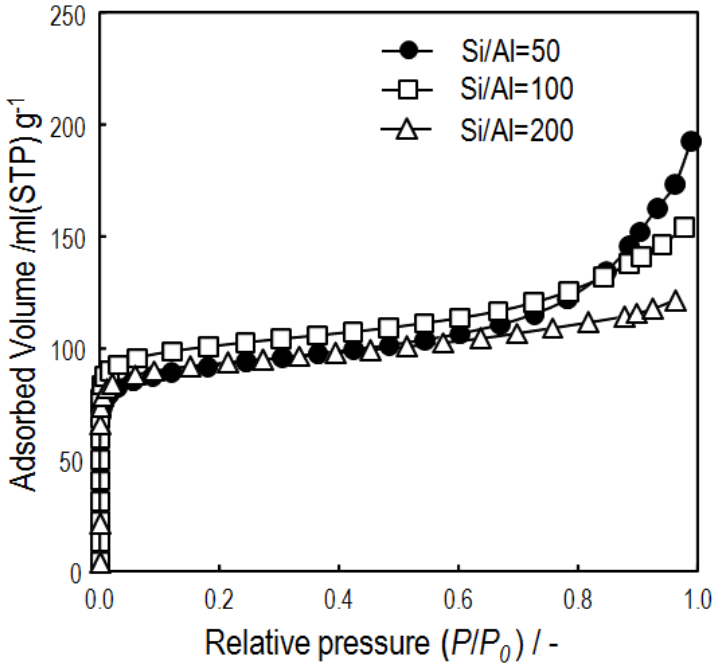

Figure 4.4 Nitrogen adsorption isotherms of nanometer-sized MTW crystals synthesized with different Si/Al ratios.

4.3.2. MTW zeolite nanocrystals membrane synthesis with different OSDAs

MTW zeolite crystals were hydrothermally synthesized by using MTEACl or TEABr as OSDA. Figs. 4.5 FE-SEM images for the obtained MTW zeolites, respectively. As shown in Fig. 4.5, long stick like crystals were formed when using the MTEACl as the OSDA and the crystals size is about 1~3μm. On the other hand, small rounded crystals with crystal size of 50~100 nm were obtained by using TEABr as

OSDA.

After the MTW-type zeolite nanocrystals (Si/Al ratio= 34.5) were piled up on the aluminum ceramic filters, protection layers were hydrothermally formed on the MTW nanocrystal layer using different OSDAs, respectively (MTEACl and TEABr). The Si/Al ratio in the mother liquid used to prepare protection layer of both membrane samples for these trials was 50. Fig. 4.6 presents SEM photographs of cross-sections ((a) and (b)) and an overhead view (c) of the resulting membranes. An MTW nanocrystal layer with a thickness of approximately 17 μm can be clearly observed on the filter in each membrane and it is evident that a protection layer was formed on the nanocrystal layer. Differences in the crystal morphology of the protection layers are also clear. In the membrane prepared using MTEACl as the OSDA, the protection layer is composed of micrometer-sized column-shaped crystals (approximately 2 μm in size), and the Si/Al ratio in these crystals was found to be 49.1 by EDS. In contrast, the use of TEABr as the OSDA formed aggregated MTW nanocrystals with a Si/Al ratio of 43.5 as the protection layer. These variations in the crystal morphology of the protection layer are ascribed to the difference in the secondary growth rate of the MTW zeolite depending on the type of OSDA [23, 24].

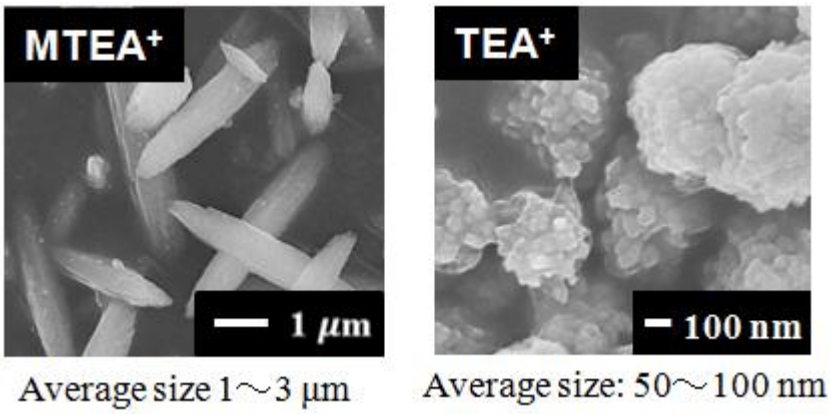

Figure 4.5 FE-SEM images of MTW crystals synthesized with different OSDAs.

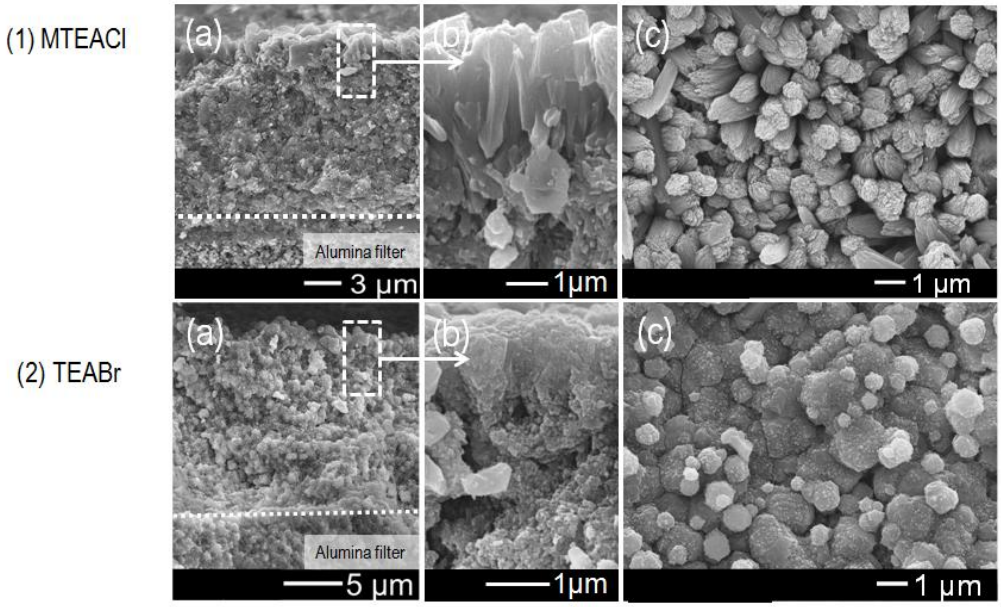

Figure 4.6 FE-SEM images of nanocrystal-layered MTW membranes with protection layers prepared using (1) MTEACl and (2) TEABr as the OSDA. Legend: (a) cross-sectional view, (b) magnified view of the indicated area and (c) overhead view.

4.3.3. Effects of mother liquid concentration of hydrothermal synthesis on MTW zeolite nanocrystal-layered membrane preparation

The membranes with different mother liquid concentration of hydrothermal synthesis were prepared and the prepared conditions are showed in Table 4.1 and Figure 4.7 shows FE-SEM photographs of MTW zeolite nanocrystal-layered membranes. From Figure 4.7 (a), the crystal size of the mordenite in the protection layer became slightly smaller by decreasing the mother liquid concentration for protection layer formation. From the cross section of the membranes (Figure 4.7 (b)), the protection layer were formed when the mother liquid concentration is between [Si] = 1.5~3.0 mol/l. The protection layer of the membrane is not obtained when the concentration of Si in mother liquid under 1.5 mol/l. It was considered that high concentration of the mother liquid will accelerate the crystal growth speed and lead to the big size crystal.

Table 4.1 Composition of the mother liquid for MTW membrane protection layer formation

[Si] /mol/L	1.5～3.0
[NaOH] /mol/L	0.2
Si/Al	50
TEABr/Si	0.2

(a)

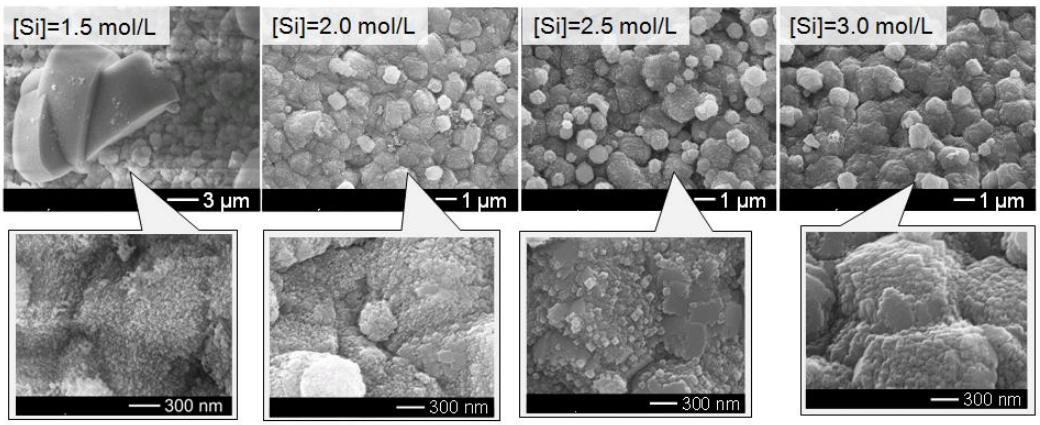

(b)

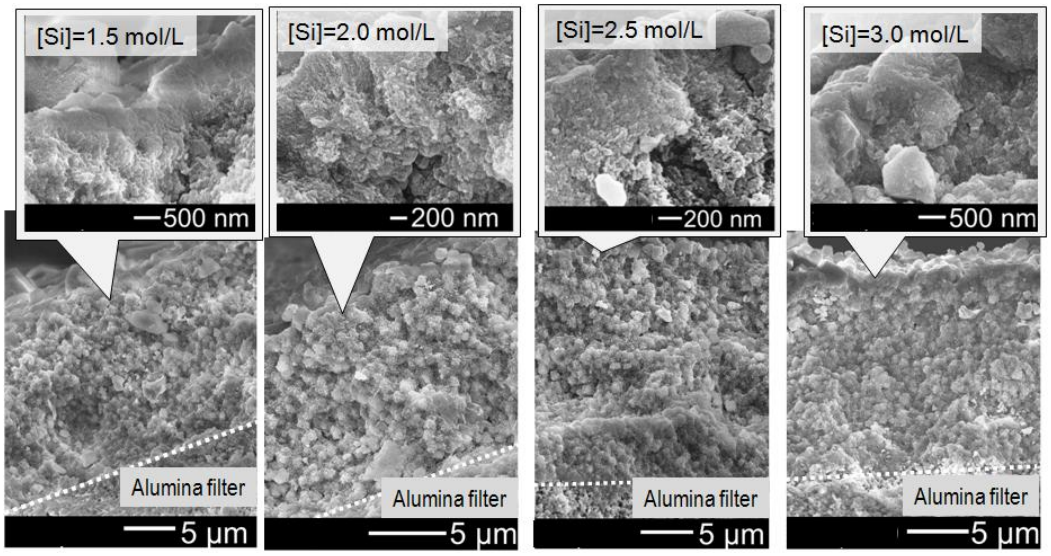

Figure 4.7 FE-SEM images of nanocrystal-layered MTW membranes with protection layers formation by using different mother liquid concentration. (a) Overhead view (b) cross-sectional view.

The XRD patterns of the powders obtained in solution after protection layer formation were show in Figure 4.8 and the SEM photographs of the powder are showed beside which can show the powder samples shape. From Fig. 4.8, powder samples obtained at Si = 0.5 mol/l show the pattern of amorphous and powder samples obtained at Si = 1.0~1.5 mol/l show the mix pattern of MFI and MTW. On the other hand, the powder samples synthesized at Si= 2.5 ~ 3.0 mol/l show the same pattern as the commercial MTW, indicating that the MTW type membranes were obtained at these conditions.

In order to check the separation performance of these membranes, the membranes prepared at Si= 2.5 ~ 3.0 mol/l were used to separate water from a water/2-propanol solution (2-propanol concentration is 88 wt %) and the results were showed in Figure 4.9. The water flux and the separation factor of the MTW type zeolite membrane prepared at Si = 2.5 mol/l show high value compared with the MTW membrane prepared at Si = 2.0 mol/l. The MTW type zeolite membrane prepared at Si = 3.0 mol/l show no separation ability during the pervaporation test and the membrane synthesized on the alumina filter falled off after one day used. Base the information discussed above, it can be concluded that the optimization of MTW zeolite nanocrystal layer membrane preparation for pervaporation is mother liquid concentration at the condition of Si = 2.5 mol/l.

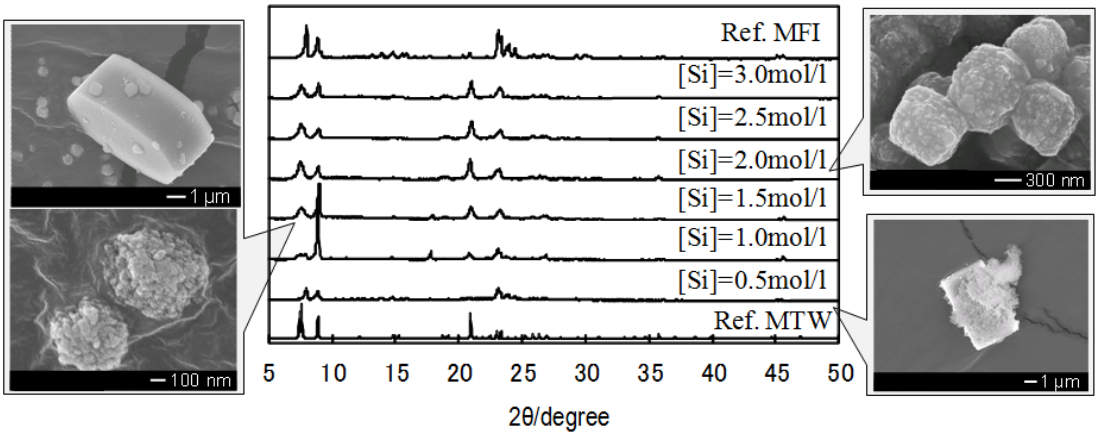

Figure 4.8 XRD patterns for MTW powders obtained in solution after protection layer formation in different concentration mother liquid.

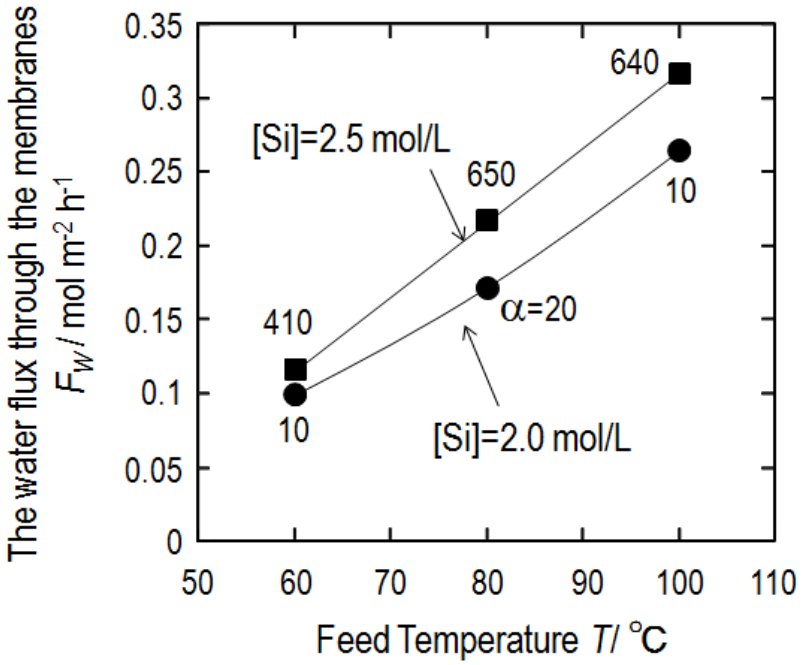

Figure 4.9 Water flux of membrane prepared with different concentration.

4.3.4 The acid-stability of the MTW zeolite nanocrystal-layered membrane

As mention in the introduction section, the MTW zeolite crystals are supposed to resist to the acidic solution. The MTW zeolite crystals with crystal size about 50 nm were used to acid-stability test at the temperature of 80 °C for 5 days, and the crystals were synthesis at the condition as follow: TEABr was using as OSDA, the ratio of Si/Al was 50. XRD patterns and N_2 adsorption were detected and the data is showed in figure 4.10 and 4.11. From the Fig.4.10 and 4.11, it is considered that the MTW zeolite crystals keep the same zeolite structure and the BET surface areas values obtained from the isotherms also keep at about 350 m^2/g. however, the EDS analysis indicate that there were alumina contents lost compared between the MTW zeolite crystals before acidic stability test (Si/Al = 34.5) and after acidic stability test (Si/Al = 74.5).

The membrane acid stability was examined by separation of water from acetic acid/water solution (acetic acid concentration is 90 wt %) by pervaporation at the temperature of 80 °C. The membrane was prepared by using TEABr as OSDA and the concentration of Si equal to the value of 2.5 mol/l. The water flux and separation factor of the membrane during the pervaporation experiment is 0.198 kg/m^2h and 160, respectively. The membrane maintained the separation performance for 2 days and lost

the separation ability and the FE-SEM photographs of MTW nanocrystal-layered membrane before and after acetic acid /water pervaporation experiment are showed in Figure 4.12. From the figure, after 2 days acid stability test, some crystals of the MTW membrane were dissolved but the surface is not broken. Although the acidic stability test only assisted for 2 days, MTW type zeolite membranes are considered to be a good candidate for the separation of acid mixtures and wide usage in organic dehydration as a new kind of zeolite material.

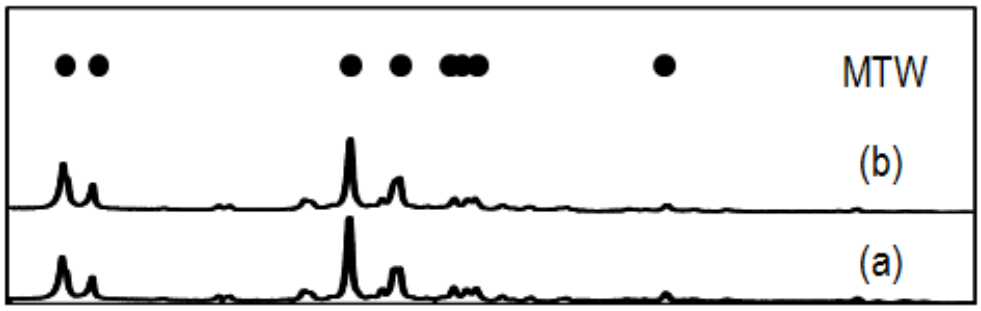

Figure 4.10 XRD patterns for (a) MTW zeolite crystal before acid stability test (b) MTW zeolite crystal after acid stability test.

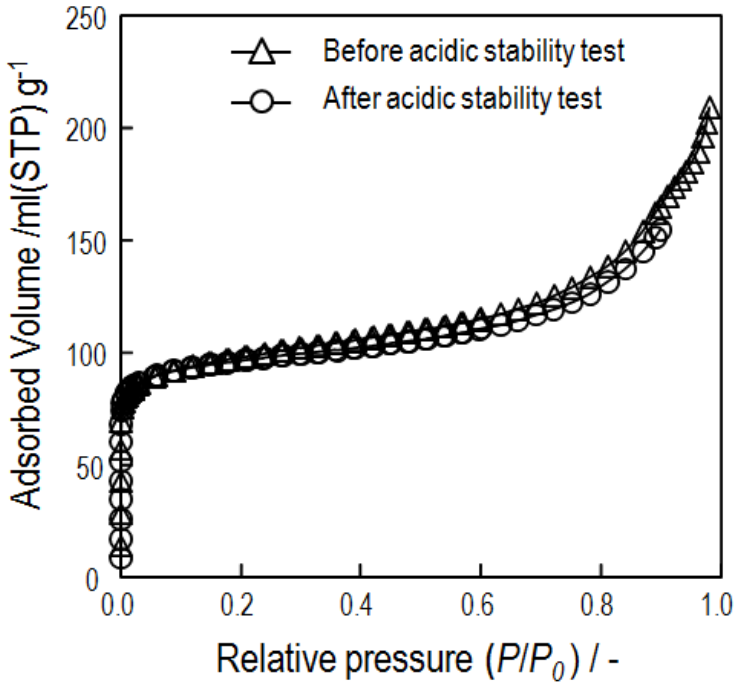

Figure 4.11 Nitrogen adsorption isotherms of MTW crystals before and after acidic stability test.

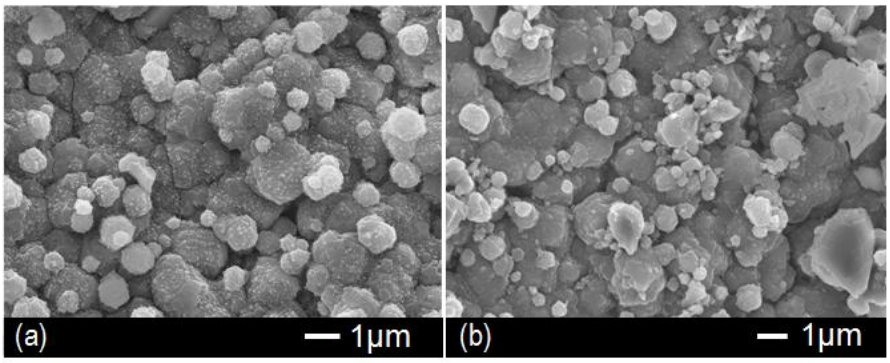

Figure 4.12 FE-SEM photographs of MTW nanocrystal-layered membrane surface areas ((a) before acetic acid /water pervaporation experiment, (b) after acetic acid /water pervaporation experiment).

4.4. Conclusions

MTW nanocrystal-layered membranes were successfully prepared using the secondary growth method. MTW nanocrystals were laminated onto an alumina filter and a MTW protection layer was clearly formed on the nanocrystal layer. The effect of nanocrystal layer thickness was discussed to determine the appropriate condition for membrane preparation. The membrane acid stability was examined by separation of water from acetic acid/water solution (acetic acid concentration is 90 wt %) by pervaporation.

Referrence

[1] C. Marcilly, *J. Sci.* 216 (2003) 47
[2] T. F. Degnan Jr, *J. Cat.* 216 (2003) 32
[3] V.N. Shetti, J. Kim, R. Srivastava, M. Choi, R. Ryoo, *J. Cat.* 254 (2008) 296
[4] K. Suzuki, Y. Aoyagi, N. Katada, M. Choi, R. Ryoo, M. Niwa, Cat. Today132 (2008) 38
[5] J.A. Rabo, M.W. Schoonover, *Applied Catalysis A: General* 222 (2001) 261
[6] F.J. Varela-Gandía, A. Berenguer-Murcia, D. Lozano-Castelló, D. Cazorla-Amorós, *J. Membr. Sci.* 351(2010)123
[7] J. Caro, D. Albrecht, M. Noack, *Sep. Purif. Technol.* 66(2009)143
[8] I. Kumakiri, K. Hashimoto, Y. Nakagawa, Y. Inoue, Y. Kanehiro, K. Tanaka, H. Kita, *Catal. Today* 236A (2014) 86

[9] N. Yamanaka, M. Itakura, Y. Kiyozumi, Y. Ide, M. Sadakane, T. Sano, *Micropor.Mesopor.Mater.* 158 (1) (2012) 141

[10] A.M. Avila, Z. Yu, S. Fazli, J.A. Sawada, S.M. Kuznicki, *Micropor. Mesopor. Mater.*190 (2014) 301.

[11] G. Li, E. Kikuchi, M. Matsukata, *Sep. Purif. Technol.* 32 (2003) 199

[12] P.S. Barcia, A. Ferreira, J. Gascon, S. Aguado, J.A.C. Silva, A.E. Rodrigues, F. Kapteijn, *Micropor. Mesopor. Mater.* 128 (2010) 194

[13] S.M. Kumbar, T. Selvam, C. Gellermann, W. Storch, T. Ballweg, J. Breu, G. Sextl, *J. Membr. Sci.* 347 (2010) 132

[14] J.B. Lee, H.H. Funke, R.D. Noble, J.L. Falconer, *J. Membr. Sci.*321(2) (2008) 309

[15] T. Lee, J. Choi, M. Tsapatsis, *J. Membr. Sci.*436 (1) (2013) 79

[16] M.O. Daramola, E.F. Aransiola, T.V. Ojumu, *Materials* 5 (2012) 2101

[17] S.J. Kim, S. Yang, G.K. Reddy, P. Smirniotis, J. Dong, *Energy fuels* 23(8) (2013) 4471

[18] Y. Morigami, M. Kondo, J. Abe, H. Kita, and K. Okamoto, *Sep. Purif. Technol.* 25 (2001) 251

[19] R.B. LaPierre, A.C. Rohrman Jr., J.L. Schlenker, J.D. Wood, M.K. Rubin, W.J. Rohrbaugh, *Zeolites* 5 (1985) 346.

[20] M.A. Camblor, L.A. Villaescusa, M.J. Díaz-Cabaňas, *Topics in Catal.* 9 (1999) 59.

[21] R. Szostak, Handbook of Molecular Sieves, Van Nostrand, Reinhold, New York, 1992, p.532

[22] A. Bhaumik, M.K. Dongare, R. kumar, *Micropor. Mater.* 173 (1995) 5.

[23] A.V. Toktarev, K.G. Ione, *Stu.Sur. Sci.Catal.*105 (1997) 333

[24] S. Ritsch, N. Ohnishi, T. Ohsuna, K. Hiraga, O. Terasaki, Y. Kubota, Y. Sugi, *Chem. Mater.*10 (1998) 3958.

[25] L. Dimitrov, M. Mihaylov, K. Hadjiivanov, V. Mavrodinova, *Micropor.Mesopor. Mater.* 143 (2011) 291

[26] B. Gil, L. Mokrzycki, B. Sulikowski, Z. Olejniczak, S. Walas, *Cat. Today* 152(2010)24

[27] Y. Zhang, Y. Nakasaka, T. Tago, A. Hirata, Y. Sato, T. Masuda, *Micropor. Mesopor. Mater.* 207 (2015) 39

[28] T. Tago, Y. Nakasaka, A. Kayoda, T. Masuda, *Sep. Purif. Technol.* 58 (2007) 7

[29] T. Tago, Y. Nakasaka, A. Kayoda, T. Masuda, *Micropor. Mesopor. Mater.* 115 (2008) 176

[30] T. Tago, D. Aoki, K. Iwakai, T. Masuda, *Topics in Catal.*52 (2009) 865

Chapter 5
Optimization of MTW nanocrystal-layer membrane for dehydration by pervaporation

5.1. Introduction

During the membrane separation process, molecules in the solution are selectively adsorbed into the membrane, permeate through it, and exit as vapor from the permeate side. The flux of molecules through the zeolite membrane from the feed side to the permeate side greatly affects the performance of the membrane. This flux can be expressed as in Eq. (1), assuming that the adsorption of molecules proceeds in accordance with a Langmuir isotherm and the effects of counter diffusion can be ignored [1].

$$J_{\mathrm{i}} = \frac{\rho \varepsilon D_{\mathrm{i,s}}}{\delta}(q_{\mathrm{i,f}} - q_{\mathrm{i,p}}) \qquad (1)$$

Here, ρ, ε, δ, $D_{\mathrm{i,s}}$, $q_{\mathrm{i,f}}$ and $q_{\mathrm{i,p}}$ are the density, porosity and thickness of the zeolite membrane, and the surface diffusivity and quantities of component *i* on the feed and permeate sides, respectively.

According to this equation, the membrane permeability will vary with the membrane thickness and surface diffusivity. The thickness is readily controlled by changing the synthesis conditions used to produce the membrane, such as the amount of seed crystals on the support filter, the Si concentration and the hydrothermal temperature. In addition, varying the crystal size/morphology and the Si/Al ratio of the zeolite will cause the surface diffusivity to change. There have been some reports regarding improvements in membrane performance by controlling the crystal morphology of MOR and MFI zeolite membranes during the secondary growth process [2-4]. In the case of MTW zeolite, the crystal size and morphology depend on the OSDA employed. Moreover, the hydrophilic/hydrophobic properties of an MTW zeolite membrane can be modified by varying the aluminum content in the zeolite lattice so as to allow for the dehydration of organic solvents [5]. Accordingly, there is the possibility of controlling the crystal size/morphology and Si/Al ratio of MTW zeolite membranes to improve separation properties.

The main objective of the present work is to optimization the preparation condition of

MTW nanocrystal layered membrane to improve the performance of the membrane and apply it to the selective separation of water from a water/2-propanol solution by pervaporation. Previously, we succeeded in preparing hydrophilic MFI and MOR zeolite nanocrystal layered membranes consisting of a zeolite nanocrystal layer and a protection layer for the removal of water from water/organic solutions [4, 6, 7]. The application of nano-sized MTW crystal as a seed crystal was effective in improving the membrane performance. The water flux of the layer membrane prepared using the nanocrystals was approximately 100 times high compared with the dense membrane prepared by in situ hydrothermal synthesis methods [2]. The protection layer is growth from the seed layer (nanocrystal layer) during the hydrothermal synthesis. It was found that the interface between the nanocrystal and protection layer is the densest area in the membrane which was considered to be the main separation region of the membrane [7]. The zeolite nanocrystal in this study, the same preparation method reported previously was applied to make the MTW zeolite membrane. As noted above, the crystal size/morphology, Si/Al ratio and thickness of the zeolite membrane can all affect the membrane performance, and so the effects of these parameters on the flux of water and on the separation factor were investigated.

5.2. Experimental

5.2.1. Preparation of MTW zeolite powders and membranes

MTW nanocrystals approximately 50 nm in size were obtained *via* hydrothermal synthesis with tetraethylammonium bromide (TEABr, Wako Chemicals) as the OSDA. An aqueous solution containing sodium aluminate (Wako Chemicals), TEABr and sodium hydroxide (Wako Chemicals) was prepared and stirred at room temperature for 3 h. Subsequently, LUDOX HS-40 colloidal silica (Si source, Aldrich Chemicals) was added followed by further stirring at room temperature for 3 h to ensure a homogeneous mixture. The composition ratio of the resulting mixture was $20Na_2O$:120TEABr:$200SiO_2$:xAl_2O_3:$11110H_2O$, where x = 1 to 2. The mixture was transferred to a Teflon-sealed stainless steel bottle and this container was heated to 150 °C and held at this temperature for 6 days with stirring. The product was washed thoroughly three times each with deionized water and 2-propanol and then dried overnight at 110 °C. The OSDA was removed by calcination in air at 550 °C for 12 h. The morphology, composition (Si/Al ratio) and crystallinity of the resulting zeolite were assessed by field emission scanning electron microscopy (FE-SEM; JEOL JSM-6500F),

energy dispersive X-ray spectroscopy (EDS, JEOL JSM-6510LA) and X-ray diffraction (XRD; JEOL JDX-8020), respectively. The porous and Brunauer-Emmett-Teller (BET) surface areas of the zeolite were determined from N_2 adsorption isotherms (BELSORP-mini).

The MTW nanocrystals were subsequently ultrasonically dispersed in a sodium hydroxide aqueous solution (approximately pH 12) at concentrations of 3.5 to 6.5 $g \cdot m^{-3}$. The dispersed nanocrystals were layered on the outer surfaces of cylindrical alumina ceramic filters (NGK insulators) *via* a filtration method driven by the application of a vacuum to the permeate side. The inner and outer diameters and the length of the filters were 6, 11 and 50 mm, respectively. Each filter consisted of two porous regions; an inner region with a pore diameter of approximately 2-3 μm (the rough region) and a dense outer region with a pore diameter of 0.1 μm. Each filter was immersed in 0.1 M HCl for 6 h and then washed in distilled water prior to preparation of the membranes. The thickness of the MTW nanocrystal layer on the ceramic filter could be controlled by changing the concentration of nanocrystals in the sodium hydroxide aqueous solution. Finally, to protect the nanocrystal layer against mechanical shock, a protection layer was hydrothermally formed on the nanocrystal layer using either TEABr or methyltriethylammonium chloride (MTEACl, Tokyo Chemical Industry) as the OSDA. The composition of the synthesis mixture when using TEABr as the OSDA was $20Na_2O$:100TEABr:$500SiO_2$:xAl_2O_3:$11110H_2O$, where x = 1.25 to 5, while the composition with MTEACl was $20Na_2O$:60TEABr:$300SiO_2$:$5Al_2O_3$:$11110H_2O$. The aqueous solution containing the MTW nanocrystal-layered membrane was heated to 150 °C for 6 days to form a protection layer on the nanocrystal layer. The zeolite membrane thus prepared was washed with distilled water and then dried in air. Further details of this process have been provided previously [6, 7].

5.2.2. Pervaporation trials

Pervaporation trials were carried out using a conventional method at temperatures ranging from 60 to 100 °C in a stainless steel autoclave, with water/2-propanol (2-propanol concentration is 88 wt%) as the feed solution. After the membrane was immersed in this solution, the air in the autoclave was replaced with room temperature nitrogen and the vessel was heated to the desired pervaporation temperature. Molecules permeating through the membrane were swept out with a flow of nitrogen that was continuously fed to the permeate side of the membrane. The composition of the exit gas from the permeate side was analyzed using an on-line gas chromatograph equipped with

a molecular sieve 5Å column and TCD and FID detectors. Details of this procedure have been described in previous reports [6, 7].

The separation factor, α, was defined as

$$\alpha = \frac{F_w / F_i}{C_w / C_i}$$

where F_w and F_i are the molar flux of water and 2-propanol on the permeate side, respectively, and C_w and C_i are the molar concentrations of water and 2-propanol on the feed side, respectively.

The membrane separation ability and water flux are tested to become stable after the pervaporation test carried out for 5 h in the same temperature. Therefore, all of the pervaporation data were detected in the membrane stable condition (after 5 h pervaporation experiment in the same temperature). The duration of the every test was 8 h and after each pervaporation test, the membrane was at first washed by water and then dried in air for 12 h. The total amount of water and organic solvent permeating through the membrane during each experiment was less than 3 wt%. Accordingly, the initial concentrations were used to calculate the separation factor.

5.3. Results and discussion

5.3.1. Effect of crystal size in the protection layer on separation properties

In our previous study of the hydrophilic silicalite-1 nanocrystal-layered membrane and mordernite membrane, the water-silanol networks that formed on non-zeolitic pore spaces among the crystals acted as one of the main channel for water permeation, and the interface between the nanocrystal layer and protection layer was important for the separation because this area became the densest area in the membrane [4, 6]. The morphology and crystal size around the interface formed by hydrothermal synthesis are the important factors affecting the membrane permeability and separation ability.

Therefore, the effects of the crystal size and morphology of the protection layer on the water separation from water/2-propanol solutions were examined by pervaporation. The membranes were prepared by the same method as show in the last chapter (chapter 4, result and discussion 4.3.2) and the resulting water flux and separation factor data obtain in the pervaporation test are summarized in Fig. 5.1. The layered membrane with nanocrystals in the protection layer (prepared using TEABr) exhibited a much higher separation factor and a water flux more than four times that of the membrane with

micrometer-sized crystals in the protection layer (prepared using MTEACl). It has been reported that the crystal morphology plays an important role in the overall quality of the zeolite membrane [7-9]. Since there were only slight differences in the Si/Al ratios of the protection layers in these two membranes, it was concluded that the evident difference in the pervaporation abilities of these membranes resulted from the different crystal morphologies of their protection layers. In these zeolite nanocrystal-layered membranes, water permeation occurred not only through the ordered nanopores of the zeolite crystal (that is, through the zeolite pores or intracrystalline pathways) but also through the spaces between the crystals (the non-zeolite pores or intercrystalline pathways) [10-12].

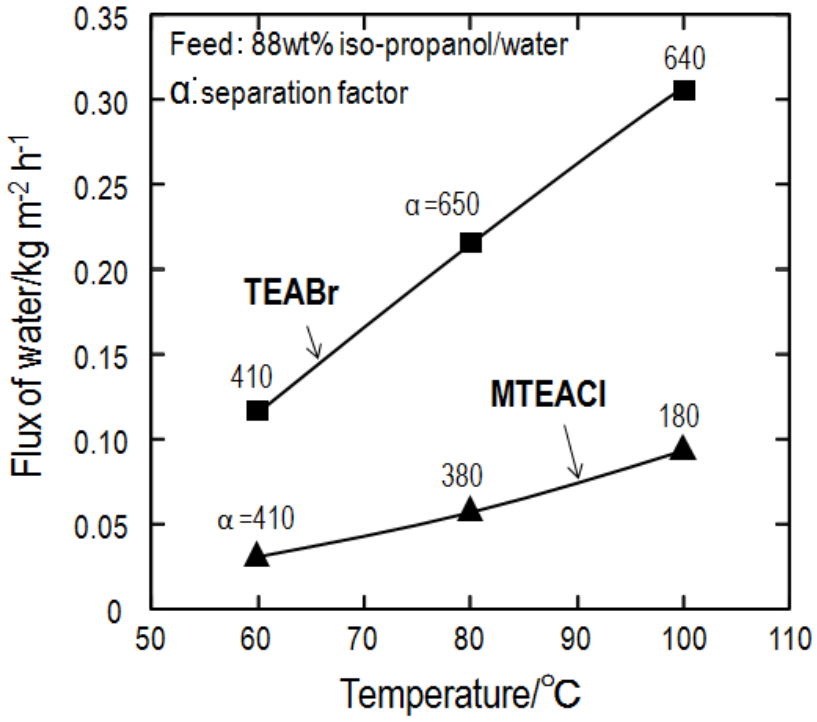

Figure 5.1 Water fluxes from water/2-propanol solutions through MTW membranes prepared using TEABr or MTEACl as the OSDA. The numerical values close to the lines indicate separation factors (a).

Since the MTW zeolite membranes were prepared by the same procedure as the silicalite-1 membranes and Mordenite membranes, it was considered that there were some non-zeolitic pores among the crystals. During the pervaporation to separate water from water/2-propanol mixtures, water molecules were adsorbed on the surfaces of

zeolitic and non-zeolitic pores, on which the water adsorption layer was formed, were the important channel for water permeation. The water molecules can diffuse through the non-zeolitic pore surrounded by the water adsorption layer, and consequently the size of non-zeolitic pores mainly affects the separation properties. The MTW membrane prepared using TEABr would possess a larger number of intercrystalline pores among the crystals, the pore size of which was appropriate for water selective permeation, compared with the membrane prepared using MTEACl. The larger number of pores and the smaller crystal size increased the water permeation rate through the intercrystalline and intracrystalline pathways within the membrane, respectively. Accordingly, the nanocrystal-layered membrane with a nano-crystalline protection layer prepared using TEABr exhibited higher water flux and enhanced separation ability compared with the membrane prepared using MTEACl.

5.3.2. Effects of the Si/Al ratio on the membrane performance

In a zeolite membrane, its hydrophilicity/hydrophobicity, which depends on the Si/Al ratio, affects the adsorbed quantity and diffusivity of molecules permeating through the membrane [13]. These MTW nanocrystal-layered membranes were composed of a nanocrystal layer and a protection layer, and so the Si/Al ratio of the MTW zeolite in both layers was expected to affect the membrane properties. Accordingly, MTW zeolite membranes with different Si/Al ratios in the nanocrystal and protection layers were prepared, and the effects of the ratio on the separation ability (as assessed by the water flux and separation factor) were examined. The membrane synthesis conditions and the Si/Al ratios in the nanocrystal and protection layers are listed in Table 5.1, along with the pervaporation results.

The pervaporation results for specimens M1, M2 and M3 show that the water flux varied with the Si/Al ratio in the protection layer, which was controlled by changing the Si/Al ratio of the mother liquid. With increasing aluminum content in the protection layer (while holding the Si/Al ratio in the nanocrystal layer at 34.5), the water flux was increased, and maintaining a high separation factor. Moreover, all of the membrane (M1, M2 and M3) show the highest separation ability at pervaporation temperature of 80 °C, and show the decreasing trend to 100 °C. This is because when the pervaporation temperature reach up to the boiling point of water, the water adsorption layer formed on the outside of the non-zeolitic pore will become unstable or broken and the non-zeolitic pores without the water adsorption layer will lose the selectivity leading to decrease in membrane separation ability.

Table 5.1 Experimental conditions used to form the protection layer and separation properties of the resulting membranes.

Sample	Si/Al ratio of mother liquid (-)		Si/Al ratio analyzed by EDS (-)		Pervaporation temperature					
	Nanocrystal layer	Protection layer	Nanocrystal layer	Protection layer*	60 °C		80 °C		100 °C	
					F_w [a]	a [b]	F_w [a]	a [b]	F_w [a]	a [b]
M1	50	50	34.5	43.6	0.117	410	0.217	650	0.316	640
M2	50	100	34.5	53.4	0.073	660	0.158	1200	0.281	770
M3	50	200	34.5	144.0	0.007	700	0.021	1300	0.043	310
M4	100	100	77.7	58.6	0.019	25	0.041	25	0.088	15

a: water flux through the membrane (kg m^{-2} h^{-1}).

b: separation factor (-).

* as-synthesized MTW membrane

Next, the effect of the Si/Al ratio in the nanocrystal layer was examined, keeping the Si/Al ratio of the mother liquid used to make the protection layer constant at 100 (corresponding to specimens M2 and M4). The water flux and separation factor were observed to increase with increasing aluminum content. As the discussed in the first section, the MTW nanocrystals have the same size and BET surface area regardless of Si/Al ratio, but the performance MTW membranes is depended on the Si/Al ratio. Even the densest area in the membrane is the interface between the nanocrystal layer and protection layer, and this place is important for the separation. The influence of the nanocrystal layer on the membrane separation ability could not be ignored. The enhancement of the Al content in MTW nanocrystal of the membrane increased its hydrophilic ability. Due to the high hydrophilicity of the nanocrystal layer of M2, the amount of adsorbed water molecules increased, leading to increases in the flux for water permeation through the membrane. On the other hand, when decreasing the Al contents in nanocrystal layer of M4, the main part of the membrane became less hydrophility. The water adsorption layers cannot be well formed on the surface side of the non-zeolitic pores and the zeolitic pores also became hydrophobicity. Therefore, the membrane showed low selectivity and low water flux during the pervaporation.

Based on the above discussion, the Si/Al ratio in both layers strongly influenced the separation of water through the membrane, as the result of the relationship between the quantity of adsorbed water molecules and the hydrophilicity (or Si/Al ratio) of the zeolite. As the hydrophilicity of the zeolite increased (the Si/Al ratio decreased), the quantity of adsorbed water molecules increased as the intracrystalline and

intercrystalline pores within the membrane were filled with water molecules, leading to the enhanced separation properties. Moreover, since the crystal morphology of the protection layer and the Si/Al ratios in the protection and nanocrystal layers affected the separation properties, both layers played important roles in water separation from water/2-propanol mixtures by pervaporation.

5.3.3. Effect of the nanocrystal layer thickness on membrane permeation properties

Those membranes with high fluxes and good separation abilities were deemed to have regions suitable for separation. As discussed above, the results indicated that separation in the membranes prepared using TEABr as the OSDA for the protection layer occurred both in the area close to the outer surface (the protection layer) and in the MTW nanocrystal layer. In order to prepare membranes with suitable separation areas, the effect of the nanocrystal layer thickness on the separation properties of the membranes were also investigated. In these trials, the layer thickness was controlled by varying the concentration of nanocrystals in a sodium hydroxide aqueous solution while loading the alumina filter. The second growth of the protection layer is mainly happened on the surface of the nanocrystal layer since it directly connected with the mother liquid during the hydrothermal synthesis. Therefore, the effect of the nanocrystal layer thickness on the growth of the protection layer is considered to be small or can be ignored. In this manner, membranes with nanocrystal layer thicknesses of 7.5, 10, 12 and 17 μm were prepared, maintain the Si/Al ratio in the nanocrystals and in the mother liquid employed to make the protection layer at 50. Fig. 5.2 presents cross-sectional FE-SEM images of the resulting membranes. An MTW zeolite layer consisting of dense nanometer-sized crystals was evidently formed over the outer surface of each membrane. Fig. 5.3 shows the effects of the nanocrystal layer thickness on the water flux through the layered membranes and on the separation factor (α). This figure demonstrates that the water flux increased as the thickness of the nanocrystal layer decreased. In contrast, the separation factor increased with increasing thickness and plateaued at values as high as approximately 1200 at thicknesses above 12 μm. This result indicated that both the flux and separation ability were dependent on the amount of nanocrystals loaded on the alumina filter. Thus it is considered that membrane regions that supported the selective permeation of water were formed during the second growth process. During the pervaporation to separate water from water/2-propanol mixtures, water molecules were adsorbed on the ion-exchange sites of zeolitic and non-zeolitic pores in the MTW

nanocrystal-layered membranes. The adsorbed water layers formed on the surfaces of both the zeolite pores (the intracrystalline pores) and the non-zeolite pores (the intercrystalline pores), which acted as channels for selective water permeation, such that the permeation and diffusion of the organic molecules were inhibited. From the results above, MTW zeolite membranes approximately 12 μm thick appear to possess adequate separation ability when applied to the pervaporation of water/2-propanol mixtures.

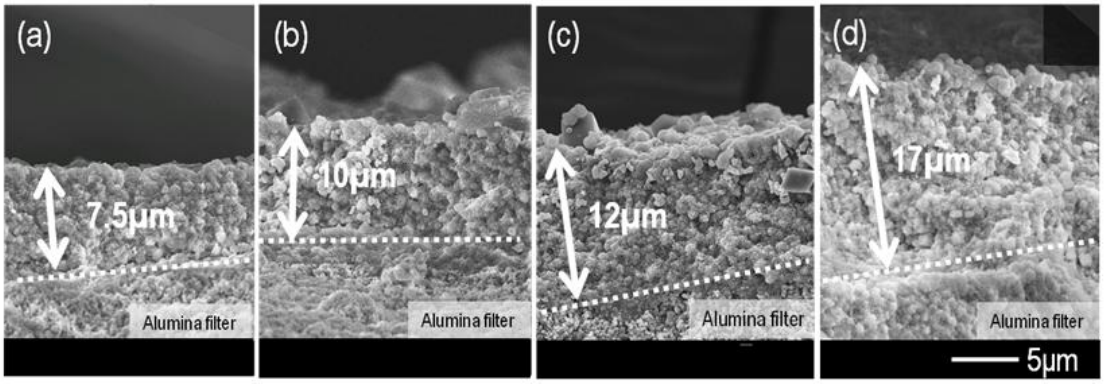

Figure 5.2 FE-SEM images of nanocrystal-layered MTW membranes prepared with different thicknesses.

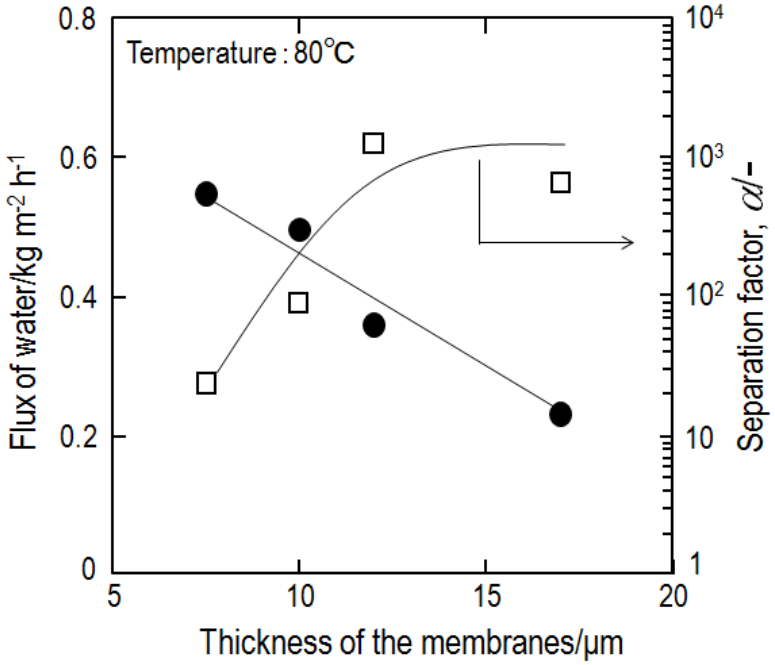

Figure 5.3 Effect of nanocrystal layer thickness in MTW membranes on permeability and separation ability from water/2-propanol solutions.

5.4. Conclusions

MTW-type zeolite membranes composed of a nanocrystal layer and a protection layer were successfully prepared by a secondary growth method and pervaporation trials involving the separation of water from water/2-propanol solutions were conducted to evaluate their performance. The crystal size of the MTW zeolite in the protection layer could be controlled by using different OSDA molecules (TEABr and MTEACl). The MTW membranes prepared using TEABr showed dense layers composed of nanometer-sized crystals and also exhibited higher water flux values as well as enhanced separation factors compared to the membranes prepared using MTEACl. The Al content in both the protection and nanocrystal layers was found to affect the performance of the membranes, such that MTW membranes with high aluminum contents showed elevated water fluxes. Moreover, the membrane flux was determined to depend on the thickness of the membrane, such that the water flux increased with decreasing thickness. It is believed that both the protection and nanocrystal layers are important factors in determining the membrane performance, and that comparatively thin membranes with high Al contents will provide the highest water flux values during the separation of water from water/2-propanol mixtures.

Reference

[1] D. Shah, K. Kissick, A. Ghorpade, R. Hannah, and D. Bhattacharyya, *J. Membr. Sci.* 179 (2000) 185
[2] M. Matsukata, K. Sawamura, T. Shirai, M. Takada, Y. Sekine, E. Kikuchi, *J. Membr. Sci.*316 (2008) 27
[3] G. Li, E. Kikuchi, M. Matsukata, *Micropor. Mesopor. Mater.* 62 (2003) 218
[4] Y. Zhang, Y. Nakasaka, T. Tago, A. Hirata, Y. Sato, T. Masuda, *Micropor. Mesopor. Mater.* 207 (2015) 39
[5] J. Coronas, J. Santamaria, *Sep. Purif. Methods* 28 (1999) 127
[6] T. Tago, Y. Nakasaka, A. Kayoda, T. Masuda, *Sep. Purif. Technol.*58 (2007) 7
[7] T. Tago, Y. Nakasaka, A. Kayoda, T. Masuda, *Micropor. Mesopor. Mater.* 115 (2008) 176
[8] J.B. Lee, H.H. Funke, R.D. Noble, J.L. Falconer, *J. Membr. Sci.*321(2) (2008) 309
[9] T.C. Bowen, R.D. Noble, J.L. Falconer, *J. Membr. Sci.* 245 (2004) 15
[10] M. Nomura, T. Yamaguchi, S. Naka, *J. Membr. Sci.* 187 (2001) 203

[11] A.K. Pabby, S.S.H.Rizvi, A. M. Sastre, Handbook of Membrane Separations, 2008, P289

[12] T.C. Bowen, H. Kalipcilar, J.L. Falconer, R.D. Noble, *J. Membr. Sci.* 215 (2003) 235

[13] M. Noack, P. Kölsch, V. Seefeld, P. Toussaint, G. Georgi, J. caro, *Micropor. Mesopor. Mater.*79 (2005) 329

Chapter 6
ZIF-8 membrane preparation

6.1. Introduction

Zeolitic imidazolate frameworks (ZIFs) are a subclass of MOFs which are composed of tetrahedrally-coordinated transition metal ions (e.g. Fe, Co, Cu, Zn) connected by organic imidazole linkers. Since the metal-imidazole-metal angle is similar to the 145° Si-O-Si angle in zeolites, ZIFs take on zeolite-like topologies. Moreover, ZIFs possess the advantages of both zeolites and MOFs, such as large surface areas, high crystallinities and exceptional thermal and chemical stabilities. ZIFs hold great promise in many application areas including catalysis, separation and sensing [1-3].

ZIF materials possess promising future and can be applied in many areas. ZIF based membranes using for separation is one of the most attractive applications and different kinds of ZIFs membrane have been developed for different kind separation processes [4-10]. So far, various synthesis methods for ZIF membranes have been explored. Generally, the preparation method can be classified into three categories: in situ preparation [11], secondary growth preparation [12] and the counter-diffusion preparation [13].

The remaining challenge is to produce ZIFs on a large scale to meet the potential commercial application and the methods for ZIFs membrane which with high reproducibility, scalability and cost-effectiveness in the future. The present work focuses on the synthesis, characterization, and the performance of ZIF-8 nanocrystal-layer membrane by selective separation of organic from water/organci mixtures. We have also studied the permeance of organic molecules through ZIF-8 membrane and application for the separation organic/water solution by pervaporation.

6.2. Experimental

6.2.1. Synthesis of ZIF-8 membranes

ZIF-8 was synthesized by mixing 2-methylimidazole (Hmim, Sigma-Aldrich) with

Zn nitrate hexahydrate ($Zn(NO_3)_2 \cdot 6H_2O$, Sigma-Aldrich) in the presence of the nonionic surfactant in the water solution. A water solution containing polyoxyethylene-(15)-oleylether (O-15, Nikko Chemicals), and 2-methylimidazole (Sigma-Aldrich) stirred until the surfactant dissolved. After that, zinc nitrate water solutions were then added into the Hmim solution and kept stirring for 24 h at room temperature. The Zn^+: Hmim: surfactant: water molar ratio of the solution was 1: 40: 0.01: 2210.

A cylindrical alumina ceramic filter (NGK insulators, LTD.) was used as a membrane support. The inner and outer diameters and the length of the filter were 6 mm, 11 mm, and 50 mm, respectively. This filter was constructed in two porous regions; the pore diameter of the inner region was about 2-3 μm (rough region), and the outer region was dense and its pore diameter was 0.1μm. The filter was immersed in a 0.1 N hydrochloride solution for 6 h, and washed in distilled water. The ZIF-8 nanocrystals were dispersed ultrasonically in an ethanol solution at a concentration of 2-13 $g \cdot m^{-3}$. The dispersed nanocrystals were layered on the outer surface of cylindrical alumina ceramic filters using a filtration method under low-pressure vacuum on the permeate side. The thickness of the nanocrystal layer is about 4-22 μm. To protect the nanocrystal layer against mechanical shock, a protection layer with micrometer-sized ZIF-8 was formed hydrothermally (secondary growth) on the nanocrystal layer without surfactant (O-15). An aqueous solution (mother liquid) containing Zn^+ and Hmim sources prepared by of $Zn(NO_3)_2 \cdot 6H_2O$ and 2-methylimidazole was used to form the protection layer and the molar composition was: Zn^+: Hmim: surfactant: water molar ratio of the solution was 1: 70: 4420x, where x equal to 2 to 4.

Then the alumina filter with a ZIF-8 nanocrystal layer was immersed in the precursor solution and kept at the room temperature for 24 h to form the protection layer on the nanocrystal layer.

6.2.2. Analysis method

The powders obtained in the solution during hydrothermal synthesis for the protection layer of ZIF-8 membrane were characterized by X-ray diffraction (XRD, JEOL JDX-8030), thermogravimetry analysis (TGA) and nitrogen adsorption and desorption experiment. The membrane morphology was characterized by scanning electron microscopy (SEM, JEOL JSM-6500F).

6.2.3. Pervaporation trials

Pervaporation experiments were conducted using a conventional method at room temperatures using the stainless-steel autoclave vessel shown in Fig. 1. Water and organic solutions (organic solvent: ethanol, butanol, hexane, or benzene) were used as feed solutions for the pervaporation experiment. The new water or organic solutions were used at each pervaporation temperature. After the membrane was immersed in the feed solution, nitrogen was fed into the gas phase of the vessel at room temperature to replace the air. The vessel was then heated to pervaporation temperatures. Molecules that permeated through the membrane were swept out with the nitrogen. The composition of the exit gas obtained from the permeate side of the membrane was analyzed using an on-line gas chromatograph equipped with a Porapak-Q column and TCD and FID detectors. The procedure has been described in detail previously.

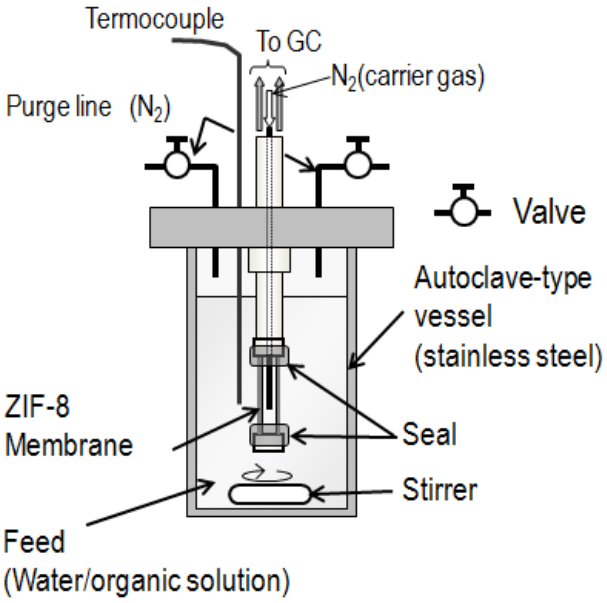

Fig. 6.1 Schematic of the stainless steel autoclave vessel used for pervaporation experiments.

The separation factor, α, is defined as:

$$\alpha = \frac{F_o / F_w}{C_o / C_w} \tag{1}$$

where F_w and F_o are the molar flux of water and organic solvent on the permeate side, respectively, and C_w and C_o are the molar concentrations of water and organic solvent, respectively, on the feed side. The total amount of water and organic solvent permeating

through the membrane during each experiment was less than 3%. Accordingly, the initial concentrations of C_w and C_o were used to calculate the separation factor.

The permeance, P_i, is defined as:

$$P_i = \frac{F_i}{C_i} \tag{2}$$

F_i is the molar flux of water or organic molecules that permeate through the mordenite nanocrystal-layer membrane and C_i stands for the molar concentration of water or organic solvent in the feed side solution. The permeance indicated the permeability of the component (water or organic molecules) in the organic solution through the ZIF-8 nanocrystal-layer membrane.

6.3. Results and discussion

6.3.1. Synthesis of ZIF-8 crystals

ZIF-8 crystals were synthesized at room temperature using O-15 as surfactant. Figure 6.2 shows XRD patterns of white powders obtained, which showed patterns corresponding to ZIF-8. Figure 6.3 shows FE-SEM photographs of obtained ZIF-8 crystals. Round shape small crystals with size of approximately 50 nm were formed.

Nitrogen adsorption isotherms of the obtained ZIF-8 were measured at 77 K (Fig. 6.4). The isotherms exhibited Type-I behavior according Langmuir isotherm model, which reflects the presence of micropore. Brunauer-Emmett-Teller (BET) surface area obtained from the isotherms were about 1770 m^2/g which value is in good agreement with those of previously reported data [14]. Figure 6.5 shows gas adsorption result, where water, ethanol, butanol, n-hexane and benzene were used. From the figure, the ZIf-8 shows an only very low uptake of water, and the vapour-phase adsorption isotherms of ethanol and butanol show an S-shaped profiles. On the other hand, benzene and n-hexane exhibited Type-I behavior according Langmuir isotherm model.

These ZIF-8 nanocrystals thus obtained were used for ZIF-8 membrane preparation.

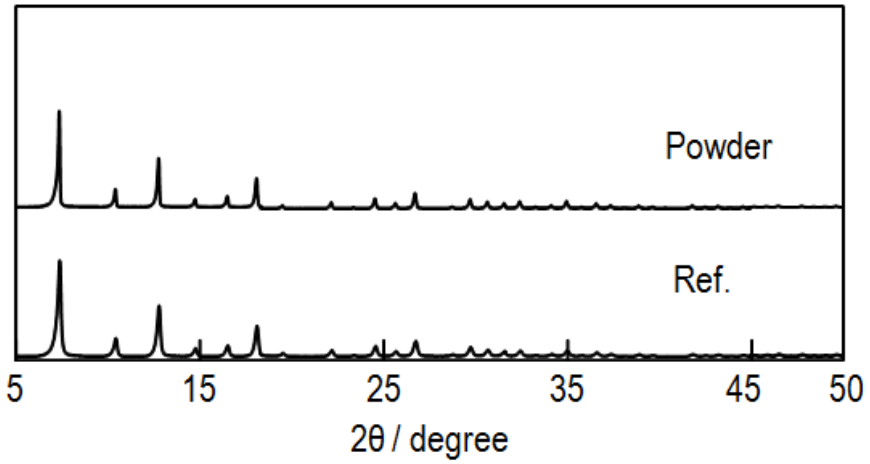

Figure 6.2 XRD patterns of (a) ZIF-8 crystals [15], (b) the powder obtained

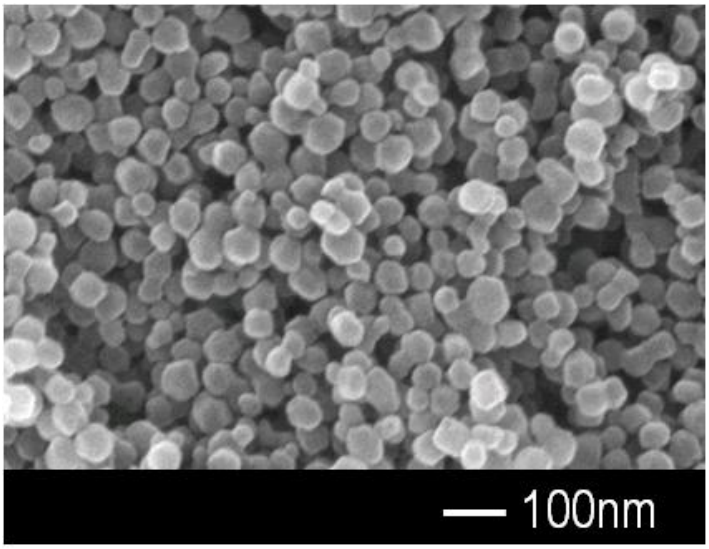

Figure 6.3 FE-SEM photographs of ZIF-8 crystals

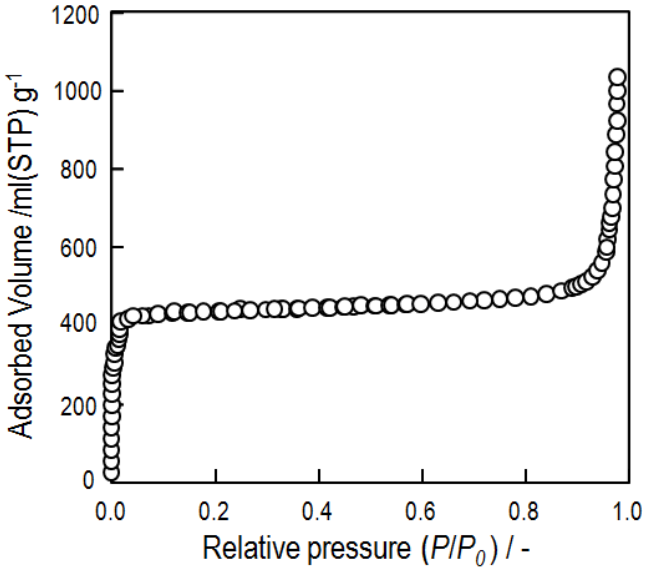

Figure 6.4 Nitrogen adsorption isotherms of ZIF-8 crystals.

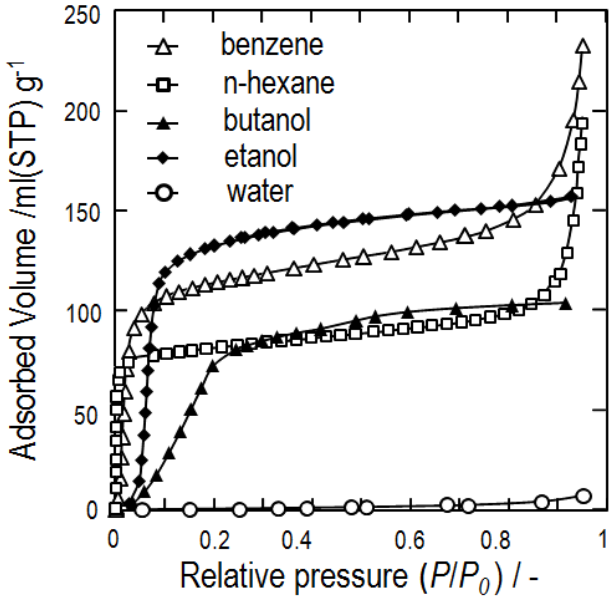

Figure 6.5 Gas adsorption isotherms of ZIF-8 nanometer size crystals.

6.3.2 ZIF-8 membrane prepared by second growth method

After the ZIF-8 nanocrystals were piled up on the aluminum ceramic filter, protection layer of the membranes were synthesized at room temperature. In order to prepare the membranes with appropriate separation areas, the effect of the nanocrystals layer thickness onto the separation properties of the membranes were investigated. The thickness was controlled by changing the concentrations of nanocrystals in the ethanol solution piling up on the alumina filter.

ZIF-8 membranes with nanocrystal layer thickness of 4.1, 5.6, 16.8 and 22μm were prepared. Figure 6.6 shows FE-SEM photographs of the cross sectional area of the membranes. A ZIF-8 membranes consists of dense micro meter sized crystals have been formed on the top of the outer surface of membrane when the nanocrystal layer equal to 5.6, 16.8 and 22μm, respectively and the thickness of the protection layer is nearly the same.

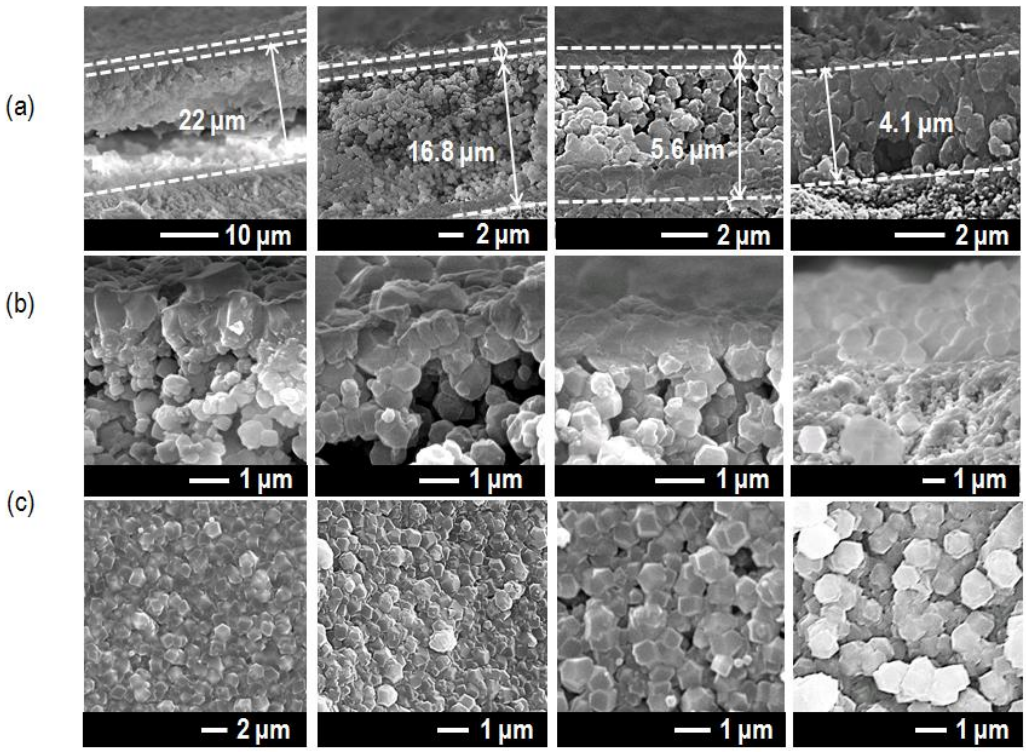

Figure 6.6 FE-SEM photographs of ZIF-8 membranes prepared with different thickness (a) cross section area, (b) protection layer by large magnification, and (c) top view.

In the case of the thickness of nanocrystal layer equal to 16.8 and 22 μm, there are some part of nanocrystal fall off from the nanocrystal layer, which indicating that the second growth was only proceeded around on the top of outer surface of the membrane. Since ZIF-8 crystal could be synthesis in a very short time, a dense layer was formed instantly in the mother liquid which preventing the further growth of the nanocrystal layer. When the thickness of nanocrystal layer smaller than 4.1 μm, the ZIF-8 nanocrystals grew and connected with each other but the protection layer of membrane was not been formed.

As the thickness of nanocrystal layer is equal to 5.6 μm, from the figure, it was found that there is a connection between ZIF-8 protection layer and nanocrystal layer. It is considered that when the thickness of nanocrystal is about 5.6 μm, after synthesis for the protection layer of the membrane, a integrity ZIF-8 membrane can be obtain.

6.3.3. ZIF-8 membrane prepared by repeated synthesis

From the top-view FE-SEM photos of ZIF-8 membrane prepared with the thickness of 5.6 μm, it was found that the surface of the membrane is not continuous and there were still some apparent defects. For the preparation of continuous well intergrow polycrystalline membranes, it is important to supply sufficient nutrients for crystal growth. However, in the case of zif-8 crystals, the homogeneous nucleation predominantly occurs due to the extremely-fast formation rate of ZIF crystals in the aqueous system. In order to supply sufficient nutrients for crystal growth, the repeated synthesis method was used.

Figure 6.7 shows the ZIF-8 membrane which prepared by repeating the synthesis for 4 times. From the top-view of the photos, it was found that the dense structural was formed and the crystal become bigger compared with the membrane synthesis only for one time. From the cross section SEM photos, the thickness of the protection layer is increased comparing with the membrane synthesis only for one time.

The density of the protection layer of ZIF-8 membrane is increased and the thickness of the protection layer could be controlled by repeated the synthesis procedure. However, the connection between the alumina filter and the nanocrystal layer is still weak, this is because that the nucleation rate of the ZIF-8 crystals at the interface beween the seed layer and the synthesis solution is very fast. Therefore, a continuous ZIF-8 layer formed on the outer surface of the seed layer. This continuous layer hindered the permeation of nutrient into the seed layer below, and thus the seed layer could not fully develop.

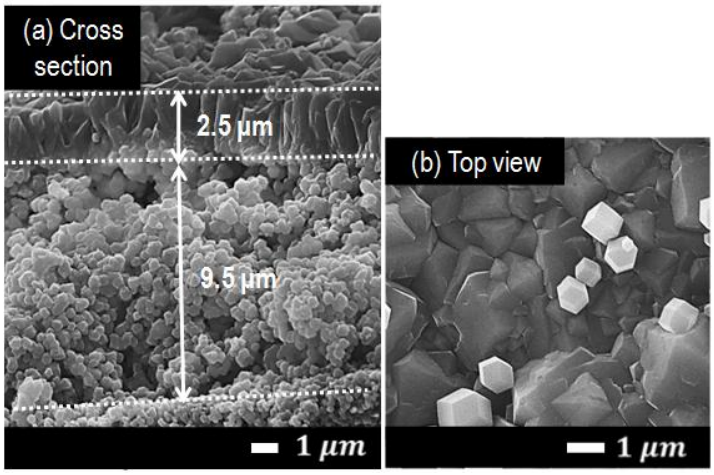

Figure 6.7 FE-SEM photographs of ZIF-8 membranes prepared by repeated synthesis. (a) cross section area, (b) top view.

6.3.4. The density of the nanocrystal layer

A counter diffusion method is using the supports physically separate the metal ions from the ligand molecules. This method enables the synthesis membranes to be healed readily which made the poorly inter−grown membranes to be healed.

In order to increase the density of the nanocrystal layer and strengthen the connection between the nanocrystal layer and alumina filter. The counter diffusion method is carried out. After pile up the nanocrystals on the surface of the alumina filter, the counter diffusion method is conducted, and then the hydrothermal synthesis for the protection layer of the ZIF-8 membrane. Figure 6.8 shows the ZIF-8 membrane prepared with the counter diffusion method to modify the density of the nanocrystal layer. From the SEM photoes (cross section), the protection layer was formed on the nanocrystal layer and the connection between the nanocrysal layer and alumina filter is closely, the boundary could not be distinguished clearly.

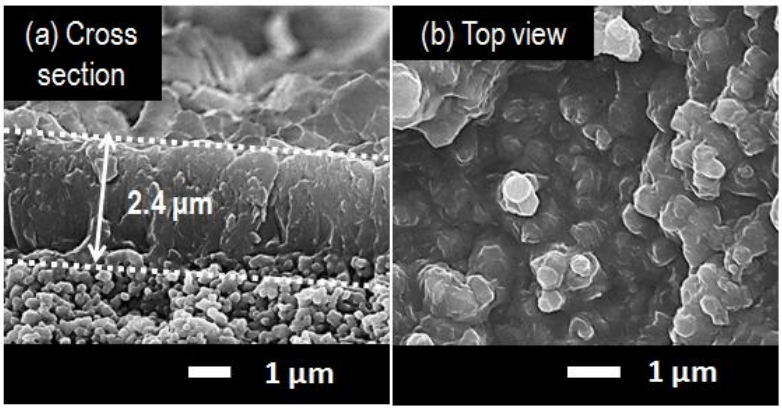

Figure 6.8 FE-SEM photographs of ZIF-8 membranes prepared by counter diffusion method (a) cross section area, (b) top view.

6.3.5. Separation performance of ZIF-8 membrane

The pervaporation performance of ZIF-8 membrane was verified by measuring their single-component permeation, using water, ethanol, butanol, benzene and hexane. As shown in Fig. 6.6, the amounts of single-component permeation follow as: hexane, benzene, ethanol, butanol, water. The ZIF-8 is hydrophobic material and favors non-polar adsorbates over polar ones. This is complete accordance with the result shown in Fig. 6.9. Even with a big molecule size, benzene shows a large permeation only a little lower than the hexane but higher than alcohol and water.

To investigate ZIF-8 membrane separation ability for water/organic mixtures. The water/ethanol (ethanol, 10%, weight percentage) was used as the feed solution for ethanol separation at room temperature. The result showed that the separation factor is 2.3. From the figure 6.9, an ideal separation factor α=8.1 can be predicted. For the water/ethanol solution, the real mixture separation factor was found to be less.

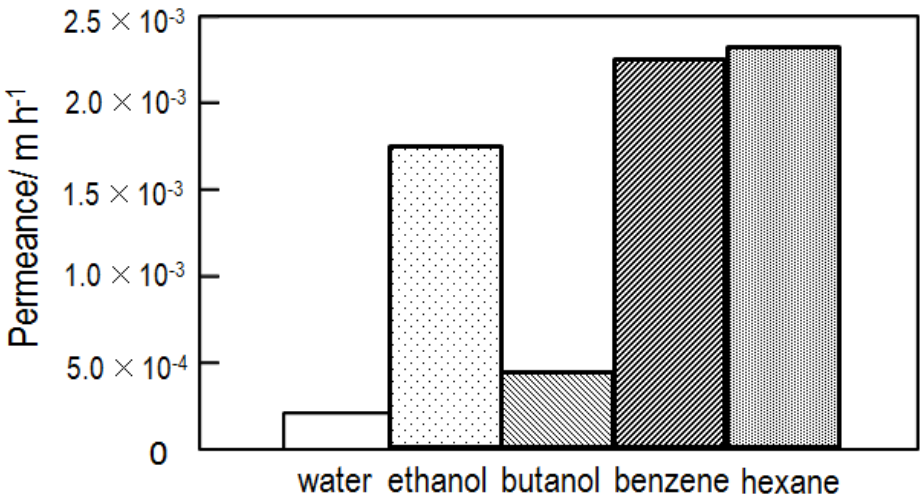

Figure 6.9 Permeance of single component through ZIF-8 membrane.

6.4. Conclusions

ZIF-8 membranes were successfully prepared and the membranes were evaluated by single liquid permeation experiment by using water, ethanol, butanol, hexane and benzene as feed solutions. It was reveal that compared with the water molecules, the permeance of hexane, benzene and ethanol molecules are high through ZIF-8 membrane.

Reference

[1] S.A. Moggach, T.D. Bennett, A.K. Cheetham, *Angew. Chem.* 121 (2009) 7221

[2] D. Fairen-Jimenez, S. A. Moggach, M.T. Wharmby, P.A. Wright, S. Parsons, T. Düren, *J. Am. Chem. Soc.* 133(2011) 8900

[3] F. Wang, Y.X. Tan, H. Yang, H.X. Zhang, Y. Kang, J. Zhang, *Chem. Commun.* 47 (2011) 5828

[4] Y.S. Li, F.Y. Liang, H. Bux, A. Feldhoff, W.S. Yang, J. Caro, *Angew. Chem., Int.Ed.*49 (2010) 548

[5] V.M. Aceituno Melgar, H.T. Kwon, J. Kim, *J. Membr. Sci.* 459 (2014) 190

[6] X. Dong, K. Huang, S. Liu, R. Ren, W. Jin, Y. S. Lin, *J. Mater. Chem.* 22 (2012) 19222

[7] M.C. McCarthy, V. Varela-Guerrero, G.V. Barnett, H.K. Jeong, *Langmuir* 26 (2010) 14636

[8] L. Ge, A. Du, M. Hou, V. Rudolph, Z. Zhu, *RSC Adv.* 2(2012) 11793

[9] Y. Pan, Z. Lai, *Chem. Commun.* 47 (2011) 10275

[10] N. Hara, M. Yoshimune, H. Negishi, K. Haraya, S. Hara, T. Yamaguchi, *J. Membr. Sci.* 450 (2014) 215

[11] H. Bux, F. Liang, Y. Li, J. Cravillon, M. Wiebcke, J.R. Caro, *J. Am. Chem. Soc.* 131 (2009) 16000

[12] S.R. Venna, M.A. Carreon, J. Am. Chem. Soc. 132 (2009) 76

[13] N. Hara, M. Yoshimune, H. Negishi, K. Haraya, S. Hara, T. Yamaguchi, *J. Membr. Sci.* 450 (2014) 215

[14] T. Xing, Y. Lou, Q. Bao, *J. Chen, CrystEngComm* 16 (2014) 8994

[15] Y. Pan, Y. Liu, G. Zeng, L. Zhao, Z. Lai, *Chem. Commun.* 47 (2011) 2071

Summary

In chemical processes, liquid mixtures are usually separated by distillation, which utilizes the vapor-liquid equilibrium difference. Purification of chemicals derived from biomass, such as ethanol, acetic acid, and acetone, requires a distillation column with a large number of plates and a high reflux ratio, plus a complex process for purification of azeotropes, which consumes a large amount of energy. Thus, a new high-purity, low-energy consumption separation process is needed. A pervaporation is a promising technique to achieve this goal and the pervaopration technique by using membrane is proposed.

The membrane process can separate certain molecular mixtures effectively and economically without any toxic or by-production. The materials used for membrane preparation are not limited but cover in a wide range. The structures and properties of the materials decided the membrane performance and the field of membrane applications. This research is focus on developing the new kinds of the membranes with different structure zeolite crystals and ZIFs crystals. The mordenite and MTW type zeolite which the Si/Al ratio can be controlled over a wide range of values were used for synthesis of the membrane. Moreover, ZIFs possess the advantages of both zeolites and MOFs, such as large surface areas, high crystallinities and exceptional thermal and chemical stabilities were also selected to synthesis of the membrane. The membrane preparation method and optimization of the membrane preparation for separation of water from water/organic mixtures by pervaporation were discussed in the works. Summary of each chapter explain as follows.

In chapter 1, the different kind of porous materials and the development of porous materials based membrane were introduced. The zeolite molecular sieve and the representative structure of zeolites, such as zeolite A, zeolite ZSM-5 and Mordenite were presented. The application of the zeolite crystal especially the zeolite used for separation is referred to get a better understanding of the zeolite crystal. The basic knowledge of the zeolite membrane preparation method, the zeolite membrane characterization and the application of the zeolite membranes for separation were introduced. The pervaporation technique and the pervaporation mechanism in zeolite membrane were explained in order to study the membrane separation mechanism.

In chapter 2 and 3, the methods of preparation, optimization of the Mordenite

membranes and application were discussed, respectively. In chapter 2, Mordenite nanocrystal-layered membranes consisting of a mordenite nanocrystal layer and protection layer were successfully prepared. Four types of water/organic solvent solutions were prepared for pervaporation experiments using the mordenite nanocrystal-layered membranes. Permeance of water through the mordenite nanocrystal-layered membrane was similar regardless of the polarity of the organic solvent in the feed solutions however the permeances of the organic molecules depended on their polarities. The mechanisms of water permeation through the mordenite nanocrystal-layered membranes can be considered as the adsorbed water layer formed on both of the zeolitic pores and non-zeolitic pores among crystals for water permeation. The appropriate pore space was formed around the interface between the nanocrystal and protection layer which was expected to be the main separation area of the membranes. Formation of small size mordenite crystals in the protection layer enhanced the separation ability as well as permeability of the mordenite nanocrystal-layered membranes.

In chapter 4 and chapter 5, a new type high-silica material with a unidimensional 12-membered ring channel were used to prepare the membrane. A MTW-type zeolite nanocrystal-layered membrane composed of nanocrystal and protection layers were successfully prepared by a secondary growth method under hydrothermal conditions. The crystal size of the MTW zeolite in the protection layer could be controlled by using different OSDA molecules (TEABr and MTEACl). The MTW membranes prepared using TEABr showed dense layers composed of nanometer-sized crystals and also exhibited higher water flux values as well as enhanced separation factors compared to the membranes prepared using MTEACl. The Al content in both the protection and nanocrystal layers was found to affect the performance of the membranes, such that MTW membranes with high aluminum contents showed elevated water fluxes. Moreover, the membrane flux was determined to depend on the thickness of the membrane, such that the water flux increased with decreasing thickness. It is believed that both the protection and nanocrystal layers are important factors in determining the membrane performance, and that comparatively thin membranes with high Al contents will provide the highest water flux values during the separation of water from water/2-propanol mixtures.

In chapter 6, the synthesis method of ZIF-8 crystals and ZIF-8 membranes were discussed, respectively. The ZIF-8 membranes were evaluated by single liquid permeation experiment by using water, ethanol, butanol, hexane and benzene as feed solutions. It was reveal that compared with the water molecules, the permeance of

hexane, benzene and ethanol molecules are high through ZIF-8 membrane.

In conclution, the new type hydrophilic membranes have been prepared successfully, and applied to selective water separation from organic/water mixtures. Moreover, the separation mechanisms in the zeolite membranes have been clarified from their permeation performance. The results from this work are considered to be useful for developing a new membrane technology in the separation process.

Outlook

Zeolite membrane

Compared with the organic membrane, some special characteristic is existed in the inorganic membrane. In pervaporation, the separation mechanism can be explanation as adsorption-diffusion process. In the case of zeolite membranes which are composed by zeolite crystals, the diffusion process is different than the dense polymeric membranes.

Firstly, the permeation in zeolite membrane is not only through the intracrystalline pathways (zeolite pores), but also through the spaces between the zeolite crystals.

Secondly, the selective separation by zeolite membrane is not only according to the molecule size but also according to the hydrophilic/hydrophobic ability of the molecules. The siloxane group existed in the zeolite crystals can adsorb the water molecules to form a water network which helping the separation.

The special characteristics which zeolite membranes possess decided the separation process carried by zeolite membrane is complicate and difficult. Compared with the removing organic compounds from water, zeolite membrane is supposed successful in dehydrating organic compounds because of the silanol groups existed between the zeolite crystals.

The separation ability of the zeolite membrane can be affected by many factors such as the hydrophilic/hydrophobic ability of zeolite crystals (the ratio of Si/Al), the morphology of the zeolite crystals, and the density of the membrane.

It is a challenge topic to build the separation model of the zeolite membrane. Some researchers using the dusty gas model and the M-S equation to modified the chemical potential with the permeation flux. In this model, some conditions were supposed as follow: there is no counter diffusion, the adsorption species follows Langmuir isotherm, single-file diffusion of molecules can through the pores and presence of trace amount of solvent species inside the pores. The flux through the membrane can be described as equation (1).

$$J_{\mathrm{i}} = \frac{\rho \varepsilon D_{\mathrm{i,s}}}{\delta}(q_{\mathrm{i,f}} - q_{\mathrm{i,p}}) \qquad (1)$$

Here, ρ, ε, δ, $D_{\mathrm{i,s}}$, $q_{\mathrm{i,f}}$ and $q_{\mathrm{i,p}}$ are the density, porosity and thickness of the zeolite membrane, and the surface diffusivity and quantities of component *i* on the feed and

permeate sides, respectively.

According to this equation, the membrane permeability will vary with the membrane thickness and surface diffusivity. The thin membrane with high surface diffusivity will lead to the high permeability.

The model above is base on the ideal condition by admit lots of factor which affecting the membrane separation process. In fact, the effect of supporter also cannot be ignored. A more accurate model is needed to access the membrane performance.

There is still lots of places could make improvement in membrane technique and in order to enlarge the industrialization of the zeolite membrane. The following areas have potential to make improvements:

- Optimize the membrane preparation method to prepare thin membrane to enlarge the membrane permeability.
- Improvement the membrane reproducibility and investigate the simple synthesis method and less expensive synthesis route.
- Improve the modeling and make simulation of transport through the zeolite membrane. Not only limited in binary system but also develop the investigation on pervaporation using multicomponent.
- Zeolite membranes are vulnerable to fouling. The method to clean membrane should been studied. The useful life period of zeolite membrane is short. In order to get industrialization, the method to extent the membrane useful life period is important.

Membrane reactor

Membrane technique can be used not only in separation process, but also be coupled to a chemical reaction. By shift the chemical equilibrium to make the reaction to the final with consuming less energy. The membrane reactor can remove certain production to shift the reaction to the right side and enhance the conversion rate or productivity. Moreover, by combine the reaction process and separation process together, the system become simple and compact. Usually, by using catalyst, the kinetics of the chemical reactions can be enhanced. In the case of membrane reactor, the catalyst can be combined with the membrane system and there are many kinds of design of the catalytic membrane reactors (CMR). The design of the CMR showed in Fig. (a) is the most simple system. The advantage of this design is the membrane preparation and the catalyst synthesis is separated. The catalyst can be change easily if the catalyst is poisoned. The design of the CMR showed in Fig. (b) and (c), either of them is suitable

for removing one of the end productions to help the reaction to shift to the right hand side which can enhance the productivities. The chemical reactions can be used in CMR systems include of dehydrogenation, hydrogenation and oxidation.

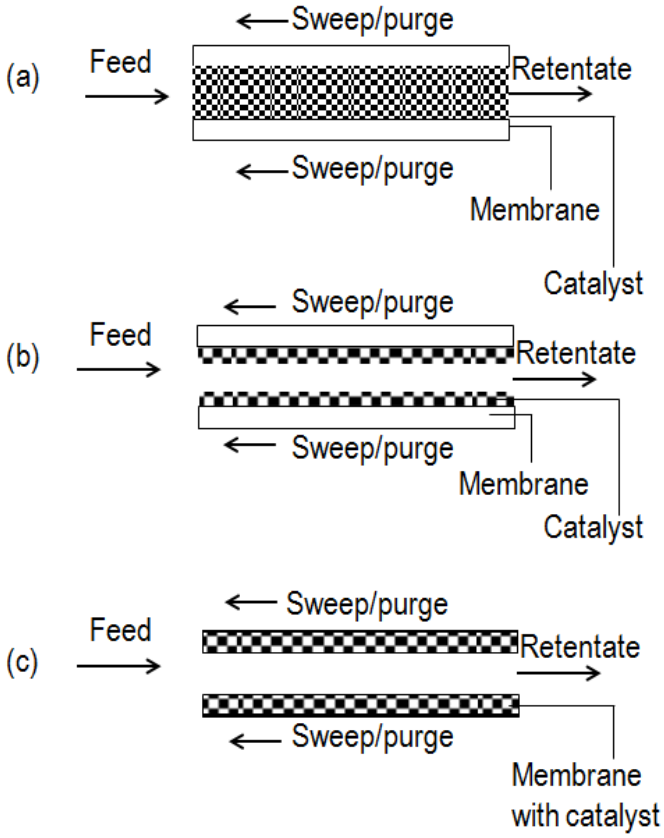

Different types of catalytic membrane reactors: (a) bore of tube filled with catalyst, (b) top layer with catalyst and (c) membrane wall with catalyst.

Even using CMR system possesses lots of merits, there are still far way to go to the commercial application. The efforts need to improve in the membrane technique include:

- Improve the membrane separation ability and permeability.
- Decrease the cost of the membrane synthesis.
- Develop more types of the membrane which can fit for all kinds of chemical reaction.
- Fine the solution to decrease the poisoning of the catalyst

Acknowledgements

The research for this thesis was carried out at the Chemical System Engineering Laboratory, Organics Process Engineering Department, Hokkaido University.

I gratefully acknowledge my supervisors Prof. Takao Masuda, Prof. Teruoki Tago and Assistant Prof. Yuta Nakasaka for providing me with the opportunity to undertake PhD Studenties. I highly appreciate their patience and support throughout the research process, conferences, and publications.

Special thanks go to Hisaki Kondoh for his assistance in both study and daily lives as foreign student in Japan. I also thank Taichi Taniguchi and Gaku Watanabe for their guidance at the different area of research. I also wish to thank membrane group members such as Yuki Satoh, Aya Hirata, Miho Haswgawa and Jihye Choi for their help and cheerful discussions. I am also grateful to all my colleagues in Chemical System Engineering Laboratory for their support and friendships.

My warmest thanks go to my family in China and friends for their support and encouragement to finish my study in Japan.

Study Achievements

Original papers

1. Yaqi Zhang, Yuta Nakasaka, Teruoki Tago, Aya Hirata, Yuki Sato, Takao Masuda: "Preparation and Optimization of Mordenite Nanocrystal-Layered Membrane for Dehydration by Pervaporation" *Microporous and Mesoporous Materials,* Vol. 207, 2015, pp. 39-45
2. Yaqi Zhang, Aya Hirata, Yuta Nakasaka, Teruoki Tago, Taichi Taniguchi, Takao Masuda: "Effects of crystal morphology, Si/Al ratio and thickness of MTW zeolite membrane on water/2-propanol separation by pervaporation" *Microporous and Mesoporous Materials,* Vol. 222, 2016, pp. 178-184

Conferences

3. ○Yaqi Zhang, Aya Hirata, Yuta Nakasaka, Teruoki Tago, Taichi Taniguchi, Takao Masuda: "Selective Separation of Water from Water/Organic Mixtures by Pervaporation using MTW type zeolite membrane" XIth European Congress on Catalysis, France, September, 2013
4. ○Yaqi Zhang, Yuta Nakasaka, Teruoki Tago, Aya Hirata, Yuki Sato, Takao Masuda: "Optimization of MOR zeolite membrane preparation for separation of water from water/organic mixtures by pervaporation" The 6th Asia-Pacific Congress on Catalysis (APCAT-6), Taiwan, October, 2013
5. ○Yaqi Zhang, Aya Hirata, Yuta Nakasaka, Teruoki Tago, Taichi Taniguchi, Takao Masuda: "Preparation of MTW type zeolite Membrane for high purification of organic solution production by pervaporation" The 26th International Symposium on Chemical Engineering, Korea, December, 2013
6. ○Yaqi Zhang, Yuta Nakasaka, Teruoki Tago, Aya Hirata, Yuki Sato, Takao Masuda: "Optimization of MOR zeolite membrane preparation for separation of water from water/organic mixtures by pervaporation" The 4th CSE Summer School Post ISHHC-16 CRC International Symposium, Japan, August, 2013
7. ○Yaqi Zhang, Aya Hirata, Yuta Nakasaka, Teruoki Tago, Taichi Taniguchi, Takao Masuda: "Preparation of MTW type zeolite membrane for the dehydration of the organic solution by pervaporation" The Seventhe Tokyo Cnference on Advanced

Catalytic Science and Technology (TOCAT7), Japan, June, 2014

8. ○Yaqi Zhang, Aya Hirata, Yuta Nakasaka, Teruoki Tago, Takao Masuda: "High purification of organic solution by pervaporation with MTW type zeolite membrane" The 3rd Frontier Chemistry Center International Symposium, Japan, June, 2014
9. ○Yaqi Zhang, Miho Hasegawa, Yuta Nakasaka, Canan Gucuyener, Teruoki Tago, Jorge Gascon, Freek Kaoteijn, Takao Masuda: "Stnthesis of size-controlled ZIF-8 nanocrystals by addition of nonionic surfactant in water solution"International Symposium on Zeolite and Microporous Crystals 2015 (ZMPC2015), Japan, July, 2015.
10. ○Yaqi Zhang，平田彩，中坂佑太，多湖輝興，増田隆夫：“含水有機溶液からの高選択的脱水を可能とするモルデナイトナノクリスタル積層膜の開発” 第 29 回ゼオライト研究発表会，2013 年 7 月，北海道
11. ○Yaqi Zhang，中坂佑太，多湖輝興，佐藤由貴，平田彩，増田隆夫:“含水有機溶液からの高選択的脱水を可能とするモルデナイトナノクリスタル積層膜の開発” 第 29 回ゼオライト研究発表会，2013 年 12 月，宮城
12. ○Yaqi Zhang，平田彩，中坂佑太，多湖輝興，増田隆夫：“MTW 型ゼオライト膜による水/有機物質共沸混合液からの選択脱水” 化学系学協会北海道支部 2014 年冬季研究発表会，2014 年 1 月，北海道
13. ○Yaqi Zhang，平田彩，中坂佑太，多湖輝興，増田隆夫：“水/2-プロパノール共沸混合液からの選択脱水を達成する MTW 型ゼオライト膜の開発” 2014 化学工学会第 79 年会，2014 年 3 月，岐阜
14. 平田彩，Yaqi Zhang，中坂佑太，多湖輝興，増田隆夫：“MTW 型ゼオライト膜による水/2-プロパノール共沸混合液からの選択脱水” 第 53 回オーロラセミナー，2013 年 7 月，旭川
15. 平田彩，Yaqi Zhang，中坂佑太，多湖輝興，増田隆夫：“MTW 型ゼオライト膜を用いた浸透気化分離法による水/2-プロパノール共沸混合液からの選択脱水” 化学工学会第４５回秋季大会，2013 年９月，岡山
16. 平田彩，Yaqi Zhang，中坂佑太，多湖輝興，増田隆夫：“MTW 型ゼオライト膜による水/有機物質共沸混合液からの選択脱水” 化学系学協会北海道支部 2014 年冬季研究発表会，2014 年１月，北海道